



**HAL**  
open science

## Tackling the Challenges of Enzymatic (Bio)Fuel Cells

Xinxin Xiao, Hong-Qi Xia, Ranran Wu, Lu Bai, Lu Yan, Edmond Magner,  
Serge Cosnier, Elisabeth Lojou, Zhiguang Zhu, Aihua Liu

► **To cite this version:**

Xinxin Xiao, Hong-Qi Xia, Ranran Wu, Lu Bai, Lu Yan, et al.. Tackling the Challenges of Enzymatic (Bio)Fuel Cells. Chemical Reviews, 2019, 10.1021/acs.chemrev.9b00115 . hal-02167914

**HAL Id: hal-02167914**

**<https://amu.hal.science/hal-02167914>**

Submitted on 28 Jun 2019

**HAL** is a multi-disciplinary open access archive for the deposit and dissemination of scientific research documents, whether they are published or not. The documents may come from teaching and research institutions in France or abroad, or from public or private research centers.

L'archive ouverte pluridisciplinaire **HAL**, est destinée au dépôt et à la diffusion de documents scientifiques de niveau recherche, publiés ou non, émanant des établissements d'enseignement et de recherche français ou étrangers, des laboratoires publics ou privés.

## Tackling the challenges of enzymatic (bio)fuel cells

Xinxin Xiao<sup>†,‡,⊥</sup>, Hong-qi Xia<sup>†,⊥,Σ</sup>, Ranran Wu<sup>‡,⊥</sup>, Lu Bai<sup>†</sup>, Lu Yan<sup>†</sup>, Edmond Magner<sup>‡</sup>, Serge Cosnier<sup>Δ,¶</sup>, Elisabeth Lojou<sup>\*,§</sup>, Zhiguang Zhu<sup>\*,‡</sup> and Aihua Liu<sup>\*,†,ζ,γ</sup>

<sup>†</sup>Institute for Biosensing, and College of Life Sciences, Qingdao University, 308 Ningxia Road, Qingdao 266071, China

<sup>‡</sup>Tianjin Institute of Industrial Biotechnology, Chinese Academy of Sciences, 32 West 7th Road, Tianjin Airport Economic Area, Tianjin 300308, China

<sup>ζ</sup>College of Chemistry & Chemical Engineering, Qingdao University, 308 Ningxia Road, Qingdao 266071, China

<sup>γ</sup>School of Pharmacy, Medical College, Qingdao University, Qingdao, 266021, China

<sup>§</sup>Aix Marseille Univ, CNRS, BIP, Bioénergétique et Ingénierie des Protéines UMR7281, Institut de Microbiologie de la Méditerranée, IMM, FR 3479, 31, chemin Joseph Aiguier 13402 Marseille Cedex 20, France

<sup>‡</sup>Department of Chemical Sciences, School of Natural Sciences and Bernal Institute, University of Limerick, Limerick V94 T9PX, Ireland

<sup>Δ</sup>Université Grenoble-Alpes, DCM UMR 5250, F-38000 Grenoble, France

<sup>¶</sup>Département de Chimie Moléculaire, UMR CNRS, DCM UMR 5250, F-38000 Grenoble, France

<sup>⊥</sup>These authors contributed equally to this work.

\*To whom correspondence should be addressed: E-mails: liuah@qdu.edu.cn (A.L.); zhu\_zg@tib.cas.cn (Z.Z.); lojou@imm.cnrs.fr (E.L.)

<sup>Σ</sup>Present address: School of Biomedical Engineering, Sun Yat-sen University, Guangzhou 510006, China

## **ABSTRACT**

The ever-increasing demands for clean and sustainable energy sources combined with rapid advances in bio-integrated portable or implantable electronic devices have stimulated intensive research activities in enzymatic (bio)fuel cells (EFCs). The use of renewable biocatalysts, the utilization of abundant green, safe, and high energy density fuels, together with the capability of working at modest and biocompatible conditions, make EFCs promising as next generation alternative power sources. However, the main challenges (low energy density, relatively low power density, poor operational stability and limited voltage output) hinder future applications of EFCs. This review aims at exploring the underlying mechanism of EFCs and providing possible practical strategies, methodologies and insights to tackle of these issues. Firstly, this review summarizes approaches in achieving high energy densities in EFCs, particularly, employing enzyme cascades for the deep/complete oxidation of fuels. Secondly, strategies for increasing power densities in EFCs, including increasing enzyme activities, facilitating electron transfers, employing nanomaterials, and designing more efficient enzyme-electrode interfaces, are described. The potential of EFCs/(super)capacitor combination is discussed. Thirdly, the review evaluates a range of strategies for improving the stability of EFCs, including the use of different enzyme immobilization approaches, tuning enzyme properties, designing protective matrixes, and using microbial surface displaying enzymes. Fourthly, approaches for the improvement of the cell voltage of EFCs are highlighted. Finally, future developments and a prospective on EFCs are envisioned.

## CONTENTS

ABSTRACT.....	2
<b>CONTENTS</b> .....	3
1. Introduction.....	5
1.1 Enzymatic (bio)fuel cells (EFCs), general considerations.....	5
1.2 Potential applications of EFCs.....	7
1.3 Identification of main challenges in EFCs.....	9
2. Strategies for achieving high energy density in EFCs.....	24
2.1 Range of fuels in EFCs.....	24
2.2 Enzyme cascades for the deep/complete oxidation of fuels.....	26
3. Strategies for increasing power density in EFCs.....	31
3.1 Evaluation of different power output results.....	31
3.2 Increasing intrinsic enzyme activities.....	35
3.3 Facilitating electron transfer.....	36
3.4 Employment of nanomaterials.....	47
3.5 Gas diffusion bioelectrode.....	50
3.6 Fluidic EFCs.....	54
3.7 Combined EFCs/(super)capacitor devices.....	56
4. Strategies for improving stability in EFCs.....	60
4.1 Enzyme immobilization approaches.....	60
4.2 Tuning enzyme properties.....	67
4.2.1 Employing extremophile enzymes.....	67
4.2.2 Protein engineering for better stability.....	68
4.3 Microbial surface displayed enzymes as biocatalysts to enhance EFCs' stability.....	70
4.3.1 Microbial surface display.....	70
4.3.2. Efficient EFCs based on microbial surface displayed enzyme as biocatalysts.....	71
4.4 Strategies for enzyme protection against O <sub>2</sub> and reactive oxygen species (ROS).....	74
4.5 Anti-biofouling of implantable glucose/O <sub>2</sub> EFCs.....	78
5. Approaches for the improvement of EFCs' cell voltage.....	81
5.1 Mediator optimization.....	84
5.2 Serial connection.....	89
5.3 Employment of external boost converter.....	91
6. Conclusions and perspectives.....	92

Acknowledgements .....	95
References.....	95
Bios.....	134

## 1. Introduction

### 1.1 Enzymatic (bio)fuel cells (EFCs), general considerations

The uneven geographical distribution of fuels associated with the increasingly serious effects of environmental pollution provides the driving force for the pursuit of green and sustainable energy sources. To this end, fuel cells are considered environmentally friendly electrochemical devices to directly convert chemical energy into electrical energy without intermediate steps.<sup>1</sup> In general, conventional fuel cells use noble metals (*e.g.* platinum, ruthenium, palladium, *etc.*) and/or their alloys as catalysts for the oxidation of pure fuels (*e.g.* hydrogen, methanol) at the anode and the reduction of the oxidant (*e.g.* oxygen) at the cathode, which work in optimized basic and/or acid electrolytes, resulting in a very high efficiency. However, noble metals are costly and, more importantly, are non-renewable resources only available in few countries in the world. The use of electrolytes at extremes of pH, accompanying with the requirement for expensive membranes to separate reactions into individual compartments, poses additional challenges.

In addition to the need for clean and renewable energy, recent rapid advances in bio-integrated implantable or portable electronic devices underline the urgent need to develop technologies that can harvest energy from biological sources.<sup>2</sup> A range of potential applications in microelectronic, biomedical, and sensor devices have inspired research in energy conversion systems utilizing sources such as body heat, muscle stretching, blood flow, walking or running, *etc.*<sup>3</sup> However, low levels of biocompatibility and durability pose potential health and safety concerns, raising significant challenges in the successful development of such devices.

EFCs are a subclass of fuel cells employing redox enzymes as catalysts<sup>4-9</sup>. The concept of an EFC was first described by Yahiro and co-workers in 1964.<sup>10</sup> Depending on emerging possible applications, EFCs have been designed in various configurations that may be quite

different from the traditional fuel cell stacks. However, they all retain the same key components. Similar to other fuel cells, EFCs consist of a two-electrode cell separated by a proton conducting medium, which can also be an electrolyte (**Figure 1**): using appropriate redox enzymes, fuels are oxidized at the bioanode, electrons flow through the external electric circuit to the biocathode, where the oxidants, usually oxygen<sup>11</sup> or peroxides<sup>12</sup>, are reduced to water. Using bioelectrocatalysts, EFCs have several advantages. Firstly, the catalyst is renewable. Redox enzymes can be extracted from a wide range of living organisms in a renewable manner. Secondly, fuels can be diverse. In principle, sugars<sup>13</sup>, alcohols<sup>14</sup>, organic acids<sup>15</sup>, hydrogen<sup>16</sup>, and mixtures of these materials that can be digested by living organisms, can be used as fuels for EFCs. Thirdly, the operational conditions are very mild and safe. The properties of enzymatic reactions enable EFCs to operate at physiological pH, room temperature and ambient pressure, although the recent use of stable extremophilic enzymes offers the possibility to work at temperatures of up to 85 °C or at a pH value as low as 2.<sup>17,18</sup> In addition, redox enzymes provide exceptional specificity towards their natural substrates, thus allowing the assembly of the bioanode and biocathode in a single membrane-less cell and the miniaturization of EFCs.<sup>19</sup> Another consequence of high enzyme specificity is that EFCs can use fuels without the need for intensive purification steps. Finally, EFCs can be considered as disposable systems as the components can potentially be biologically degraded. These properties demonstrate the potential use of EFCs in next-generation green power source for a range of applications.

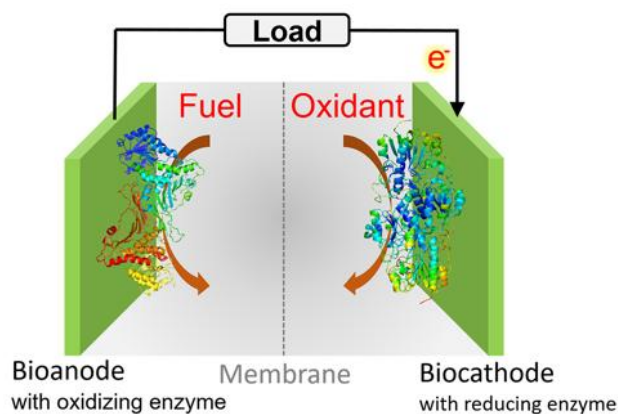


**Figure 1.** Schematic drawing of a typical EFC consisting of a bioanode and a biocathode.

Bioelectrocatalysis, in which the electrons involved in an enzymatic reaction are collected at an electrode surface, is a key element of EFCs. Due to the size and structure of the enzymes, electron transfer (ET) within the enzyme and between the enzyme and the electrode is specific. In general, the electron transfer mechanisms between enzymes and electrodes are classified into two types: mediated electron transfer (MET) and direct electron transfer (DET)<sup>8,20,21</sup>. In a MET-type system, extrinsic redox-active compounds such as ferrocene<sup>22</sup>, methyl viologen, ABTS are used as redox mediators to shuttle electrons between the enzyme cofactor (for example, glucose oxidase (GOx) uses flavin adenine dinucleotide (FAD) as the cofactor) and the electrode<sup>23</sup>. In this case, the redox enzyme catalyzes the oxidation or reduction of the mediator as a co-substrate. The reverse transformation (regeneration) of the mediator occurs on the electrode surface. The use of small, low molecular weight electron mediators that require low overpotentials can be beneficial as they can enable rapid rates of electron transfer between an enzyme and an electrode with low power losses. However, the cost, stability, selectivity and ability to exchange electron in the immobilized state of such mediators must also be considered. In contrast, in a DET-type system, fast electron transfer to or from a solid electrode occurs through an intrinsic electron relay system in the protein<sup>20</sup> (e.g. iron-sulfur clusters<sup>24,25</sup>, heme groups<sup>26,27</sup> or copper sites<sup>28,29</sup>).

## **1.2 Potential applications of EFCs**

The early development of EFCs focussed on obtaining electrical energy mainly through the oxidation of glucose or other organic fuels in living organisms, in order to drive implantable electronic devices. The power output of an average human body is approximately 100 W, and the constant presence and availability of the fuel from the body provides sufficient support for running EFCs<sup>30</sup>. The oxygen or other oxidant supply for the biocathode in such EFCs is important as EFCs are implanted in a relatively closed system. Since the first total surgical implantation of a EFC in a rat in 2010,<sup>31</sup> several recent studies on implantable EFCs have been reported. In particular, biocathodes modified by chitosan implanted in a rat can exhibit a stability of up to 167 days<sup>32</sup>. Cyborg lobsters with partially implanted EFCs were able to



power an electrical watch and a pacemaker<sup>33</sup>, while a fully implanted EFC in rats can power a light-emitting diode (LED), or a digital thermometer<sup>34</sup>. Mountable EFCs using trehalose in insect hemolymph were also successfully demonstrated<sup>35</sup>. However, special attention should be focused on solving sterilization and biocompatibility issues, as well as their poor operational stabilities, before such implantable or mountable EFCs can become practical, especially when used in human patients<sup>36-40</sup>.

During the past decades, significant improvements in the power output and stability of EFCs have been achieved, paving the way for the use of EFCs to power portable electronic devices such as music players, cellphones, sensors, and even laptops. Many studies have demonstrated the use of EFCs as power sources for LEDs or for digital clocks<sup>41-43</sup>. In 2007, Sony demonstrated that a music player could be powered by a stack of EFCs. Later, they demonstrated the operation of a toy car using a glucose-fueled EFC. However, there are considerable challenges to the development of these devices as cost effective power sources that can be manufactured on a large scale<sup>44</sup>.

Another potential application of EFCs is emerging with the rapid development of wearable electronic devices that are shaping our life in healthcare, communication, entertainment, etc. Such wearable electronic devices can potentially be powered by EFCs operating using external fuels, or directly from fuel in the body<sup>45,46</sup>. In contrast to implantable EFCs, non-invasive EFCs have attracted considerable interest<sup>47</sup>. Several wearable EFCs have been constructed using lactate in sweat or in tears as the fuel and generate reasonable power outputs<sup>48,49</sup>. Such wearable EFCs need to be flexible in order to withstand frequently bending or folding. A number of layer-by-layer or printed EFCs have been developed that exhibit good flexibility, high performances, and a potential of low fabrication costs<sup>50,51</sup>. In the following sub-section, the main challenges of these EFCs will be discussed and the particular limitations of each application will be described.

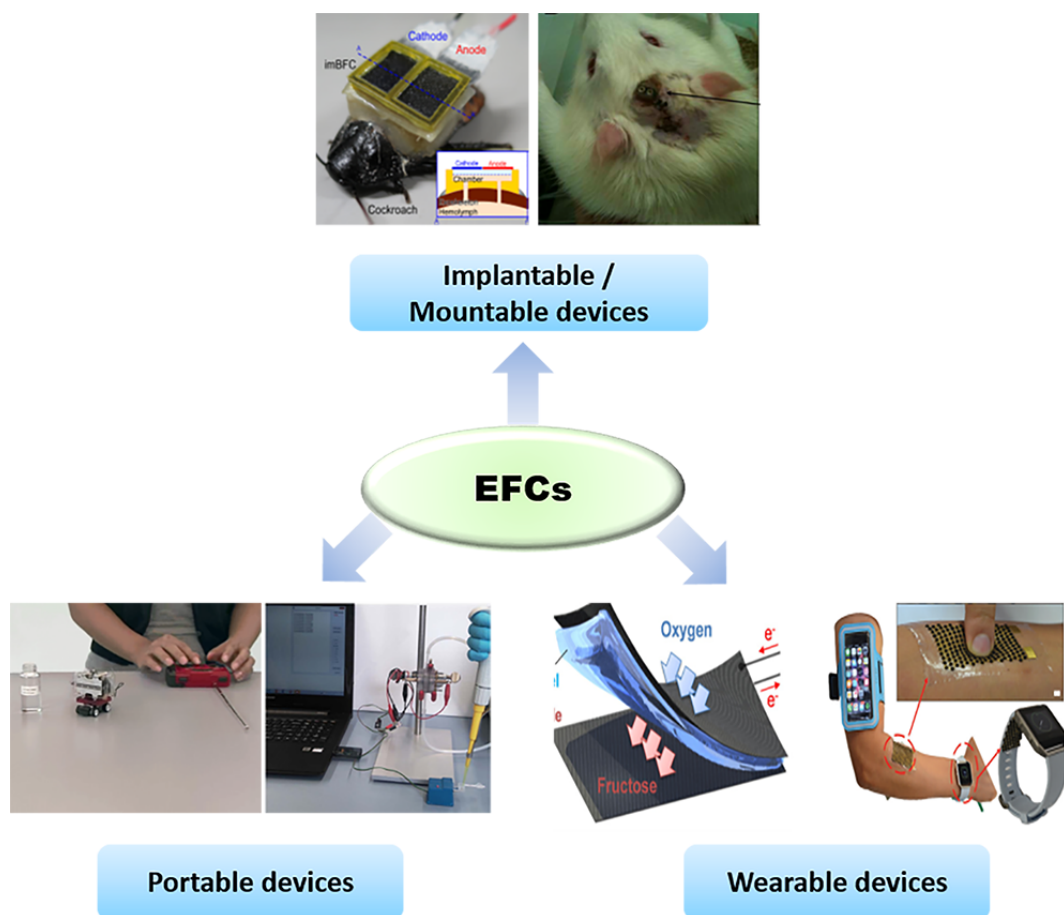


**Figure 2.** Possible applications of EFCs activating implantable, portable and wearable devices. Reprinted with permission<sup>34,35,50,52-54</sup> Copyright 2013, 2016, 2018 Elsevier; Copyright 2009, 2017 Royal Society of Chemistry; Copyright 2013 Nature Publishing Group.

### 1.3 Identification of main challenges in EFCs

The development of EFCs faces four significant challenges: inability to completely oxidize fuels, low power density, poor operational stability, and limited voltage output. Although each of these challenges can be addressed from multiple aspects, some potential solutions are too complex to implement and may also be detrimental factors in terms of other aspects of cell performance. Due to the complexity of these challenges, a systematic analysis should be made to identify the key reasons behind each challenge and to then carefully evaluate multiple possible solutions<sup>55</sup>.

Firstly, most EFCs employ one or two oxidoreductases. Depending on the fuel, complete oxidation cannot be achieved, leading to low efficiency and energy density, critical parameters for all power sources. As one of the principle advantages of EFCs mentioned above, sugars or alcohols can store much higher energy per weight or volume than most secondary batteries<sup>56</sup>. However, exploitation of such energy storage potential requires a series of cascade reactions that oxidize the fuel in a step by step manner. The use of one or two enzymes makes it impossible to implement the complete oxidation of a fuel. As a consequence, the cost of fuels, inhibition (by products or intermediates), the difficulties in reusing cells, and decreased power output pose significant obstacles to the successful development of EFCs.

The issue of low power output of EFCs has been a major problem that constrains potential use to applications<sup>57</sup>. Compared with metal-catalyzed fuel cells or lithium-ion batteries, the power output produced from EFCs is significantly lower. The power densities of the majority of EFCs lie in the range of 1-1000  $\mu\text{W cm}^{-2}$ , with few surpassing 1  $\text{mW cm}^{-2}$  (**Table 1**). A principal reason for this is that the active site of enzyme is buried inside a large insulating protein moiety. Typically, a 0.5  $\text{mg cm}^{-2}$  Pt loading on the electrode of a metal-catalyzed fuel cell represents 2.5  $\mu\text{mol}$  of catalyst  $\text{cm}^{-2}$ , while the catalyst loading for a GOx or laccase (Lac)-immobilized electrode is only at the level of  $10^{-6}$  to  $10^{-1}$   $\mu\text{mol cm}^{-2}$ <sup>58,59</sup> in an EFC depending on the electrode of choice. The overall reaction rate per volume or area, in terms of power density, for enzyme biocatalysts is decreased by orders of magnitude. In addition, the availability of the fuel may become a limiting factor in power generation, especially for implantable EFCs, which may have limited oxidant supply<sup>60</sup>. Tackling this issue requires a combinatorial strategy of engineering electrode materials, enzymes, and their interfaces as well as smart configuration design<sup>4</sup>.

**Table 1.** Full EFCs with a maximum power density ( $P_{\max}$ ) greater than  $1 \text{ mW cm}^{-2}$ 

Glucose/O <sub>2</sub> EFCs							
No.	Bioanode	Biocathode	Note	$P_{\max}$ ( $\text{mW cm}^{-2}$ )	OCV (V)	Stability	Ref.
1	CF/GDH/DI/VK <sub>3</sub> /NADH (1.5 mm thick); MET; 400 mM glucose	CF/K <sub>3</sub> [Fe(CN) <sub>6</sub> ]/BOD; MET; Air-breathing	Two-compartment; limited by anode	1.45	0.8	Continuous operation over 2 h	<sup>52</sup>
2	CF/GDH/DI/ANQ/NADH; MET; 400 mM glucose	CF/K <sub>3</sub> [Fe(CN) <sub>6</sub> ]/BOD; MET; Air-breathing	Two-compartment; limited by cathode	3	0.8	n/a	<sup>61</sup>
3	MWCNTs-PEDOT yarn/Os-complex modified polymer(I)/GOx; MET; 60 mM glucose	MWCNTs-PEDOT yarn/Os-complex modified polymer(II)/BOD; MET; O <sub>2</sub> -saturated	One-compartment; limited by cathode	2.18	0.7	83% remaining after 24 h	<sup>62</sup>
4	HPC/AQ2S/DI/NAD <sup>+</sup> /GDH; MET; 800 mM glucose	CF/K <sub>3</sub> [Fe(CN) <sub>6</sub> ]/BOD; MET; Air-breathing	Two-compartment; limited by anode	1	0.8	Can be used for > 10 cycles	<sup>63</sup>
5	GCE/MWCNTs/NQ-4-LPEI/GDH; MET;	CP/anthracene-MWCNTs/ BOD;	One-compartment; limited by	2.3	0.86	Potential decreased from	<sup>64</sup>

	Stirred 100 mM glucose	MET; Air-equilibrated	anode			0.86 to 0.71 V after 24 h operation	
6	MWCNTs/NQ/GOx/catalase; MET; 50 mM glucose	MWCNTs/Lac; DET; O <sub>2</sub> -saturated	One-compartment; limited by anode	1.54	0.76	60% decrease over 7 days' storage	<sup>41</sup>
7	MWCNTs/GOx/catalase(3 mm thick); MET; 50 mM glucose	MWCNTs/Lac; DET	One-compartment	1.3	0.95	Stable for 1 month	<sup>59</sup>

H <sub>2</sub> /O <sub>2</sub> EFCs							
	Bioanode	Bio-/cathode	Note	P <sub>max</sub> (mW cm <sup>-2</sup> )	OCV (V)	Stability	Ref.
8	CNF/ <i>Aquifex aeolicus</i> (Aa) [NiFe] hydrogenase; DET; H <sub>2</sub> -saturated	CNF/ <i>Bacillus pumilus</i> (Bp) BOD; DET; O <sub>2</sub> -saturated	Two-compartment; limited by cathode	1.5 at 60 °C	1.06	Decreased by 60% at 0.5 V after 24 h	<sup>65</sup>
9	WPCC/KB/ <i>Desulfovibrio vulgaris</i> (Dv) [NiFe] hydrogenase; DET; H <sub>2</sub> diffusion electrode	WPCC/KB/ <i>Myrothecium verrucaria</i> (Mv) BOD; DET; Air-breathing	Dual gas-diffusion type; One-compartment; limited by	6.1	1.12	n/a	<sup>16</sup>

			cathode				
10	CMC/ <i>E. coli</i> hydrogenase-1; DET	CMC/ <i>Mv</i> BOD; DET	In a 78% H <sub>2</sub> -22% air mixture; One-compartm ent; limited by cathode	1.67 (per anode area)	1.068	Retained 90% output after continuously working for 24 h	<sup>66</sup>
11	CF/CNTs/ <i>Aa</i> [NiFe] hydrogenase; DET; H <sub>2</sub> -saturated	CF/CNTs/ <i>Bp</i> BOD; DET; O <sub>2</sub> -saturated	Two-compartm ent; limited by anode	1.7 at 50 °C	1.02	5% loss after 17 h operation	<sup>67</sup>
12	WPCC/KB/ <i>Dv</i> [NiFe] hydrogenase; DET; 100% H <sub>2</sub>	WPCC/KB/ <i>Mv</i> BOD; DET; 100% O <sub>2</sub>	Dual gas-diffusion; not a real EFC assembly	8.4	1.14	n/a	<sup>68</sup>
13	Carbon cloth/ <i>Dv</i> [NiFe] hydrogenase/ P(N <sub>3</sub> MA-BA-GMA)-vio/ P(GMA-BA-PEGMA)-vio; MET; 100% H <sub>2</sub>	Carbon cloth/ <i>Mv</i> BOD; DET; 100% O <sub>2</sub>	Dual gas-diffusion; One-compartm ent; limited by anode	3.6	1.13	Retained 46% output after 24 h continuous operation	<sup>69</sup>

Fructose/O<sub>2</sub> EFCs

Bioanode	Bio-/cathode	Note	$P_{\max}$ (mW $\text{cm}^{-2}$ )	OCV (V)	Stability	Ref.	
14	CP/CCG/FDH; DET; 500 mM fructose	CP/KB/ <i>Mv</i> BOD; DET; Air-breathing	DET-type EFC; One-compartment; limited by anode	2.6	0.79	n/a	<sup>70</sup>
15	CNTs/FDH; DET; 200 mM fructose	CNTs/Lac; DET; $\text{O}_2$ -saturated	One-compartment; limited by cathode	1.8	0.77	Retained 84% output after 24 h continuous operation	<sup>71</sup>
16	GCE/MWCNTs/PPy/FDH; DET; 100 mM fructose	GCE/MWCNTs/PPy/AB TS/Lac; MET; $\text{O}_2$ -saturated	One-compartment; limited by cathode	2.1	0.59	60% loss after 1 week operation	<sup>72</sup>
Formate/ $\text{O}_2$ EFCs							
Bioanode	Bio-/cathode	Note	$P_{\max}$ (mW $\text{cm}^{-2}$ )	OCV (V)	Stability	Ref.	
17	NG/AuNPs/FoDH; 5 mM $\text{NAD}^+$ and 50 mM formic acid	NG/AuNPs/Lac; MET; 0.5 mM ABTS	One-compartment; limited by cathode	1.96	0.95	Not directly measured	<sup>73</sup>
18	WPCC/KB/viologen-functionalized	WPCC/KB/ <i>Mv</i>	One-compartment	12	0.78	n/a	<sup>15</sup>

polymer/FoDH;  
MET;  
300 mM formate

BOD/ABTS;  
MET;  
O<sub>2</sub> diffusion electrode

ent;  
Thick  
electrode;  
limited by  
anode

Sucrose/O <sub>2</sub> EFCs							
Bioanode	Bio-/cathode	Note	P <sub>max</sub> (mW cm <sup>-2</sup> )	OCV (V)	Stability	Ref.	
19	Carbon felt/CNTs/TTF/GO <sub>x</sub> /FDH/MUT/INV ; MET; 50 mM sucrose	Carbon felt/CNTs/ABTS/BOD; MET; O <sub>2</sub> -saturated	Deep oxidation of sucrose	2.9	0.69	Bioanode displayed good stability for 0.5 h	<sup>74</sup>
Ethanol/O <sub>2</sub> EFCs							
Bioanode	Bio-/cathode	Note	P <sub>max</sub> (mW cm <sup>-2</sup> )	OCV (V)	Stability	Ref.	
20	MDB/AuNPs/gel/ADH; MET; 1 mM NAD <sup>+</sup> and 1 mM ethanol	AuNPs/gel/Lac; DET; Air-equilibrated	One-compartm ent	1.56	0.86	80% loss after 36 days	<sup>75</sup>
21	PAN nanofiber/Au/Super-P/ADH/NAD <sup>+</sup> /D I//VK <sub>3</sub> ;	PAN nanofiber/Au/Super-P/Lac/ ABTS;	Two-compartm ent; limited by cathode	1.6	0.99	Pronounced loss of NAD <sup>+</sup>	<sup>76</sup>



MET;  
~69 mM ethanol

MET;  
O<sub>2</sub>-saturated

---

Abbreviations: CF: Carbon fiber; GDH: glucose dehydrogenase; DI: diaphorase; VK<sub>3</sub>: vitamin K<sub>3</sub>; NADH: β-Nicotinamide adenine dinucleotide disodium salt (reduced form); BOD: bilirubin oxidase; ANQ: 2-amino- 1,4-naphthoquinone; Lac: laccase; MET: mediated electron transfer; MWCNTs: multi-walled carbon nanotubes; PEDOT: poly(3,4-ethylenedioxythiophene); Os-complex modified polymer(I): poly(*N*-vinylimidazole)-[Os(4,4'-dimethoxy-2,2'-bipyridine)<sub>2</sub>Cl]<sup>+2+</sup>; Os-complex modified polymer(II): poly(acryl  
5 amide)-poly(*N*-vinylimidazole)-[Os(4,4'-dichloro-2,2'-bipyridine)<sub>2</sub>]<sup>+2+</sup>; HPC: hierarchical porous carbon; AQ2S: anthraquinone-2-sulfonate; NQ-4-LPEI: naphthoquinone(NQ)-modified linear polyethyleneimine; CP: carbon paper; CNF: carbon nanofibers; WPCC: water proof carbon paper; KB: Ketjen black; CMC: compacted mesoporous carbon; P(N<sub>3</sub>MA-BA-GMA)-vio: poly(3-azido-propyl methacrylate-co-butyl acrylate-co-glycidyl methacrylate)-viologen; P(GMA-BA-PEGMA)-vio: poly(glycidyl methacrylate-co-butyl acrylate-co-poly(ethylene glycol) methacrylate)-viologen; CCG: carbon cryogel; CPPy: cellulose/polypyrrole composite; NG: nitrogen-doped graphene; FoDH: formate dehydrogenase; ABTS: 2,2'-azinobis(3-ethylbenzothiazoline-6-sulfonate);  
10 CNTs: carbon nanotubes; TTF: tetrathiafulvalene; GOx: glucose oxidase; FDH: fructose dehydrogenase; MUT: mutarotase; INV: invertase; MDB: Meldola's blue; AuNPs: gold nanoparticles; PAN: polyacrylonitrile.

Moreover, as a typical enzyme-catalyzed system, EFCs suffer from poor operational stability, resulting in short lifetimes and higher costs.<sup>77,78</sup> Instability arises not just with the enzyme, but also arises from the use of cofactors such as nicotinamide adenine dinucleotide (NAD<sup>+</sup>), adenosine triphosphate (ATP), and coenzyme A (CoA), which are necessary for many redox enzymes, and of other components that include mediators. The complexity of biological systems can pose additional detrimental effects on the stability of EFCs, such as biofouling of the electrode in implantable EFCs, or enzyme inhibition by O<sub>2</sub> for H<sub>2</sub>/O<sub>2</sub> EFCs. In contrast to relatively stable proton exchange membrane fuel cells and metal-based batteries that can last for years, or microbial fuel cells (MFCs) utilising self-reproducing microorganisms that can be reused for months, the majority of EFCs can operate only for hours or days<sup>79-81</sup>.

For almost all reported EFCs, the voltage at which usable power can be extracted is below the minimal requirement to power commercially available electronic devices. This drawback is inevitable as, from a thermodynamic point of view, the maximum redox potential gap between two electrodes in most biological fuel cells (e.g. ~1.18 V for glucose/O<sub>2</sub> EFCs with two-electron oxidation of glucose) is much less than that of lithium-based batteries (e.g. ~4.2 V)<sup>36</sup>. In many cases, the involvement of electron mediators leads to additional decreases in the voltage output of EFCs. In addition, the actual voltage output of EFCs is decreased by factors such as ohmic and concentration losses. Such losses can also depress the current output, and further reduce the overall power output.

Significant developments in EFCs have occurred since the first report in 1964. A number of reviews on EFCs have recently been published<sup>3,7,39,79,82-88</sup>, the majority of which have focused on either the electrode materials<sup>40,87-95</sup>, enzyme immobilization<sup>40,90,96-98</sup>, bioelectrocatalysis<sup>8,11,99-101</sup> or their applications<sup>39,40,45,47,86,88,102</sup>. **Table 2** summarizes a list of the reviews reported since 2015 on bioelectrodes and EFCs. This review identifies the main scientific challenges hindering the development of EFCs, low energy and power densities,

poor operational stability as well as limited voltage output, and summarizes the corresponding approaches to solve them.

**Table 2.** Reviews relevant to bioelectrodes and EFCs since 2015

Topic	Title	Year and ref.
Nanostructured materials	Wired Enzymes in Mesoporous Materials: A Benchmark for Fabricating Biofuel Cells	2015 <sup>103</sup>
	Graphene Based Enzymatic Bioelectrodes and Biofuel Cells	2015 <sup>93</sup>
	3D Graphene Biocatalysts for Development of Enzymatic Biofuel Cells: A Short Review	2015 <sup>104</sup>
	Tailoring Biointerfaces for Electrocatalysis	2016 <sup>105</sup>
	Magneto-Switchable Electrodes and Electrochemical Systems	2016 <sup>106</sup>
	Application of Carbon Fibers to Flexible Enzyme Electrodes	2016 <sup>81</sup>
	Paper Electrodes for Bioelectrochemistry: Biosensors and Biofuel Cells	2016 <sup>107</sup>
	An Overview of Dealloyed Nanoporous Gold in Bioelectrochemistry	2016 <sup>108</sup>
	Enzymatic Biofuel Cells on Porous Nanostructures	2016 <sup>92</sup>
	Conformational Changes of Enzymes and Aptamers Immobilized on Electrodes	2016 <sup>109</sup>
	Progress on Implantable Biofuel Cell: Nano-Carbon Functionalization for Enzyme Immobilization Enhancement	2016 <sup>40</sup>
	Enzymatic Reactions in Confined Environments	2016 <sup>110</sup>

---

Biomimetic and Bioinspired Approaches for Wiring 2016<sup>78</sup>  
Enzymes to Electrode Interfaces

Nanostructured Material-Based Biofuel Cells: 2017<sup>87</sup>  
Recent Advances and Future Prospects

Nanostructured Inorganic Materials at Work in 2017<sup>91</sup>  
Electrochemical Sensing and Biofuel Cells

Carbon Felt Based-Electrodes for Energy and 2017<sup>111</sup>  
Environmental Applications: A Review

Advanced Materials for Printed Wearable 2017<sup>112</sup>  
Electrochemical Devices: A Review

Recent Advance in Fabricating Monolithic 3D 2017<sup>95</sup>  
Porous Graphene and Their Applications in  
Biosensing and Biofuel Cells

Enzyme Immobilization on Nanoporous Gold: A 2017<sup>113</sup>  
Review

Recent Developments in High Surface Area 2017<sup>114</sup>  
Bioelectrodes for Enzymatic Fuel Cells

Graphene and Graphene Oxide: Functionalization 2018<sup>115</sup>  
and Nano-Bio-Catalytic System for Enzyme  
Immobilization and Biotechnological Perspective

Molecular Engineering of the Bio/Nano-Interface for 2018<sup>116</sup>  
Enzymatic Electrocatalysis in Fuel Cells

Buckypaper Bioelectrodes: Emerging Materials for 2018<sup>117</sup>  
Implantable and Wearable Biofuel Cells

Recent Applications of Bacteriophage-Based 2019<sup>118</sup>  
Electrodes: A Mini-Review

---

## Redox polymers

Current Trends in Redox Polymers for Energy and 2016<sup>119</sup>

---

Medicine

Redox Polymers in Bioelectrochemistry: Common 2017<sup>120</sup>

Playgrounds and Novel Concepts

---

Gas diffusion electrodes

Application of Gas Diffusion Electrodes in 2016<sup>121</sup>

Bioelectrochemical Syntheses and Energy

Conversion

Gas Diffusion Bioelectrodes 2017<sup>102</sup>

---

Enzyme engineering

The Use of Engineered Protein Materials in 2016<sup>122</sup>

Electrochemical Devices

---

Enzyme cascades

Oxidative Bioelectrocatalysis: From Natural 2016<sup>123</sup>

Metabolic Pathways to Synthetic Metabolons and

Minimal Enzyme Cascades

Enzyme Cascades in Biofuel Cells 2017<sup>124</sup>

---

Electron transfer

processes

Direct Enzymatic Bioelectrocatalysis: Differentiating 2017<sup>125</sup>

Between Myth and Reality

Mathematical Modeling of Nonlinear 2017<sup>126</sup>

Reaction-Diffusion Processes in Enzymatic Biofuel

Cells

Protein Bioelectronics: A Review of What We Do 2018<sup>127</sup>

and Do Not Know

Controlling Redox Enzyme Orientation at Planar 2018<sup>128</sup>

Electrodes

Electrochemistry of Surface-Confined Enzymes: 2018<sup>129</sup>

---

---

Inspiration, Insight and Opportunity for Sustainable  
Biotechnology

Direct Electron Transfer of Enzymes Facilitated by  
Cytochromes 2019<sup>130</sup>

---

Sugar oxidation

Direct Electron Transfer (DET) Mechanism of FAD  
Dependent Dehydrogenase Complexes ~From the  
Elucidation of Intra- and Inter-Molecular Electron  
Transfer Pathway to the Construction of Engineered  
DET Enzyme Complexes~ 2018<sup>131</sup>

Direct Electron Transfer of Dehydrogenases for  
Development of 3rd Generation Biosensors and  
Enzymatic Fuel Cells 2018<sup>132</sup>

---

Enzymatic oxidation of  
H<sub>2</sub>

Guiding Principles of Hydrogenase Catalysis  
Instigated and Clarified by Protein Film  
Electrochemistry 2016<sup>133</sup>

New Perspectives in Hydrogenase Direct  
Electrochemistry 2017<sup>134</sup>

---

Enzymatic reduction of  
O<sub>2</sub>

Recent Progress in Oxygen-Reducing Laccase  
Biocathodes for Enzymatic Biofuel Cells 2015<sup>99</sup>

Oxygen Electroreduction Versus  
Bioelectroreduction: Direct Electron Transfer  
Approach 2016<sup>135</sup>

Laccase: A Multi-Purpose Biocatalyst at the 2017<sup>136</sup>

---

---

	Forefront of Biotechnology	
	O <sub>2</sub> Reduction in Enzymatic Biofuel Cells	2017 <sup>137</sup>
	Application of Eukaryotic and Prokaryotic Laccases in Biosensor and Biofuel Cells: Recent Advances and Electrochemical Aspects	2018 <sup>138</sup>

---

Biocapacitor		
	Biocapacitor: A Novel Principle for Biosensors	2016 <sup>139</sup>
	Biosupercapacitors	2017 <sup>140</sup>

---

Microfluidic biofuel cells		
	Generating Electricity on Chips: Microfluidic Biofuel Cells in Perspective	2018 <sup>141</sup>

---

Implantable enzymatic fuel cells		
	Tear Based Bioelectronics	2016 <sup>142</sup>
	<i>Quo Vadis</i> , Implanted Fuel Cell?	2017 <sup>60</sup>
	Challenges for Successful Implantation of Biofuel Cells	2018 <sup>30</sup>
	Implantable Energy-Harvesting Devices	2018 <sup>143</sup>

---

Wearable enzymatic fuel cells		
	Wearable Biofuel Cells: A Review	2016 <sup>45</sup>
	Review-Wearable Biofuel Cells: Past, Present and Future	2017 <sup>47</sup>
	Wearable Bioelectronics: Enzyme-Based Body-Worn Electronic Devices	2018 <sup>144</sup>
	Biofuel Cells - Activation of Micro- and Macro-Electronic Devices	2018 <sup>44</sup>
	Wearable Biofuel Cells Based on the Classification	2019 <sup>145</sup>

---

---

of Enzyme for High Power Outputs and Lifetimes

---

Self-powered system

- Energy Harvesting from the Animal/Human Body for Self-Powered Electronics 2017<sup>146</sup>
- Recent Advances in the Construction of Biofuel Cells Based Self-Powered Electrochemical Biosensors: A Review 2018<sup>147</sup>
- Energy-Autonomous Biosensing Platform Using Supply-Sensing CMOS Integrated Sensor and Biofuel Cell for Next-Generation Healthcare Internet of Things 2018<sup>148</sup>
- Self-Powered Bioelectrochemical Devices 2018<sup>149</sup>
- Enzymatic Fuel Cells: Towards Self-Powered Implantable and Wearable Diagnostics 2018<sup>150</sup>
- Self-Powered Biosensors 2018<sup>151</sup>

---

Enzymatic fuel cells

- Enzymatic Biofuel Cells: 30 Years of Critical Advancements 2015<sup>4</sup>
- Recent Advances on Enzymatic Glucose/Oxygen and Hydrogen/Oxygen Biofuel Cells: Achievements and Limitations 2016<sup>8</sup>
- H<sub>2</sub>/O<sub>2</sub> Enzymatic Fuel Cells: From Proof-of-Concept to Powerful Devices 2017<sup>88</sup>
- Beyond the Hype Surrounding Biofuel Cells: What's the Future of Enzymatic Fuel Cells? 2018<sup>9</sup>
-



## 2. Strategies for achieving high energy density in EFCs

Like other types of fuel cells, the available energy density of an EFC is dependent on the product of the chemical energy stored in the fuel and the faradaic efficiency. The faradaic efficiency is described by:

$$\eta_F = \int I \times dt / (c_{\text{fuel}} \times V \times n \times F) \quad (1)$$

where  $\eta_F$  = faradaic efficiency,  $I$  = current,  $t$  = reaction time,  $c_{\text{fuel}}$  = concentration of fuel,  $V$  = reaction volume,  $n$  = number of electrons generated per fuel, and  $F$  = Faraday constant (96,485 C per mole). Clearly, it is desirable to combine high-energy-density fuels with high faradaic efficiencies to achieve high energy density EFCs.

### 2.1 Range of fuels in EFCs

EFCs harness power from living and renewable biological sources. Compared with traditional rare metal-catalyzed fuel cells that are predominantly powered by hydrogen or methanol, the fuel diversity of EFCs has been greatly broadened to many organic compounds which are common intermediates metabolized in living organisms or are the main components of biomass. Although a wide variety of fuels can be used for EFCs, their energy density, cost, availability, and toxicity all need to be considered.

Hydrogen has one of the highest energy density values per mass and has been widely used in traditional fuel cells. As a clean fuel that can be produced from biomass or water splitting, it can also be used in an EFC catalyzed by hydrogenases.<sup>16,88,152-154</sup> Storage and distribution of  $H_2$  have been the subject of intensive research, enabling the use of  $H_2$  in a safe manner. Alternatively, formic acid is a stable hydrogen carrier and has been used to power some EFCs due to its advantages of high volumetric capacity (53 g  $H_2$   $L^{-1}$ ), low toxicity and flammability under ambient conditions. Methanol is another promising alternative to hydrogen as a fuel because it is accessible and easy to transport and store, although it is toxic for human beings if ingested. It has a nearly 3-fold higher volumetric energy density than that of formic acid.

Furthermore, the theoretical maximum voltage for a methanol/oxygen fuel cell (1.19 V) is close to that for a H<sub>2</sub>/O<sub>2</sub> fuel cell (1.23 V)<sup>155</sup>. Although ethanol is rarely considered as a fuel source in fuel cells, it has some advantages, such as low cost, non-toxicity and wide availability. In addition, ethanol is a renewable energy source that can be generated through fermentation of agricultural products. As another prospective fuel, glycerol has many desirable qualities and is abundant since it is a by-product of biodiesel production. Properties such as low toxicity, low flammability, extremely low vapor pressure and high energy density make glycerol very appealing as an energy source<sup>156</sup>. Pyruvate, a key intermediate from the glycolysis pathway, has also been used as a fuel in EFCs<sup>157</sup>. Finally, it is noteworthy that the most commonly used fuels are sugars as they are inexpensive, abundant, renewable, and safe to use. They can be derived from lignocellulosic biomass (ca. 1×10<sup>11</sup> tons/year globally), which can be locally grown and are more evenly distributed than fossil fuels. Among various sugars, glucose is the most widely used fuel in EFCs, and glucose-based EFCs are particularly suited for implantable applications due to its presence in blood at reasonable concentrations (mM). Many other sugars including xylose, fructose, sucrose, and polysaccharides such as maltodextrin have also been used in EFCs<sup>56,158,159</sup>.

Full exploitation of the energy stored in a substrate can provide high energy densities, a key advantage of EFCs compared with commonly available batteries. Theoretically, glucose possesses an energy density of 4,125 Wh L<sup>-1</sup> releasing 24 electrons per glucose molecule to produce carbon dioxide and water. Hence, the complete enzymatic oxidation of the glucose units of a 15% maltodextrin solution indicates that the energy-storage density of the EFC can be as high as 596 Ah kg<sup>-1</sup>, which is an order of magnitude higher than that of lithium-ion batteries and primary batteries<sup>42</sup>. Glycerol has an even higher energy density (6,260 Wh L<sup>-1</sup>) compared to glucose, or to ethanol (5,442 Wh L<sup>-1</sup>), methanol (4,047 Wh L<sup>-1</sup>), making it a very attractive fuel. Notably, pyruvate also has a high energy density (4,594 Wh L<sup>-1</sup>), and requires fewer enzymes than glucose for complete oxidation.

## 2.2 Enzyme cascades for the deep/complete oxidation of fuels

When building an EFC, maximizing both energy density and power density is of crucial importance. The majority of EFCs utilizes a single enzyme to perform partial oxidation of a fuel (i.e. glucose, lactate, pyruvate or ethanol), but the complete oxidation of the majority of fuels requires several enzymes to use the energy available in the fuel<sup>82</sup>. As a relevant example, when the degree of catalytic oxidation as well as the maximum allowable fuel concentration are taken into account, the energy density of an ethanol fuel cell based on 20% v/v ethanol with incomplete oxidation to acetic acid decreases from 5,442 to 363 Wh L<sup>-1</sup><sup>156</sup>. Therefore, one of the key issues in developing high-energy-density EFCs is the successful design of multi-enzyme systems that can completely oxidize the fuel in order to increase the overall energy efficiency.

Living cells are able to completely oxidize complex fuels into carbon dioxide and water through the tricarboxylic acid (TCA) cycle, a crucial metabolic pathway<sup>160</sup>. In the cycle, acetyl-CoA is oxidized to carbon dioxide and water, generating the reduced forms of nicotinamide-adenine dinucleotide (NADH) and flavin adenine dinucleotide (FADH<sub>2</sub>) and chemical energy in the form of ATP. Several fuels can be fed into the TCA cycle, and each requires different sets of enzyme cascades. One of these fuels is glucose, which can be oxidized through the glycolysis pathway to pyruvate, which is subsequently oxidized to acetyl-CoA by pyruvate dehydrogenase. Lactate can also enter into the TCA cycle after dehydrogenation by lactate dehydrogenase (LDH). Ethanol has also been used as a substrate by introducing alcohol dehydrogenase (ADH), aldehyde dehydrogenase (AldDH), and S-acetyl CoA synthetase to oxidize ethanol into acetyl-CoA<sup>160</sup>. By mimicking the natural TCA pathway, several EFCs have been developed that can completely oxidize glucose, ethanol, pyruvate, and lactate. For instance, in an ethanol/O<sub>2</sub> EFC, dehydrogenases along with non-energy producing enzymes necessary for the cycle were immobilized in cascades onto a carbon electrode in a tetrabutylammonium bromide modified Nafion membrane, generating an 8.71-fold increase in power density compared to a single enzyme (ADH)-based ethanol/air

EFC<sup>161</sup>. In another mitochondria-based fuel cell consisting of all the enzymes involved in the TCA cycle, pyruvate was converted to acetyl-CoA by a pyruvate dehydrogenase and further oxidized by the enzyme cascade. A 4.6-fold increase in power density was observed when using intact mitochondria as compared to that using an individual enzyme in the TCA cycle<sup>162</sup>. It should be noted however that the increased power densities obtained in these systems<sup>161,162</sup> are still significantly lower than the theoretically expected values.

In addition to mimic the natural pathways, *in vitro* synthetic pathways to completely oxidize fuels have been described. The first EFC based on enzyme cascades that can completely transform alcohols was demonstrated in 1998<sup>155</sup>, where three NAD-dependent dehydrogenases including ADH, AldDH and formate dehydrogenase (FoDH) were employed to fully oxidize methanol to carbon dioxide and water (**Figure 3**). Six electrons per methanol molecule were collected at the bioanode when NADH was re-oxidized into NAD<sup>+</sup> with the assistance of redox mediators. However, this complete oxidation process relied on enzymes in solution rather than immobilized at the electrode surface. Later, Minteer et al.<sup>124</sup> conducted a series of studies of enzyme immobilization based on this pathway, including encapsulation within hydrophobically modified Nafion<sup>163</sup> and self-assembled enzymatic hydrogel<sup>164</sup>. An EFC based on the two-step oxidation of ethanol to acetate mediated by ADH and AldDH was described<sup>161</sup>.

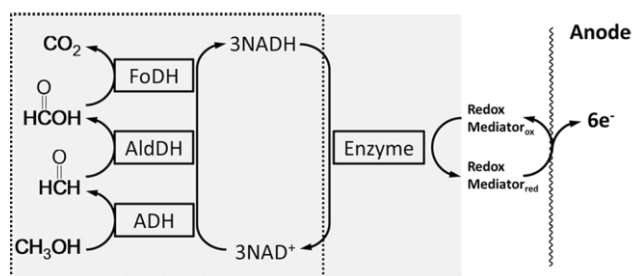


**Figure 3.** The oxidation of methanol to CO<sub>2</sub> is catalyzed by NAD-dependent alcohol-(ADH), aldehyde-(AldDH), and formate-dehydrogenases (FoDH) (shown within the box). Regeneration of NAD<sup>+</sup> is accomplished electro-enzymatically with an enzyme coupled to the anode via a redox mediator. Reprinted with permission<sup>155</sup> with modification. Copyright 1998 Elsevier.



**Figure 4.** Schematic diagram of the in vitro 15-enzyme pathway in the anode of the EFC that can completely oxidize sucrose, fructose, and glucose at the same time. Reprinted with permission<sup>167</sup>. Copyright 2018 Elsevier.

The majority of glucose-fed EFCs are based on one oxidoreductase (i.e., GOx or NAD-dependent glucose dehydrogenase (GDH)), generating only 2 of total 24 electrons per glucose<sup>52,168</sup>. In order to achieve more complete oxidation of glucose, Gorton et al. developed a highly efficient anode for glucose-based EFCs by combining pyranose dehydrogenase from *Agaricus meleagris* (AmPDH) and cellobiose dehydrogenase from *Myriococcum thermophilum* (MtCDH), resulting in up to six electrons being obtained by the oxidation of one glucose molecule<sup>169</sup>. Inspired by the metabolic pathways in living cells to fully oxidize glucose, Minter et al.<sup>170</sup> proposed a six-enzyme system at a bioanode to oxidize glucose to CO<sub>2</sub>. It was however difficult to confirm that the complete oxidation of glucose had occurred because CO<sub>2</sub> could be produced from intermediate reactions. Zhu et al.<sup>171</sup> designed a novel synthetic pathway containing two NAD-dependent dehydrogenases (i.e. glucose-6-phosphate dehydrogenase and 6-phosphogluconate dehydrogenase) to perform the oxidation of glucose, generating four electrons per molecule of glucose. The same authors designed a synthetic enzymatic pathway that was comprised of 13 enzymes in an air-breathing enzymatic fuel cell to completely oxidize the glucose units of maltodextrin and generate nearly 24 electrons per glucose unit<sup>42</sup>. Three functional modules were assembled to oxidize the substrate, transfer electron, and regenerate the intermediate. First, glucose units in maltodextrin were converted to glucose 6-phosphate (G6P) by the enzymes glucan phosphorylase and phosphoglucomutase. Next, during the two-step oxidation of G6P by glucose 6-phosphate dehydrogenase (G6PDH) and 6-phosphogluconate dehydrogenase (6PGDH), NAD<sup>+</sup> was simultaneously reduced to NADH, which was subsequently re-oxidized by diaphorase (DI), producing two electrons per NADH. Other enzymes were used to convert the 5-carbon intermediate to the 6-carbon G6P. The oxidation and regeneration steps were repeated six times in order to fully oxidize G6P, releasing 24 electrons. As a result, an EFC containing a 15% (wt/v) maltodextrin solution had

an energy-storage density of  $596 \text{ Ah kg}^{-1}$  and a faradaic efficiency of 92.3%. Nevertheless, this pathway utilized polysaccharides, such as maltodextrin and starch, and cannot be applied directly to glucose. Later, based on a combination of glycolysis and the pentose phosphate pathway, an *in vitro* synthetic enzymatic pathway was demonstrated to generate close to the theoretically available yield of electrons from glucose. This pathway does not involve ATP, CoA, or membrane proteins. The reaction rate was enhanced after replacing several enzymatic building blocks and introducing a new enzyme, 6-phosphogluconolactonase. Using this new pathway, a high faradaic efficiency of 98.8% was obtained, with a maximum current density of  $6.8 \text{ mA cm}^{-2}$ . Similarly, an *in vitro* 15-enzyme pathway that can co-utilize glucose, sucrose and fructose in EFCs was designed by incorporating the corresponding enzymes in the sugar conversion module. G6P was obtained after several sugar phosphorylation steps and then entered into the oxidation and regeneration modules as described above. The EFC achieved a faradaic efficiency of approximately 95% for these three sugars and yielded a maximum power density of  $1.08 \text{ mW cm}^{-2}$  (**Figure 4**)<sup>167</sup>. This work was the first to demonstrate the use of sugar mixtures as the fuel in EFCs and the achievement of close to the theoretically available energy density. In addition to the hexose fuels mentioned above, xylose as the second largest mono-saccharide and the most abundant pentose in plant biomass, is also a promising sugar fuel. Recently, a reconstituted bacterial pentose phosphate pathway *in vitro* was confirmed to generate a nearly theoretical yield of electricity from xylose in EFCs for the first time<sup>172</sup>. The complete oxidation of xylose can pave the way for the co-utilization of hexose and pentose in biomass and is a promising method for the production of bioresource-derived electricity<sup>172</sup>.

However, the use of enzyme cascades introduces a number of challenges such as increased complexity. The overall stability of an EFC is limited by the enzyme that possesses the lowest stability (e.g., as low as several hours at room temperature). The operation of EFCs can be compromised since specific enzymes have various optimal temperatures and pHs<sup>42</sup>. The amount of each immobilized enzyme on the surface of electrodes is limited with a fixed

number of anchoring points to host the enzymes. Electrode fouling together with enzyme or cofactor degradation is an additional concern in such systems. Therefore, it makes sense to precisely localize enzymes in a sequential manner to increase the overall flux<sup>173</sup>. Enzyme complexes or in vitro metabolons, facilitating the transfer of intermediates between enzymatic steps, have been constructed as an efficient approach to accelerate cascade reactions<sup>174</sup>. Liu et al.<sup>175</sup> synthesized an enzyme complex by covalently modifying hexokinase (HK) and G6PDH with a poly(Lys) bridge. The enzyme complex was synthetically cross-linked and able to facilitate electrostatic substrate channeling by shortening the lag time required to reach steady state. Another work reported the assembly of an ADH and AldDH enzyme cascade-based bioanode via a protein purification-free approach in a methanol biofuel cell. By using a designed DNA duplex sequence, substrate channeling between active sites of cascade enzymes was observed and the power density of the biofuel cell increased by 73%<sup>176</sup>. In addition, enzyme complex or metabolon based EFCs have also been considered as a promising alternative to obtain significantly improvement in faradaic efficiency and stability<sup>177</sup>. To understand the mechanisms involved in such cascade reactions, differential electrochemical mass spectrometry could be used to provide relevant information on the products formed at each step<sup>178</sup>.

### **3. Strategies for increasing power density in EFCs**

#### **3.1 Evaluation of different power output results**

The power output of EFCs is a vital criterion to determine which applications can actually be considered. In practice, the polarization curve (voltage-current profile) and the corresponding power output profile can be obtained using four methods<sup>179</sup>: i) discharge the EFC at specified resistances by connecting the EFC to a resistor and measuring a series of currents and voltages obtained on varying the resistance; ii) potentiodynamic discharge: record the response (voltage-current plots) at a relatively slow sweep rate (typically no more than 1 mV s<sup>-1</sup>); iii) potentiostatic discharge: apply various discharge voltages and record the currents generated; iv)



galvanostatic discharge: discharge the EFC at various currents and record the associated voltages. Accordingly, the operational stability of an EFC can also be monitored over time using these four methods. Methods i), iii) and iv) are most convenient and the most frequently used for long-term testing.

One of the issues concerned with the evaluation of the performance of EFCs is the definition of their power output. The power output is generally reported as the power density, as is widely used with batteries and other fuel cells. However, arbitrary comparison between power densities reported in the literature can be misleading in EFCs due to significant variations in the type of electrode material, method of enzyme immobilization, enzyme loading, etc.).

The majority of reports on power densities in the literature are based on the projected geometric surface area of the electrodes (**Table 1**)<sup>11</sup>. However, such reported power densities do not consider the morphology of the electrode materials nor the loading of immobilized biocatalysts. In the last decade, porous nanostructured materials with high conductivities have been employed as electrodes, due to their large hierarchical porosity, and high surface areas<sup>92</sup>. The power density of EFCs based on porous nanostructured materials increased from  $\mu\text{W cm}^{-2}$  to  $\text{mW cm}^{-2}$ , calculated according to the geometric areas of the electrodes (**Table 1**)<sup>43,62,180,181</sup>. Nonetheless, these values cannot accurately represent the real power densities as due to the high porosity of the electrodes, the real surface areas are much larger than the geometric areas. Just to give one example, a compressed multi-walled carbon nanotube (MWCNT)-based bioelectrode used in a glucose EFC exhibited an electroactive area of  $52 \text{ cm}^2$  for an interfacial geometrical area of  $1.3 \text{ cm}^2$ , which corresponds to 0.01% of its BET surface area<sup>59</sup>. Moreover, calculation of the power density is dependent on the method used to determine the electroactive surfaces area. The electroactive surface area based on capacitance measurements is more accurate than that obtained from voltametric response of redox molecule probes<sup>126</sup>. Additionally, in the case of an EFC utilizing a bioanode and a biocathode with different surface areas, the geometric surface area of the rate-limiting bioelectrode is

commonly used to calculate the power density. For example, a H<sub>2</sub>/O<sub>2</sub> EFC requires a bilirubin oxidase (BOD)-modified cathode with an area of 6 cm<sup>2</sup> to match the output of a 1.2 cm<sup>2</sup> hydrogenase (Hase)-modified anode<sup>182</sup>. Therefore, balancing of the catalytic performance of a cell requires consideration of the appropriate sizes of the electrodes.

The weight or the volume of an EFC is another critical parameter in the evaluation of performance. The specific power can be determined in mW g<sup>-1</sup> or mW cm<sup>-3</sup>, and is particularly suitable for three-dimension structured electrodes<sup>9,183</sup>. In terms of potential applications for portable power sources, the power density normalized to the overall weight is important, although few reports providing these values<sup>59</sup>. As a simple example, a net power of 10-20 W is required to power a laptop<sup>184</sup>, and a high-power-density-per-gram will help to reduce the weight. For an implantable EFC, the volumetric power density is the most important parameter (more detailed discussion is in Section 3.4). The power output of EFCs needs to be described in a manner that enables direct comparison between different systems<sup>59,185</sup>. The expression of power density in multiple forms is therefore recommended. For example, the power output of an EFC based on the naphthoquinone-mediated oxidation of glucose in a CNT 3D matrix was expressed in mW cm<sup>-2</sup>, mW mL<sup>-1</sup> and mW g<sup>-1</sup> simultaneously<sup>41</sup>. The same approach was used for a membrane- and mediator-free glucose/O<sub>2</sub> EFC utilizing novel graphene/single-wall carbon nanotube co-gel electrodes<sup>186</sup>. Reporting the data in this format makes it feasible to compare results in an effective manner.

The number of enzyme molecules involved in the biocatalytic process is an additional key factor for the evaluation and comparison of the performance of bioelectrodes. It is thus necessary to report enzyme loadings applied on the electrode and to estimate the amount of electroactive enzymes. However, this determination is not obvious, and relies on the determination of the non-catalytic signals of enzymes obtained under non-turn-over conditions. Although this information has often been reported for Lac<sup>187,188</sup> or BOD<sup>189,190</sup>, it has only once been reported for hydrogenase<sup>67</sup>. Low enzyme coverage can render such a determination difficult. Even when

obtained, it is necessary to ensure that the species involved in the baseline signal appearance are identical to those involved in the catalytic measurements. This last condition is only rarely satisfied, however, leading to misleading values. The work from Mazurenko et al., should be noted where the authors rigorously followed the evolution of the non-catalytic signals related to the FeS clusters of the *AaHase* with the decrease of the catalytic signal for H<sub>2</sub> oxidation, allowing the accurate determination of the amount of enzyme involved in the catalytic process<sup>67</sup>. In addition, it is essential to consider the fuel concentration when comparing the power density (**Table 1**).

Besides the above-mentioned factors that influence power output, an analysis of the reaction occurring in each compartment of an EFC should be carefully made. A typical bioelectrocatalytic reaction is comprised of i) mass transport of the reactant from the bulk solution to the active site on the solid surface, ii) enzymatic reaction with the reactant, iii) electron transfer between active sites of the enzyme and the electrode, and iv) diffusion of the products into the solution from the solid-liquid interface (**Figure 5**)<sup>77</sup>. The identification and enhancement of the current density of the limiting bioelectrode in a given system with fixed electrode geometries, either the bioanode or biocathode with the lower net catalytic current density, are crucial<sup>77,191</sup>. In the following sections, we will discuss the general strategies to increase the current density of a single bioelectrode using fast rates of ET<sup>80</sup>, in addition to mass transport issues and cell configuration design.

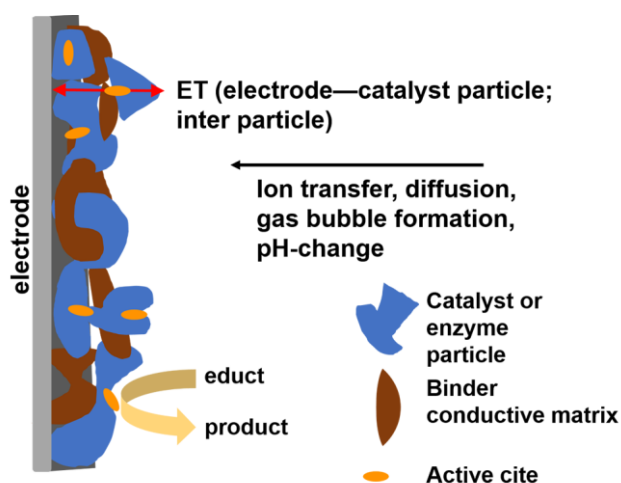


**Figure 5.** Schematic drawing of a typical electrocatalysis reaction using enzymatic or inorganic catalysts highlighting key reaction steps. Reprinted with permission <sup>77</sup>. Copyright 2018 Elsevier.

### 3.2 Increasing intrinsic enzyme activities

The catalytic response of enzymes in solution is generally characterized by the Michaelis-Menten equation <sup>192</sup>:

$$V = \frac{V_{max}[S]}{K_M + [S]} \quad (2)$$

where  $V$  is the rate of reaction,  $V_{max}$  the maximum rate of reaction,  $K_M$  the Michaelis constant (the substrate concentration at which  $V$  is equal to  $V_{max}/2$ ). The turnover frequency,  $k_{cat}$  is defined as:

$$k_{cat} = \frac{V_{max}}{[E]_o} \quad (3)$$

where  $[E]_o$  is the enzyme concentration. These kinetic parameters can be obtained by assaying the enzyme activity <sup>193</sup>. Enzyme activity is widely used as an indicator to compare the biocatalytic efficiency of a single enzyme using various substrates and of different enzymes for the same substrate <sup>194</sup>. The ratio  $k_{cat}/K_M$  is independent of the concentration of enzyme and substrate. One international unit (U) of an enzyme is defined as the amount of enzyme that catalyzes the conversion of 1  $\mu\text{mol}$  of reactant per min <sup>195</sup>. Accordingly, specific enzyme activity (in  $\text{U mg}^{-1}$  or  $\text{U g}^{-1}$ ) represents the number of units of enzyme per mg or g of protein. Actual enzyme activity after long-term storage of enzymes should be reported. It should be noted that these activities are defined based on their optimal conditions that may not be the same as the condition of running a specific EFC. In EFCs, attention needs to focus on the enzyme activity at the electrode interface. In many cases involving enzyme immobilization, the actual activity of immobilized enzyme may be not as high as predicted due to enzyme deactivation and mass transfer barriers. It is necessary to consider the number of enzymes per electrode or per cell in order to appropriately compare the performance of different EFC systems.

Naturally occurring enzymes may not possess sufficiently high activities that are required for EFCs. Therefore, substantial efforts have been made on enzyme engineering to improve the

catalytic activities and rates of electron transfer<sup>196</sup>. Here, we focus on discussing the engineering on GOx, one of the most widely used enzymes in bioelectrodes, to demonstrate general strategies including direct and random site mutagenesis as well as enzyme de-glycosylation that can be used to improve the current density. Schwaneberg et al. employed directed protein evolution in *Saccharomyces cerevisiae* to screen libraries of mutants. They found a GOx mutant (I115V), close to the FAD centre, with 1.4-1.5 times higher activity for glucose oxidation<sup>197</sup>. A similar approach led to a double mutant GOx (T30S and I94V) that displayed an increased  $k_{cat}/K_M$ <sup>198</sup>. Altering expression strains is an additional route to altering the properties of enzymes. On replacing native GOx from *Aspergillus niger* with *Penicillium pinophilum* GOx at an Os-complex modified polymer “wired” bioanode, Mano et al. reported an EFC showing an increase in power density from 90 to 280  $\mu\text{W cm}^{-2}$ <sup>199</sup>. This increase was induced by the lower  $K_M$  (6.2 mM) of *PpGOx* compared to that of *AnGOx* (20 mM), resulting in a bioanode with higher catalytic current in the presence of only 5 mM glucose. A recombinant GOx from *Penicillium amagasakiense* has been overexpressed in a secreted active form displaying a  $k_{cat}/K_M$  in homogeneous glucose solution of  $155 \text{ mM}^{-1} \text{ s}^{-1}$ , which was much higher than that of a *AnGOx* ( $38 \text{ mM}^{-1} \text{ s}^{-1}$ )<sup>200</sup>. Using ferrocene-methanol as a mediator, the electrocatalytic current observed towards glucose oxidation was two-fold higher with the recombinant GOx than with a native one<sup>200</sup>. De-glycosylated GOx in combination with an Os-polymer mediator showed an 18% increase in current density, which is likely a consequence of the shortened distance between the active site of the enzyme and the redox mediator, as well as improved mediator utilization due to the decreased molecular size after de-glycosylation<sup>201</sup>.

### 3.3 Facilitating electron transfer

The rate of ET plays an important role in determining the power output of many EFCs. According to Marcus’s theory, the reorganization energy and the distance between the donor and the acceptor determine the rate of ET<sup>202</sup>, which decreases by an order of magnitude for every 2.3 Å increase in distance<sup>203</sup>. An upper threshold of 15 Å is thus required for efficient direct electron transfer (DET)<sup>204</sup>. The structure and conformation of the enzyme may present a cofactor in close

proximity to the electrode to maximize the rate of ET<sup>205</sup>, so that the current density of the bioelectrode can be enhanced. However, many cofactors and active sites reside inside insulating protein shells, introducing barriers to effective rates of long distance ET. In this section, we start with introducing several important equations and theories of ET. A summary of the common DET-capable enzymes along with the brief description of their structural features is followed. We then discuss strategies, such as electrode surface modification for suitable enzyme orientation and enzyme engineering, to bring the enzyme cofactor closer to the electrode surface to facilitate DET for high-current-density bioelectrodes. The difference between DET and MET- based bioelectrodes will be briefly discussed, while MET will be further detailed in Section 5.1 when discussing the EFC voltage.

Protein film voltammetric techniques (PFV) can be used to characterise redox enzymes in detail<sup>206,207</sup>. It describes the noncatalytic situation of DET-capable enzymes that are in (sub-)/monolayer configuration displaying the cofactors based well-defined voltammetry on the electrode surface. The empirical Butler-Volmer equations reveal that interfacial ET rates exponentially increase with the activation potential (driving force)<sup>208</sup>. Convenient forms of the Butler-Volmer expression describing the electrochemical rate constants for a reversible redox reaction ( $k_{red}$  and  $k_{oxi}$ ) of a one-electron couple are:

$$k_{red} = k^0 \exp\left(-\frac{\alpha n F \eta}{RT}\right) \quad (4)$$

$$k_{oxi} = k^0 \exp\left(-\frac{(1-\alpha) n F \eta}{RT}\right) \quad (5)$$

where  $k^0$  is the standard first-order electrochemical rate constant,  $\alpha$  is the electron-transfer coefficient,  $\eta$  the activation potential, R the gas constant and T is the absolute temperature.  $k^0$  can be determined by Laviron's method by plotting the voltammetric peak potential versus the logarithm of the scan rate<sup>209</sup>.

Marcus theory describes the relationship between  $k^0$  and the tunnelling distance  $d$ , which is the distance between the electrode surface to the electron's entry/leaving point in the

DET-capable enzyme<sup>208</sup>:

$$k^0(d) \propto \exp(-\beta d) \quad (6)$$

where  $\beta$  is a decay constant. A dispersion of tunneling distances (i.e. various enzyme orientations) leads to a dispersion of values of  $k^0$ . The mathematic model developed by Léger et al. can describe the distribution of DET-capable enzyme orientations<sup>208,210</sup>.

The surface coverage ( $\Gamma$ ) of (sub-)/monolayered DET-active enzymes can be evaluated from the voltammetric peak current ( $I_p$ ) obtained for the oxidation/reduction of the co-factor under non-turnover conditions, which is proportional to the enzyme concentration:

$$I_p = \frac{n^2 F^2 v A \Gamma}{4RT} \quad (7)$$

where  $v$  is the scan rate of the voltammetric method and  $A$  is the surface area.

$\Gamma$  is equivalent to  $[E]_0$  in eq. 3, assuming that all of the electrochemical-addressable enzymes are involved in the catalytic reaction.  $k_{cat}$  can be obtained using the saturated electrocatalytic current ( $I_{cat}^{sat}$ )<sup>211</sup>:

$$k_{cat} = \frac{I_{cat}^{sat}}{Fn\Gamma A} \quad (8)$$

The electrochemical form of the Michaelis-Menten equation is<sup>206</sup>:

$$I_{cat} = \frac{nFA\Gamma k_{cat}[S]}{[S] + K_M} \quad (9)$$

When the bioelectrode is studied further using rotating-disc voltammetry (RDV), the limiting current ( $I_L$ ) of the bioelectrocatalytic current can be described by the Koutecky-Levich approximation:

$$\frac{1}{I_L} = \frac{1}{I_{cat}} + \frac{1}{I_{Lev}} + \frac{1}{I_E} \quad (10)$$

where  $I_{cat}$  describes the intrinsic catalytic current of the enzyme, defined by eq.9;  $I_{Lev}$  which is described by the Levich equation, is dependent on the rate of rotation and is limited by substrate diffusion between the enzyme and bulk solution<sup>206</sup>;  $I_E$  is determined by the Butler-Volmer equation (eq.4 and 5) describing the rate of interfacial electron transfer between the electrode and the enzyme. For a first order reaction,

$$|I_E| = nFA\Gamma k_E \quad (11)$$

where  $k_E$  is the heterogeneous electron transfer rate constant (i.e. either  $k_{\text{red}}$  in eq.4 or  $k_{\text{oxi}}$  in eq.5).

Detailed consideration of the 3D structure of a protein is essential to rationalize the electrode surface functionalization for a preferred DET<sup>128</sup>. X-ray crystallographic structures of many enzymes are available, and cryo-electron microscopy has the potential to significantly expand the number of structures and in particular of larger enzymes and enzyme complexes<sup>212</sup>. There has been much debate on considering ET via electronic relays within an enzyme subunit as a DET process<sup>213</sup>. As an illustration, electrons generated upon H<sub>2</sub> oxidation at the NiFe active site located in the large subunit of an hydrogenase travel through three FeS clusters in the small subunit of the protein<sup>24</sup>. Another relevant example is CDH in which the heme domain acts as the electronic relay<sup>132</sup>. In this review, ET between the electrode and the catalytic center of an enzyme via a built-in redox relay is regarded as DET (**Figure 6B**)<sup>125</sup>. These redox relays are present in a range of sugar oxidizing enzymes used at the bioanode. CDH is a flavocytochrome composed of a catalytically active flavodehydrogenase domain and a cytochrome domain acting as a built-in ET relay (**Figure 6C**)<sup>214,215</sup>. Another relevant example is FDH, a flavohemoprotein with three subunits<sup>216,217</sup>: subunit I with covalently bound FAD showing a pH-dependent formal redox potential, E<sup>o'</sup>, of -0.034 V vs. SHE at pH 5.5 for catalytic oxidation of D-fructose; subunit II containing three heme c moieties with E<sup>o'</sup> of 0.135, 0.251 and 0.537 V at pH 5.5, the heme with the lowest E<sup>o'</sup> suggested to be the exit site for ET pathway<sup>218</sup>; and subunit III, whose function is still unclear and does not carry any redox centers. Bacterial derived, hetero-oligomeric FAD-dependent GDH (FAD-GDH) consisting of a FAD based catalytic subunit, a small chaperone subunit and a multi-haem ET subunit<sup>219</sup>, is also capable of DET. A [3Fe-4S] cluster has been identified in this FAD-GDH type, acting as a ET bridge between FAD and the multi-heme cytochrome c subunit<sup>220</sup>. Quinohaemoprotein-type PQQ-dependent enzymes (e.g. GDH<sup>221,222</sup>, ADH<sup>223</sup> and LDH<sup>224</sup>) contain PQQ prosthetic group coordinated with the apoenzyme with Ca<sup>2+</sup> and heme-c moieties performing as ET relay<sup>225</sup>. As demonstrated by Sode et al., enzyme fusion can be employed to promote DET by introducing a cytochrome domain to the



catalytic domain of non-quinohemoprotein-type PQQ-GDH<sup>226</sup> and fungi-derived FAD-GDH<sup>227</sup>, suggesting a powerful strategy that can be expanded to a wide range of DET-capable fusion enzymes. The use of built-in redox relay is also the case with H<sub>2</sub> oxidizing enzymes. [NiFe]-hydrogenases catalyzing H<sub>2</sub> oxidation possess a [NiFe] catalytic site accompanied with Fe-S clusters distant less than 10 Å to facilitate intra- then intermolecular ET between the catalytic site and either c-type or the b-type cytochromes (**Figure 6D**)<sup>88,228,229</sup>. On the cathodic side, the copper site T1 of multicopper oxidases (MCOs) is the site where the natural substrate binds. It is located near the shell of the enzyme allowing ET with the electrode surface. O<sub>2</sub> is reduced to H<sub>2</sub>O with four electrons transferred over a short distance (13 Å) at the combined T2/T3 (binuclear) trinuclear cluster (TNC) (**Figure 6A**)<sup>11,230</sup>. Immobilization of the enzyme with the electronic relay facing the electrode is necessary for efficient DET to occur. Suitable electrode surfaces are crucial for appropriate enzyme orientation to ensure favorable rates of DET<sup>21,154,231-235</sup>. In this electrode-protein recognition for DET, electrostatic and hydrophobic interactions are mainly involved. In case of electrostatic driven orientation, the distribution of charges on the protein surfaces was proved to be essential for DET<sup>236</sup>. The calculation of the protein dipole moment is thus highly informative in describing favorable enzyme orientations at a charged electrode surface<sup>234,237</sup>.

Analysis of the shape of the electrochemical signal, especially using cyclic voltammetry, allows an estimation of the distribution of orientation of the enzymes on the electrode<sup>208,236</sup>. In situ surface techniques can provide additional information about any modification in enzyme orientation or conformation after immobilization on conductive supports. Furthermore, the support material (usually made of gold) used in these techniques can simultaneously act as the electrode and makes it possible to quantify any change of the enzyme conformation and orientation under turnover as a function of applied potential, concentration of substrate, temperature, time etc.<sup>128,129</sup> Ellipsometry can be used to examine the dielectric properties of thin films, and can provide details of the thickness of the enzyme layer. In situ ellipsometry measurements emphasized that MCOs immobilized on bare gold tend to adopt a flattened

conformation explaining their deactivation<sup>238</sup>. The same technique showed that monolayers of *MvBOD* were formed irrespective of composition of the self-assembled-monolayer used for gold modification, although significantly different catalytic signals were recorded. Such a result is indicative of different orientations of the enzyme, which was confirmed by the electrochemical response.<sup>239</sup> Surface plasmon resonance and quartz-crystal microbalance (QCM) can be used to quantify the total amount of enzyme immobilized on the electrode, and the variation of this quantity under turnover and as a function of the local environment<sup>240</sup>. Correlation with the electrochemical response can allow the determination of the proportion of DET-oriented enzymes<sup>234</sup>. QCM with dissipation (QCM-D) provides additional information on the viscoelasticity of the deposited element. Using QCM-D, loss of activity of *MvBOD* was demonstrated to be related to change in enzyme hydration rather than enzyme desorption<sup>241</sup>. ATR-Fourier-transform infrared (FTIR) spectroscopy is a powerful in situ method which has been used to study changes in the secondary structures of immobilized enzymes. In the case of BODs<sup>239</sup>, or hydrogenases<sup>242</sup>, the conservation of the intensity of the amide I and II bands, fingerprints of the polypeptide backbone, proved that the enzyme's secondary structure was maintained upon immobilization. Alternatively, surface enhanced resonance Raman (SERR) and surface enhanced IR absorption (SEIRA) are sensitive methods to monitor enzyme orientation in the immobilized state. Using SERRS on Lac immobilized on gold nanoparticles, Shleev et al. demonstrated that ET occurred via a pathway through the trinuclear cluster instead of Cu T1<sup>243</sup>. Heidary et al. were able to correlate enzymatic oxidation of H<sub>2</sub> to the orientation of a hydrogenase on SAMs<sup>244</sup>. Utilizing the surface selection rules, polarization modulation-infrared reflection-adsorption spectroscopy (PM-IRRAS) was successfully used to differentiate hydrogenase orientation as a function of the hydrophobicity of the electrode<sup>242</sup>. Angles of 25° and 40° between the normal to the electrode surface and the  $\alpha$ -helix as a main component of the enzyme, were found on negatively charged and hydrophobic SAMs, respectively. Different enzyme orientation could be correlated with the rate of enzymatic oxidation of H<sub>2</sub>. A similar study was conducted on Lac<sup>245,246</sup>, demonstrating that the orientation of beta-sheet moieties controlled the rate of catalysis. Finally, in situ microscopies (atomic force microscopy (AFM),

scanning tunneling microscopy (STM)) can be used to indicate the location of an enzyme and to also provide conformational information. Studies carried out by Ulstrup's group on nitrate reductase<sup>247</sup> and De Lacey's group on hydrogenases<sup>248</sup> and ATP synthase<sup>249</sup> are particularly relevant. For example, using in situ high-speed AFM, the dynamic motion of the dehydrogenase-cytochrome interdomain of CDH occurred only in the presence of the substrate, paving the way for improved understanding of the mechanism of catalysis<sup>250</sup>.

This in-depth knowledge acquired thanks to structure examination and in situ coupled techniques guide further enzyme or electrode modifications for enhanced ET rate. Different strategies have been reported in the literature. For example, a comprehensive study was reported for the immobilization of *Mv*BOD and *Bp*BOD on CNTs bearing different surface charges<sup>236</sup>. The respective surface charges and dipole moments of both BODs were shown to determine the optimal electrostatic interactions between enzymes and CNT surfaces for efficient DET. Surface bearing polyaromatic hydrocarbons that mimics the natural substrates of MCOs (e.g. bilirubin for BOD<sup>70,251</sup>) were able to orient the enzymes with the appropriate configuration minimizing the distance towards the T1 site<sup>252-254</sup>. When bilirubin was adsorbed on a carbon black based electrode for BOD immobilization, the standard ET rate constant increased by a factor of 3 with a maximum current density of 5 mA cm<sup>-2</sup><sup>70</sup>. Coupled with a FDH based bioanode, the fructose/O<sub>2</sub> EFC exhibited a considerable maximal power density ( $P_{\max}$ ) of 2.6 mW cm<sup>-2</sup>. After introduction of pyrenebutyric acid functional groups onto the electrode, the DET current density of a BOD electrode showed ca. 6-fold enhancement over randomly adsorbed system<sup>254</sup>. Some other relevant examples include, electrode surfaces functionalized with 2-carboxy-6-naphtoyl and 4-aminoaryl diazonium salt to favor DET of *Mv*BOD and *Trametes hirsuta* Lac (*Th*Lac), respectively, due to their different binding conditions surrounding Cu T1 pockets<sup>255,256</sup>. In particular, naphthoate-modified MWCNTs functionalized by electrografting induce favorable orientation of *Magnaporthe oryzae* BOD (*Mo*BOD) that can surpass *Mv*BOD in terms of both current densities and minimal overpotentials.<sup>256</sup> Otherwise, hydrophobic interactions have been widely used to enhance DET of Lac taking advantage of its hydrophobic pocket<sup>181,257,258</sup>,

achieving excellent maximum current densities several ( $\text{mA cm}^{-2}$ ) towards oxygen reduction at pH 5. For example, the efficient immobilization and orientation of *Trametes versicolor* Lac (TvLac) on MWCNT electrodes using adamantane-pyrene derivative, confirmed by electrochemistry, theoretical calculations and quartz crystal microbalance experiments led to maximum current densities of  $2.4 \text{ mA cm}^{-2}$ .<sup>259</sup>

Besides electrode surface functionalization, enzyme engineering faces a growing interest for specific enzyme wiring for enhanced ET. *Trametes sp.* Lac was designed with a single pyrene group close to the T1 Cu site<sup>260</sup>. Specific interaction via  $\pi$ -stacking with CNT sidewalls and host-guest interaction with  $\beta$ -cyclodextrin, enabled a shortened ET route to the electrode, resulting in high catalytic current densities with a 4.2 fold increase over that obtained with unmodified Lac<sup>260</sup>. One very recent strategy relies on the incorporation of noncanonical amino acids into designed sites of the target enzyme<sup>261,262</sup>. The great advantage is the possibility to graft specific functions at a desired location on the protein. Click chemistry was employed to form a covalent linkage between the alkyne moiety and the electrode surface. The anchoring position on the enzyme and the linker length can be tuned to understand the mechanism of DET<sup>262</sup>. Site-directed mutagenesis was used with CDH to enable highly site-specific immobilization via introduced cysteine residues on the protein surface and surface-grafted maleimide groups<sup>263</sup>. Covalent binding of the variants close to the heme cofactor showed 60-80% higher DET current over the physical adsorption approach due to improved enzyme orientation<sup>263</sup>. Although not widely applied but of interest, deglycosylated enzymes permit DET due to their decreased molecular weight/size and thus shortened distances for ET<sup>264</sup>. Mano et al. reported a deglycosylated *AnGOx* which preserved its activity with the direct redox reaction of FAD occurring at  $-0.687 \text{ V vs. SHE}$ <sup>265</sup>. PDH carries covalently bound FAD as the cofactor and its deglycosylated form undergoes DET on a graphite electrode<sup>266</sup>.

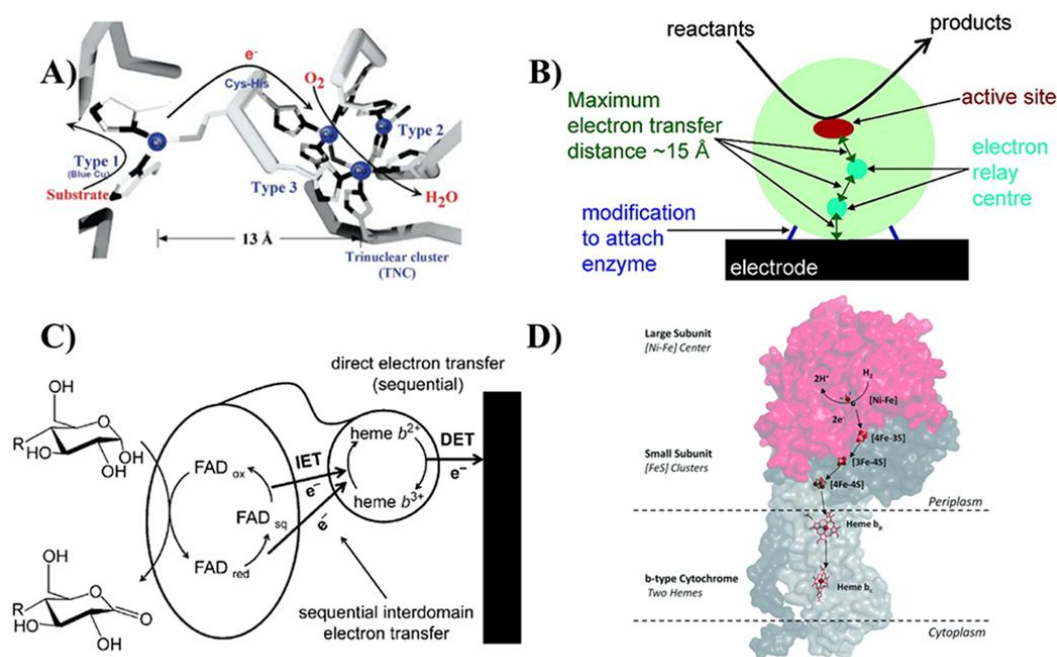


**Figure 6.** (A) Schematic drawing of the flow of electrons at the active site of MCOs. Reprinted with permission <sup>231</sup>. Copyright 2018 Royal Society of Chemistry. (B) Schematic drawing shows a DET capable enzyme with multi-redox centres immobilized on an electrode surface. Reprinted with permission <sup>7</sup>. Copyright 2018 American Chemical Society. (C) Schematic drawing of direct electron transfer from an aldehyde via CDH to an electrode surface. Reprinted with permission <sup>214</sup>. Copyright 2018 Wiley. (D) 3D structure of a membrane-bound [NiFe]-hydrogenase showing the electron pathway involved during physiological DET. Reprinted with permission <sup>88</sup>. Copyright 2018 Royal Society of Chemistry.

Many enzymes that have been identified for use in EFCs cannot be wired in an optimal manner, however, either because the structure is not known to a sufficiently high resolution so that the parameters for an orientation favouring DET are unknown, or because the active site is isolated from the surface by glycosylation or the presence of detergents in the case of membrane enzymes. It is noteworthy for example that native GOx cannot undergo DET at CNT or graphene based electrode <sup>267-269</sup>, as it is heavily glycosylated with an FAD group that is too deeply buried (at least 1.7 nm from the surface of the protein <sup>267</sup>) to allow direct ET. Small redox molecules can serve as exogenous mediators to shuttle the electrons via MET <sup>79</sup>. Redox mediators, which undergo reversible redox reaction, can be physiological redox partners such as cytochromes or ferredoxins, or artificial molecules including ferrocene derivatives, ferricyanide, conducting organic salts (for example, tetrathiafulvalene (TTF)<sup>74</sup> and mixed-valence viologen salt<sup>270</sup>, etc.), quinone

compounds, transition-metal complexes, phenothiazine and phenoxazine compounds<sup>205</sup>. To enable ET to occur, the redox potential of the mediator should be higher than that of the cofactor of the oxidizing enzyme (the opposite is true for the reducing enzyme)<sup>125</sup>. The selected mediators should also be stable in both oxidized and reduced form, access the cofactor in an efficient manner and undergo fast and reversible redox reaction on the electrode surface. Enzyme orientation is not a primary issue for MET based bioelectrode construction. For membrane-less EFCs, mediators must be co-immobilized with enzymes together on the electrode. To attain this goal, polymers bearing redox molecules on their backbones<sup>120,271,272</sup> are widely used, however, raising performance-degrading<sup>273</sup> and possible toxicity issues due to the potential leakage of the polymer. The possible toxicity issue from the redox polymer leakage has not been well studied and comprehensively understood. Recent reports find that some Os complexes with finely-tuned chelating ligands show comparable cytotoxicity to the clinical drugs<sup>274</sup>. Moreover, most polymer backbones are biocompatible and is unlikely to harm the body even after leakage into the body. The advantages of redox polymers in acting as O<sub>2</sub> scavengers will be further discussed in sub-section 5.1. Meanwhile, Gross et al. recently reported the use of freely diffusing redox-active carbohydrate nanoparticles as redox mediators for homogeneous electron transfer with enzymes in solution<sup>275</sup>. This concept was illustrated via a biocathode based on 2,2'-azino-bis(3-ethylbenzothiazoline-6-sulphonic acid) (ABTS)-nanoparticles and BOD. An example of this type of EFC avoiding the need for surface immobilization at the electrode was recently illustrated with GOx and BOD electrically wired by redox organic glyconanoparticles with entrapped quinone and thiazoline redox mediators, respectively.<sup>276</sup>

The comparison between the DET and MET currents for MCOs can be used to determine the percentage of enzymes with an orientation that is unfavorable for DET<sup>236</sup>. As illustrations, the addition of free ABTS as the redox mediator increased the current density by 20% and 24% for Lac and BOD modified electrodes, respectively, emphasizing the optimal control of the proximity of enzymes' cofactor for facilitated DET<sup>255</sup>. In another study, only approximately 9% of BOD immobilized on hierarchical carbon felt modified with CNTs was electro-active<sup>67</sup>. It

should be noted that a freely-diffusing mediator was used in these examples, with potential issues for the rate of diffusion of the mediator itself making it potentially difficult to evaluate the portion of enzyme in an orientation suitable for DET. Furthermore, examination of the DET/MET ratio demonstrated that this poor electroactive proportion was linked to unsuccessful direct enzyme wiring. On the anode side, it has been shown that Os redox polymer encapsulating CDH permitted a higher MET current density than that of DET, which can arise from a lower ratio of DET active enzymes<sup>277</sup>.

For DET-based bioelectrodes, the surface coverage of active enzymes is generally of a monolayer on the electrode. In such cases, modification of the electrode surface and the use of high-surface area electrodes is used to obtain significant currents<sup>100</sup>. In contrast, using mediators allows multilayered enzymes to be “electroactive”, resulting in high current densities. A direct proof of this is the successful concept of electrostatic layer-by-layer (LBL) assembly of enzymes with redox polymers<sup>278-280</sup>. Electrostatic LBL assembly of redox enzymes and oppositely charged polyelectrolytes enables rapid ET, tuneable modification layers. However, the faradaic response of redox polymers themselves, alongside with the biocatalytic performance, does not increase linearly with increasing number of assembled layers, indicative of a limitation in the number of layers in order for the outermost layers to be electrochemically addressable, as well as limited mass transfer rates within a relatively thick polymer layer<sup>280</sup>.

A recent report combined orientation and mediation strategies to enhance the performance of a Lac-based biocathode<sup>281</sup>. A molecular wire was synthesized, which contained an enzyme-orientation site (pyrene) to be plugged into the hydrophobic pocket of Lac, an electron redox mediator (ABTS) and a pyrrole monomer to be polymerized onto electrode surface. This combined approach resulted in the highest maximum current density ( $2.5 \text{ mA cm}^{-2}$ ) in comparison to the optimal oriented ( $1.4 \text{ mA cm}^{-2}$ ), mediated ( $2 \text{ mA cm}^{-2}$ ) and physically adsorbed approaches ( $0.6 \text{ mA cm}^{-2}$ ). Coupled with a Pt alloy/C based anode, the optimized hydroge/air fuel cell provided a  $P_{\text{max}}$  of  $7.9 \text{ mW cm}^{-2}$  (limited by the cathode).

### 3.4 Employment of nanomaterials

Implementation of high-specific-surface-area nanomaterials including porous gold and porous carbon electrodes as enzyme supports is a widely used strategy for enhancing current density<sup>88,92,103</sup>. Conductive materials with high surface-to-volume ratios enable high enzyme loading<sup>87</sup>. For DET enzymes, even though they may be randomly distributed in the conductive matrix, 3D nanomaterials provide the opportunity for favourable enzyme wiring for DET<sup>282</sup>. Moreover, the confinement effects of the porous electrodes are of advantage in the efficient coupling of enzymes<sup>282,283</sup> and redox polymers modified surface<sup>283</sup>, in comparison to planar electrodes (**Figure 7**).

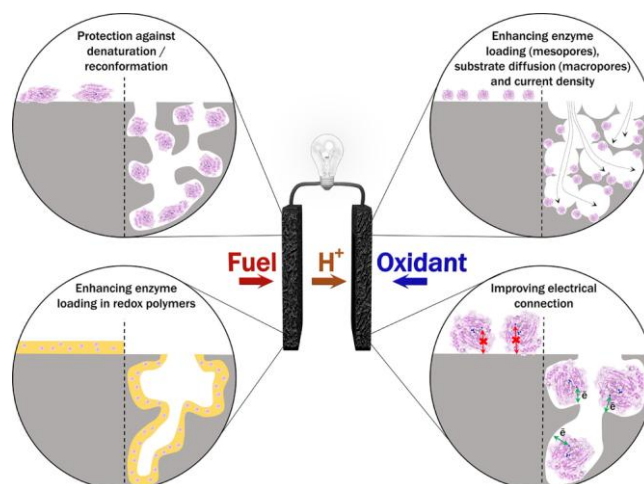


**Figure 7.** Schematic drawing of the advantages of using nanomaterial-based electrodes for the application of EFC. Reprinted with permission<sup>114</sup>. Copyright 2018 Elsevier.

Porous gold electrodes featuring good electrical conductivity, chemical stability and biocompatibility can be fabricated by dealloying<sup>282,284,285</sup>, Au nanoparticle (AuNP) assembly<sup>75,286-289</sup>, anodization<sup>290</sup>, or hard-<sup>291-293</sup> and soft-<sup>294</sup> template methods. Au electrodes can be easily modified with self-assembled monolayers (SAMs) of thiols<sup>242,295</sup>, diazonium grafting<sup>283,296,297</sup> and electropolymerization<sup>298,299</sup> for enzyme immobilization to achieve direct and mediated ET. A dealloyed porous gold (thickness: 100 nm, pore size: 30 nm, roughness factor: 9) based EFC utilizing electrodeposited Os-complex modified polymer with BOD and GDH, respectively, showed a  $P_{\max}$  of  $1.3 \mu\text{W cm}^{-2}$  in the presence of 20 mM glucose, in contrast to  $0.08 \mu\text{W cm}^{-2}$



using planar Au electrodes<sup>283</sup>. When the same amounts of enzyme/Os-complex modified polymer were drop-cast onto electrodes<sup>300</sup>, the CDH/BOD based EFC in 5 mM lactose displayed 41 and 13  $\mu\text{W cm}^{-2}$  on dealloyed porous and planar gold electrodes, respectively. Such a difference arises from the larger surface area of the porous electrode. Highly ordered microporous gold electrodes assembled by AuNPs were utilized to immobilize GDH and Lac at a bioanode and biocathode respectively, and exhibited a  $P_{\text{max}}$  of 178  $\mu\text{W cm}^{-2}$  in 30 mM glucose, in comparison with 12.6  $\mu\text{W cm}^{-2}$  on flat electrodes<sup>301</sup>. This increase in power density was mainly attributed to the higher enzyme loading in microporous gold. Coupling a MWCNT/GDH based bioanode with a 3D microporous gold/Lac biocathode displaying high DET current densities resulted in a  $P_{\text{max}}$  of 56  $\mu\text{W cm}^{-2}$  in 10 mM glucose, while 7  $\mu\text{W cm}^{-2}$  was obtained when a planar Au/Lac biocathode was used<sup>286</sup>. These reports highlighted the enhancement of the power density observed with porous gold electrodes. The pore size, inversely proportional to the specific surface area<sup>282,302</sup>, is an important factor for the performance of the bioelectrode. An optimal DET current for BOD was observed on porous gold electrodes with a pore size of ca. 20 nm which was large enough to accommodate the enzyme while providing a high surface area for sufficient enzyme loading<sup>283</sup>.

Examination of values of  $P_{\text{max}}$  greater than 1  $\text{mW cm}^{-2}$  (**Table 1**) indicates that the majority of high-power-density EFCs are based on carbon nanomaterials (CNMs)-based electrodes. CNMs including buckypaper<sup>46,117,303</sup>, carbon felt<sup>74</sup>, carbon cloth, carbon black<sup>16</sup>, CNTs<sup>62,72,303-313</sup>, carbon fiber<sup>65,273,314-318</sup>, graphene<sup>73,93,255,319</sup>, porous carbon<sup>11,63,66,320,321</sup>, carbon nanodots<sup>322</sup>, and their combinations thereof<sup>15,35,185,323-327</sup> have been widely used for the preparation of bioelectrodes. They enjoy advantages including low cost, affordable industrial scalability, wide operating potential window, chemical stability, hierarchical micro/nanostructures and flexible structures. The high specific surface area of CNMs ensures high loadings of enzymes<sup>67</sup>. For example, the modification of graphite electrode with hydrophobic carbon nanofibers (CNFs, BET surface area: 131  $\text{m}^2 \text{g}^{-1}$ ) resulted in a 1500-fold increase in the active area, so that a high current density of 4.5  $\text{mA cm}^{-2}$  (100-fold increase) was obtained for enzymatic  $\text{H}_2$  oxidation<sup>328</sup>. Graphene coated 3D

micropillar arrays were used to immobilize GOx and Lac, respectively, allowing an EFC with a  $P_{\max}$  of  $136 \mu\text{W cm}^{-2}$  in 100 mM glucose, much higher than a bare carbon based cell ( $22 \mu\text{W cm}^{-2}$ )<sup>329</sup>. As discussed previously in Section 3.3, varying the surface properties enables the electrostatic interactions between the enzyme and the electrode, resulting in the optimal preferred enzyme orientation for DET, and possible covalent attachment. CNMs are very attractive for that purpose. Versatile surface modification methods are based on diazonium salt reduction<sup>255,330-332</sup>, electropolymerization<sup>333,334</sup> and pyrene based  $\pi$ -stacking interactions<sup>185,335-337</sup>. One example is that a  $\text{H}_2/\text{air}$  EFC showed a  $P_{\max}$  of  $12 \mu\text{W cm}^{-2}$  when the hydrogenase and BOD were randomly adsorbed on pyrolytic graphite (PG) electrode, in contrast to  $119 \mu\text{W cm}^{-2}$  using functionalized pyrenyl MWCNTs<sup>254</sup>. By replacing PG with SWCNT-COOH, 35 and 300 fold increases in the hydrogenase-bioanode and BOD-biocathode currents, respectively, have been reported<sup>338</sup>. Accordingly, the  $P_{\max}$  of the resultant  $\text{H}_2/\text{O}_2$  EFC attained to a value of  $300 \mu\text{W cm}^{-2}$ , much higher than that for the cell based on PG ( $1 \mu\text{W cm}^{-2}$ )<sup>338</sup>.

CNMs are versatile and can be used in various formats<sup>81</sup>, allowing the miniaturization of EFCs towards implantable applications with significant volumetric power densities. Pioneering work by Heller et al. demonstrated a glucose/ $\text{O}_2$  EFC consisting of two 7- $\mu\text{m}$  diameter and 2-cm long carbon fibers, which delivered a maximum power density of  $137 \mu\text{W cm}^{-2}$  (estimated to be  $10 \mu\text{W cm}^{-3}$  in volumetric power density normalized to the whole cell size) at  $37 \text{ }^\circ\text{C}$ <sup>339</sup>. The implantation of this miniaturized EFC into a grape containing more than 30 mM glucose registered a maximum power density of  $240 \mu\text{W cm}^{-2}$  (ca.  $18 \mu\text{W cm}^{-3}$  in volumetric power density) when the cathode fiber was near the grape skin<sup>340</sup>. A glucose/ $\text{O}_2$  EFC with a needle bioanode inserting into a rabbit ear using ketjenblack as the electrode material produced a volumetric power density of ca.  $42 \mu\text{W cm}^{-3}$  (estimated by the volume of the sealing tip:  $0.01 \text{ cm}^3$ )<sup>341</sup>. A functional and implantable glucose/ $\text{O}_2$  EFC in a freely moving rat based on graphite particles electrodes was reported in 2010, featuring a size of  $0.13 \text{ cm}^3$  and a volumetric power density of ca.  $24.4 \mu\text{W cm}^{-3}$  (excluding the volume of the encapsulating bag)<sup>31</sup>. Crespilho et al. constructed a miniaturized glucose/ $\text{O}_2$  EFC made with flexible carbon fiber microelectrodes

(length ca. 0.05 cm; diameter ca. 10  $\mu\text{m}$ ) modified with enzyme and mediator and implanted into the jugular vein of a living rat, yielding a maximum power density of  $95 \mu\text{W cm}^{-2}$ <sup>342</sup>.

Although allowing significantly improved current densities, two main challenges of using CNMs based high-surface-area electrodes need to be addressed. Firstly, the potential toxicity of CNMs<sup>343</sup> particularly in implantable applications, needs to be considered<sup>344</sup>. Since direct *in vivo* contact should be circumvented, biocompatible polymers can be used to avoid biofouling<sup>341</sup>. When used in portable devices, the possible dispersion of CNMs into the environment may cause chronic diseases with long-term exposure time<sup>345</sup>. Secondly, fuel diffusion limitations can arise at high enzyme loadings<sup>67,346</sup>. Open, hierarchical porous carbon materials with macropores for improved mass transport and mesopores with nanostructured surface for efficient enzyme-electrode communication are promising<sup>320,321</sup>. A study of the pore size effect of MgO-templated carbon on the performance of [NiFe]-hydrogenase showed that larger pores (150 nm) afforded enhanced current density than small pores (35 nm) due to the more favourable enzyme loading in the large pores<sup>347</sup>.

### 3.5 Gas diffusion bioelectrode

Mass transport plays a vital role in the power output of EFCs. For gaseous fuel-powered EFCs, gas diffusion bioelectrodes may overcome the substrate diffusion issue as the consumed substrate (e.g.  $\text{H}_2$  and  $\text{O}_2$ ) in the electrolyte will be compensated from the gas phase. The concentration of  $\text{O}_2$  available in aqueous solutions at room temperature is less than 1 mM, limiting power output to only a few  $\text{mW cm}^{-2}$ <sup>79</sup> for EFCs based on oxygen-reducing cathodes. In the case of hydrogenase-based bioanodes, modeling of substrate diffusion showed that a thickness limited to 100  $\mu\text{m}$  of porous carbon material was catalytically active, mainly restricted because of fast substrate depletion in the inner layers<sup>67</sup>. Therefore, the gas diffusion bioelectrode (GDBE) is envisioned as a type of porous electrodes allowing the direct contact with gaseous substrates, eliminating the supply limitations due to the relatively low substrate solubility<sup>102</sup>. The concept of GDBE emanates from developments in conventional fuel cells. A viable GDBE consists of

(Figure 8):<sup>102</sup> i) a catalytic layer comprising enzymes, carbon additives for improved conductivity, binders for enhanced attachment and tuning the hydrophobicity/hydrophilicity balance and ET mediators if necessary; ii) a porous and conductive catalytic support layer such as carbon paper<sup>348</sup>, carbon cloth<sup>349</sup>, carbon felt<sup>50</sup> etc.; iii) a protective layer that is gas permeable and prevents leakage of the liquid electrolyte, for example Nafion®<sup>350</sup> and polytetrafluoroethylene (PTFE)<sup>351,352</sup>.

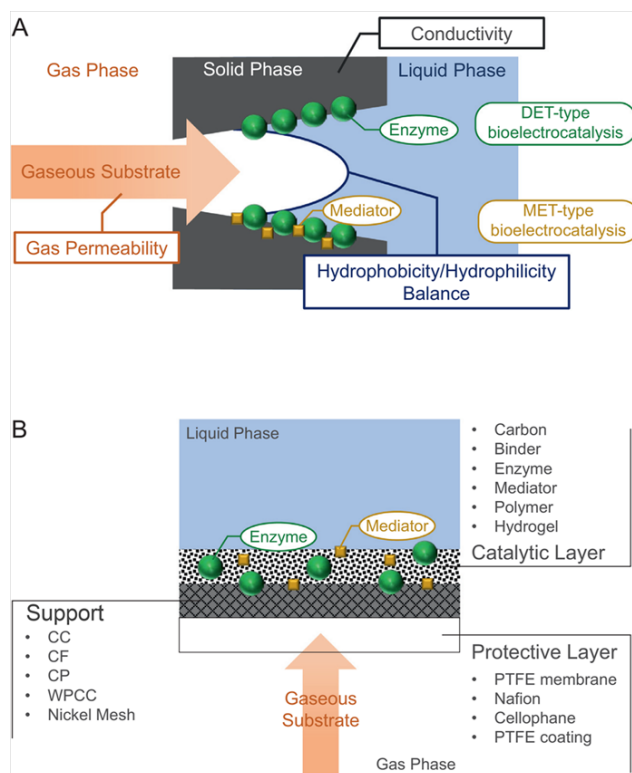


**Figure 8.** Schematic drawings of (A) bio-triple-phase boundary highlighting relevant properties including gas permeability, electrode conductivity and surface hydrophobicity/hydrophilicity balance; (B) structure and material candidates of a gas diffusion bioelectrode. Reprinted with permission<sup>102</sup> with modification. Copyright 2018 Elsevier.

Initial attempts in using oxygen-reducing GDBEs were conducted by Tarasevich et al. in 2003 by immobilizing Lac at highly dispersed colloidal graphite or acetylene carbon black<sup>353</sup>. Additional reports using ferricyanide mediated O<sub>2</sub> reduction by BOD in 2009<sup>52</sup>, a GDBE using multi-copper oxidase undergoing DET in 2009<sup>348</sup>, and Lac undergoing DET<sup>350</sup> have been described. In pioneering work Atanassov's lab described a range of GDBEs based on *Mv*BOD<sup>354</sup> and Lac<sup>355-357</sup> adsorbed on hydrophobized carbon black composite, and Lac on MWCNTs<sup>358</sup>. High catalytic

current densities were reported based on GDBE not only for O<sub>2</sub> reduction but also for other gaseous substrate enzymatic transformation such as CO<sub>2</sub> reduction<sup>270</sup> or H<sub>2</sub> oxidation<sup>16,68,69</sup>. The reduction of N<sub>2</sub> into ammonia has been possible<sup>153</sup>, which could also be developed into a gas diffusion type electrode. Recent examples demonstrate steady-state catalytic current densities at water-repellent-treated porous carbon felt/*Mv*BOD bioelectrode as high as 24 and 32 mA cm<sup>-2</sup> using air and oxygen, respectively<sup>351</sup>. A highly gas-permeable water-proof carbon cloth/hollow MWCNTs/*Mv*BOD displayed a DET based catalytic current density of 32 mA cm<sup>-2</sup> under atmospheric oxygen conditions<sup>153</sup>. On the anode side, the first use of GDBE for H<sub>2</sub> oxidation was published in 2014 based on *Hydrogenovibrio marinus* [NiFe]-hydrogenase undergoing DET<sup>359</sup>. A H<sub>2</sub>/O<sub>2</sub> EFC based on DET and dual GDBEs delivered a P<sub>max</sub> of 8.4 mW cm<sup>-2</sup> at 0.7 V under quiescent conditions, the highest value ever reported for such device<sup>68</sup>. More recently, a dual GDBE-based H<sub>2</sub>/O<sub>2</sub> EFC was constructed based on O<sub>2</sub>-sensitive hydrogenase incorporated in redox polymers and BOD directly wired to carbon cloth<sup>69</sup>. A maximum power density of 3.6 mW cm<sup>-2</sup> was obtained, one of the highest values ever reported for an EFC (**Table 1**)<sup>69</sup>. Beside EFC applications, GDBEs are also promising for applications in bioelectrosynthesis. The reduction of CO<sub>2</sub> to formate using MET-type GDBEs with tungsten-containing FoDH showed a current density of 17 mA cm<sup>-2</sup><sup>360</sup>.

Special care has been paid to the architecture of GDBEs allowing these high catalytic performances. Bio-triple-phase boundary (BTPB) is the interface between a gaseous fuel, liquid electrolyte (buffer solution) and solid electrode, at which the catalytic reaction occurs<sup>102</sup>. The active enzymes need to be hydrated to enable catalytic activity, highlighting the importance of tuning the surface hydrophobicity/hydrophilicity properties<sup>102</sup>. The reduction of O<sub>2</sub> at the air-breathing biocathode nicely illustrates the main issues associated with GDBEs. Biocatalytic O<sub>2</sub> reduction involves the following steps: i) O<sub>2</sub> from the gas phase is dissolved in the thin liquid layer around the enzymes, ii) O<sub>2</sub> and protons diffusing from the electrolyte meet at the active site of the enzyme with production of H<sub>2</sub>O, iii) excess water is repelled by the hydrophobic surface enabling the reaction to continue. An accumulation of water at the biocathode affects the final

performance of the GDBEs over time as the flow of gases is impeded. A subtle optimization of the hydration level at the BTPB is of importance to ensure the water content is sufficiently high for efficient proton transfer in the liquid phase, and sufficiently low to ensure adequate gas permeability at the interface. In practice, the hydrophobicity/hydrophilicity balance of GDBEs can be optimized by adjusting the hydrophilic binder/hydrophobic carbon additive ratio<sup>68,348</sup>. Besides biocathode flooding, local pH change at BTPB also resulted in decreased operational stability of GDBEs<sup>102</sup>, which can be alleviated by using concentrated buffer solutions<sup>52</sup>. Quantitative stability performance of various GDBEs has been described in a recent review<sup>102</sup>. The observed decay in the current density can be related to changes in hydrophobicity/hydrophilicity arising from increased water flooding and decreased gas permeability. Atanassov et al. combined oxygen-reducing GDBEs with paper based lateral-flow microfluidic systems by immobilizing enzymes with carbon based inks on nitrocellulose paper<sup>361</sup>, which broadened the range of applications of EFCs, such as microfluidic paper-EFC stacks<sup>362-364</sup>.

It should be noted that GDBEs are not suitable for implantable EFCs since gaseous substrates are not substantially available in the body, but can be feasible in subcutaneous devices<sup>341</sup>. Future efforts should be devoted to optimizing the utilization levels of the immobilized enzyme, since the widely-used enzyme/binder/additive slurry casting method maybe not sufficient enough. New strategies to engineer the hydrophobicity/hydrophilicity balance of the gas permeability and porosity should be developed. For example, a gold coated porous anodic alumina (PAA), whose surface wettability can be tailored by the properties of self-assembled monolayers, has been recently used for GOx immobilization (**Figure 9**)<sup>365</sup>. It is found that O<sub>2</sub> can participate to the enzymatic reaction directly from the gas phase through the channels, resulting in an 80-fold increase compared with that of an immersion type electrode.

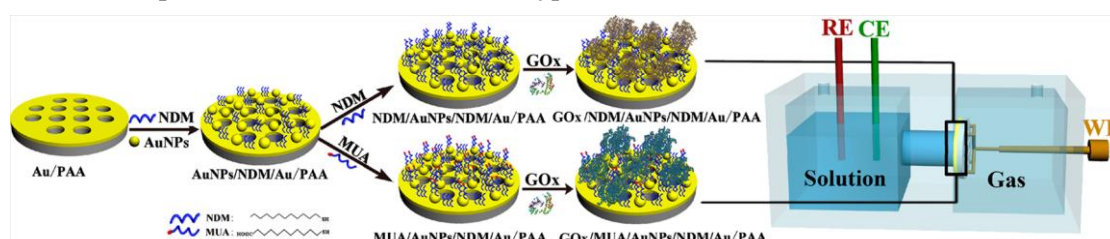


**Figure 9.** Schematic drawing of the assembly of an Au/PAA based air diffusion bioelectrode and the testing setup. The surface wettability of the Au electrode is tuned by using two different types of self-assembled monolayers of thiols. Reprinted with permission <sup>365</sup> with modification. Copyright 2018 American Chemical Society.

### 3.6 Fluidic EFCs

Fluidic configuration is one hydrodynamic strategy to overcome substrate depletion and thus increase the power density. EFCs in implanted medical devices use sugars and oxygen available under physiologically ambient conditions in soft tissue or blood vessels <sup>5</sup>. The surrounding tissue leads to additional resistance for mass transport of reactants and waste products. In contrast, EFCs implanted in blood vessels can be regarded as flow-through devices with mass transport improved in the blood stream which has a flow velocity of 1-10 cm s<sup>-1</sup> <sup>5</sup>. A wide range of recent studies has used a combination of enzymatic microfluidic devices to mimic the flow conditions in blood vessels<sup>350,366</sup>. Initial attempts focused on flowing enzyme<sup>367-369</sup> and/or cofactor<sup>370</sup> and/or mediator<sup>371</sup> solutions into micro-channels, where enzyme immobilization is essential<sup>350</sup>. Immobilization methods such as electrostatic interaction <sup>76,372,373</sup>, covalent bonding<sup>294,371</sup> and cross-linking<sup>374,375</sup> will be discussed further in Section 4.1.

One interesting example is a hybrid microfluidic fuel cell based on a GOx bioanode and an air-exposed Pt/C cathode <sup>375</sup>. At a flow rate of 0.5 mL h<sup>-1</sup> (under laminar flow), the fuel cell exhibited a decrease in P<sub>max</sub> from 0.6 to 0.2 mW cm<sup>-2</sup> when tested in buffer and human blood respectively. The decrease was proposed to be a consequences of higher viscosity and the adsorption of chemical species, including protein fragments, onto the electrode surface. A single compartment lactate/O<sub>2</sub> EFC in a pH 5.6 buffer containing 40 mM lactate registered a P<sub>max</sub> of 61.2 μW cm<sup>-2</sup>, which was increased to 305 μW cm<sup>-2</sup> when operated at 3 mL h<sup>-1</sup> in a microfluidic configuration <sup>376</sup>. The power density increased further on raising the flow rate to 9 mL h<sup>-1</sup>, but levelled off at 12 mL h<sup>-1</sup> indicating that the response is likely due to flow-induced instabilities in the enzyme immobilization, as explained by the authors <sup>376</sup>. Porous carbon paper has been introduced into a co-laminar microfluidic ethanol/O<sub>2</sub> EFC <sup>377</sup>. In this case, a low flow rate (50 μL

$\text{min}^{-1}$ ) generated higher power density than that from a higher flow rate ( $100 \mu\text{L min}^{-1}$ ), a result that can arise from the longer residence times in the enzyme layer at lower flow rates.

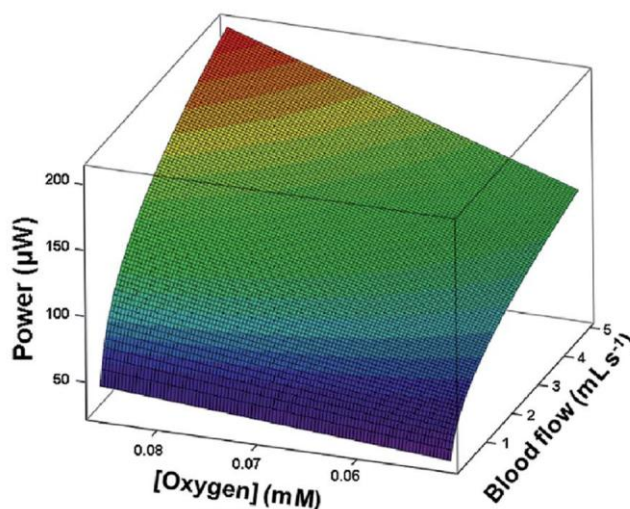


**Figure 10.** The calculated dependence of power output on  $\text{O}_2$  concentration and blood flow rate in a channel mimicking a human blood vessel. Reprinted with permission <sup>378</sup>. Copyright 2018 Royal Society of Chemistry.

Pankratov et al. prepared a tubular graphite electrode with inner and outer diameters of 1.00 and 3.01 mm, respectively, sizes that resemble that of a vein <sup>378</sup>. CDH and BOD were used to modify the inner tubular surface to form a bioanode and biocathode respectively. The tube was operated *ex vivo* with a laminar flow of blood from a human volunteer under homeostatic conditions. Experimental data, as well as theoretical calculations, showed that the power density of such an EFC was dependent on fuel concentration and blood flow rate (**Figure 10**).

Detachment arising from hydrodynamic flow, however, hindered the long-term operation of the bioelectrode, highlighting the importance of robust anchoring of enzymes to electrode surfaces. Specifically, poly(ethylene glycol) diglycidyl ether (PEGDGE) cross-linked enzyme layers could be washed off by the fluid at a flow rate of  $0.2 \text{ mL h}^{-1}$  <sup>371</sup>. In contrast, covalently bound enzymes appeared to be much more resistant towards flow at  $2 \text{ mL h}^{-1}$  <sup>371</sup>. The response of a hybrid fuel cell using a GOx/MWCNTs anode and a Pt/carbon cathode was tested in human blood at a flow rate of  $0.5 \text{ mL h}^{-1}$ , decreased by over 65% after 3 h of operation <sup>375</sup>. Gonzalez-Guerrero et al.



described a pyrolyzed photoresist film (PPF) electrode based EFC employing a ferrocenium-based PEI linked GOx anode and MWCNTs/Lac cathode that displayed a decreased in power density of 50% after 24 h of operation at a flow rate of 4.2 mL h<sup>-1</sup> in buffer solution<sup>374</sup>.

The Reynolds number is a measurement of degree of convective mixing of co-laminar streams<sup>350</sup>. In microfluidic channels, the Reynolds number is low, and mixing of the adjacent flowing streams is limited to a very thin interfacial width. Careful adjustment of the dimensions of these microchannels can avoid the need for a physical barrier to separate the fuel and the oxidant. Ion-exchange membranes are typically used to avoid mixing of H<sub>2</sub> and O<sub>2</sub> and to limit exposure to O<sub>2</sub> inactivation of hydrogenases<sup>88</sup>. A Y-shape microfluidic channel<sup>369</sup> with co-laminar flows of H<sub>2</sub> and O<sub>2</sub> enriched solution could eliminate the need for separation membranes, while ensuring rapid rates of transport of the substrates.

Other hydrodynamic environments introduced by magnetic stirring<sup>273</sup>, electrode rotation<sup>230,287</sup> and flow cell<sup>33,294</sup> are widely used to compensate for diffusion limitations in order to increase the power output of a EFC. However, the additional power, sometimes even greater than that generated by the EFC itself, is usually required, making these stirred and rotated EFCs impractical.

### **3.7 Combined EFCs/(super)capacitor devices**

The energy generated in EFCs can be stored in energy storage devices in a 'stationary' mode. Rechargeable batteries and supercapacitors are the most widely studied energy storage devices, and can store and release electrical energy by electrochemical reactions<sup>379</sup>. Supercapacitors, also known as electrochemical capacitors, utilize the electrical double layer capacitance (EDLC) via ion adsorption or pseudocapacitance attained during reversible faradaic reactions<sup>379</sup>. Unlike EFCs suffering from low power density and stability, supercapacitors possess high specific power density and long lifetime. A range of reports have combined EFCs with (super)capacitors<sup>140</sup>.

Initial attempts focussed on the external connection of EFCs with capacitors or supercapacitors. The coupled capacitor element accumulates the charge generated by the EFCs in the circuit, which can be released by output pulses with much higher power densities than that possible by EFCs themselves. Skunik-Nuckowska et al. used MWCNT based supercapacitors in parallel as complementary power units coupled with a Lac cathode and zinc anode based biobattery. The biobattery alone delivered a power output of 1.3  $\mu\text{W}$ , in comparison to 8.5 mW from the biobattery/supercapacitor hybrid system<sup>380</sup>. Sode et al. developed the concept of a “BioCapacitor” by integrating an EFC with a charge pump/capacitor combination (**Figure 11**)<sup>139,381</sup>. The capacitor was gradually charged and then discharged to power the electric device<sup>139</sup>. The high-power levels generated resulted in very short discharge intervals. A similar setup was used to design a wireless sensor fed by a  $\text{H}_2/\text{O}_2$  EFC<sup>382</sup>. The concentration of fuel determines the rate of charge/discharge of the biocapacitor, which enables a self-powered biosensor to determine the concentration of the fuel via the rate of charge/discharge of the capacitor<sup>139</sup>. Liu et al. coupled two series-connected glucose/ $\text{O}_2$  EFCs consisting of a buckypaper/MWCNT/FAD-GDH bioanode and a buckypaper/MWCNT/Lac biocathode with a flexible all-solid-state supercapacitor<sup>303</sup>. The self-charged system achieved a  $P_{\text{max}}$  of 608  $\mu\text{W cm}^{-2}$  when the capacitor was discharged, 90% higher than the value for series-connected EFCs.

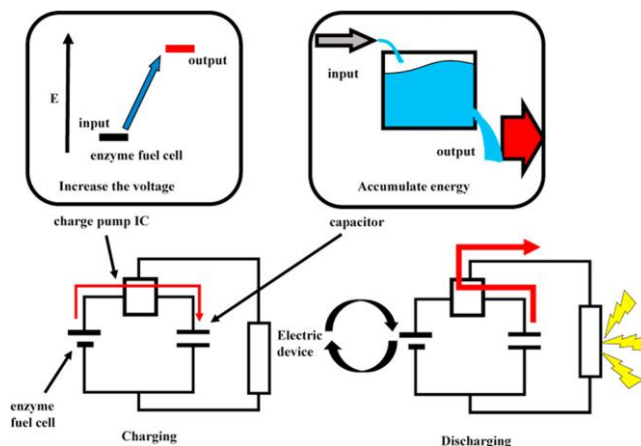


**Figure 11.** Schematic drawing of the principle of a biocapacitor. A charge pump can scale up the voltage of the EFC and a capacitor is used to store the electrical energy. The stored electric

energy can be discharged from the capacitor to activate a device (e.g. a LED bulb) when the capacitor voltage attains to the set value. Reprinted with permission <sup>139</sup>. Copyright 2018 Elsevier.

Closer examination of the configuration of EFCs and supercapacitors indicate that i) two electrodes hosting active materials (namely the anode and cathode) connected to the external circuit; ii) an electrolyte solution with conducting ions; iii) a separator if necessary to prevent possible short-circuit. Carbon nanomaterials that are widely used for the preparation of bioelectrodes have significantly high EDLC. Agnès et al. developed an EFC consisting of a compressed porous CNT matrix modified GOx bioanode and a Lac based biocathode, delivering 3 mA and 2 mW pulses with a short duration of 10 ms per 10 s for 5 days in the presence of glucose and O<sub>2</sub> <sup>383</sup>. In this case, the electricity generated by the EFC was stored continuously in the EDLC of CNTs. In parallel, Pankratov et al. reported a hybrid device based on flat graphite foil electrodes, with one face bearing an EFC using an AuNPs-CDH bioanode and an AuNPs-BOD biocathode, and the other face configured with capacitive materials (CNT/polyaniline) <sup>384</sup>. It displayed an initial power output of 1.2 mW cm<sup>-2</sup> at a voltage of 0.38 V which is 170 times higher than that of the EFBC alone.

It should be clarified that a biodevice simultaneously functioning as an EFC and a supercapacitor is different from systems based on the external connection of an EFC to a (super)capacitor. The former can be termed a hybrid EFC/supercapacitor device, which can be prepared from bifunctional electrodes<sup>140,385</sup>. The integration of such systems enables miniaturization. The self-powered capacitor functions in a sequence of charging and discharging<sup>283,386</sup>. Under charging conditions, the cell is at open-circuit, and the open-circuit potential (OCP) between the two electrodes gradually increases to the open-circuit voltage (OCV) of the EFC, as a result of the higher potential on the biocathode catalyzing oxygen reduction and the lower potential at the bioanode catalyzing the oxidation of fuels. Such a potential difference drives the polarization of the capacitive biocathode and bioanode. In other words, the capacitive cell is electrostatically charged by the biocatalytically induced potential difference. In the discharge step, the accumulated charge can be released at a fixed resistance<sup>384</sup> or current

density<sup>283</sup>. Based on such a methodology, Kizling et al. reported a fructose/O<sub>2</sub> EFC/supercapacitor hybrid device composed of a cellulose/polypyrrole/FDH bioanode<sup>387,388</sup> and a naphthylated CNTs/Lac biocathode<sup>388</sup>. Three biodevices in a series could generate pulses for 45 s with potentials above 1 V. Villarrubia et al. prepared a buckypaper based glucose/O<sub>2</sub> EFC/supercapacitor hybrid device<sup>364</sup>, which could be self-charged and discharged by a range of current densities as high as 4 mA cm<sup>-2</sup> for 0.01 s with a P<sub>max</sub> of 0.87 mW cm<sup>-2</sup> (absolute maximum power: 10.6 mW), 10 times higher than that of the EFC itself.

In addition to carbon nanomaterials with high EDLC, the pseudocapacitance behavior of redox polymers has also been examined. Knoche et al. prepared a hybrid device consisting of a carbon felt/MWCNT/dimethylferrocene-modified linear poly(ethylenimine) (FcMe<sub>2</sub>-LPEI)/FAD-GDH bioanode and a biocathode based on a carbon felt/anthracene terminated MWCNT/BOD<sup>389</sup>. The FcMe<sub>2</sub>-LPEI redox polymer served as mediator, enzyme immobilization matrix and as a supercapacitor whose pseudo-capacitance increased with polymer loading. The device generated 1 mA pulses for 1 s with a power output of 1 mW energy. Pankratov et al. developed a capacitive EFC using the same Os-complex modified polymer on a GDH anode and a BOD cathode<sup>378</sup>. The capacitance of the polymer was used for energy storage with an OCP up to 0.45 V, which could be discharged with 8-fold higher power output than that obtained in steady state<sup>378</sup>. Xiao et al. doped an Os-complex modified polymer based FAD-GDH bioanode and a BOD cathode with poly(3,4-ethylenedioxythiophene) (PEDOT) that showed enhanced capacitance<sup>283</sup>. The hybrid device was charged by the internal glucose/O<sub>2</sub> EFC and discharged as a supercapacitor at various current densities up to 2 mA cm<sup>-2</sup> registering a P<sub>max</sub> of 609 μW cm<sup>-2</sup>, a 468-fold increase when compared to that from the EFC itself. Connection of three devices in series produced 10 μA for 0.5 ms at a frequency of 0.2 Hz, mimicking the power requirement of a cardiac pacemaker. Interestingly, Alsaoub et al. demonstrated that the pseudo-capacitance of Os-complex modified polymers can be used in a so-called “biosupercapacitor” which can be discharged<sup>390</sup>. However, such a biodevice, comprised of a high-potential Os complex modified

polymer for glucose oxidation and a low one for oxygen reduction, is not an EFC as it cannot provide a usable OCV.

To briefly summarize this section, unconventional configurations of EFCs enable additional functionalities. However, as already discussed, the output voltage is still limited by the OCV of the EFC. The arbitrary combination of EFC and supercapacitor may be problematic, as shared electrodes configuration may reduce the efficiency of EFCs due to diffusion limitation. Insulating biomolecules are unlikely to be very beneficial for high-performance supercapacitors, although there are some reports indicating that proteins could contribute additional capacitance<sup>391</sup>. Additional research is needed to understand the mechanism of operation<sup>392,393</sup> and to develop practical applications<sup>392</sup> of hybrid devices.

## **4. Strategies for improving stability in EFCs**

### **4.1 Enzyme immobilization approaches**

The primary consideration of immobilization upon the bioelectrode's operational stability is to avoid enzyme detachment and other co-factors from the electrode<sup>76</sup>. Once immobilized, enzymes usually exhibit extended lifetime compared to those in solution<sup>394</sup>. Rigidification of the structure of the enzyme can enhance enzyme stability<sup>395</sup>. In EFCs, enzymes can be immobilized onto solid electrode surfaces by a range of approaches that include physical adsorption, covalent binding, entrapment and cross-linking<sup>6,40,90,96,396</sup> (**Figure 12**).

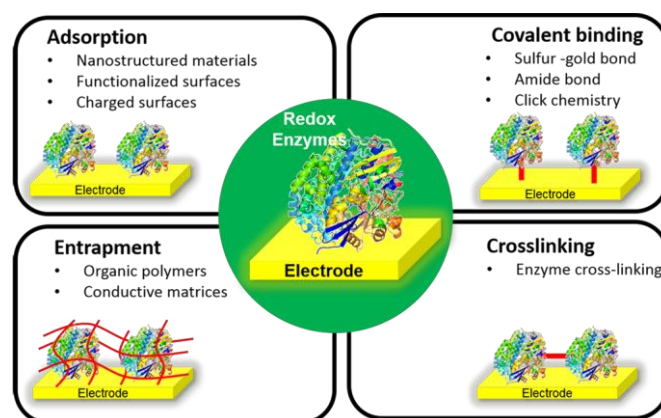


**Figure 12.** Scheme of various enzyme immobilization methods for bioelectrode fabrication.

Physical adsorption is generally considered as the simplest and mildest technique for enzyme immobilization, whereby enzymes are adsorbed directly onto electrode surfaces. However, enzymes physically adsorbed onto bare metal electrode surfaces often suffer from reduced operating lifetimes.<sup>238</sup> The self-assembly of a monolayer of thiols on the electrode surface may protect the enzymes from denaturation caused by metal-enzyme interactions<sup>397</sup> or at the electrode solution interface<sup>398</sup>. On the contrary, in comparison with planar electrodes, bioelectrodes fabricated by adsorbing enzymes at nanomaterials often exhibit not only improved electrocatalytic activity but also improved operational stability.<sup>399-401</sup> The improved activity and stability of nano-structure-based bioelectrode was ascribed to the 3D structure of the electrode, providing a mild microenvironment to effectively avoid enzyme desorption and denaturation.<sup>402</sup> A glucose/O<sub>2</sub> EFC prepared by the physical adsorption of GOx and BOD onto hierarchical metal-oxide mesoporous electrodes showed only 10% loss in voltage output after 30-h continuous operation.<sup>403</sup> Furthermore, the effect of pore size of porous electrodes on the stability of bioelectrode was investigated<sup>321,347,404,405</sup>. *AaHase* adsorbed onto MgO-templated carbon (MgOC) with pore size of 35 nm (larger than the size of *AaHase* *ca.* 17.7 ± 1.3 nm), exhibited a half-time of 81 h at 50 °C, much longer than that of *AaHase* in solution (7 h) (**Figure 13**).<sup>347</sup> A dialysis membrane (cut-off-molecular-weight of 12-14 kDa) was placed on the electrodes to prevent enzyme leakage to the solution during the measurement. The enhanced stability was ascribed to interactions between the pore materials and enzymes which decreased the conformational flexibility of the enzymes.<sup>347</sup>

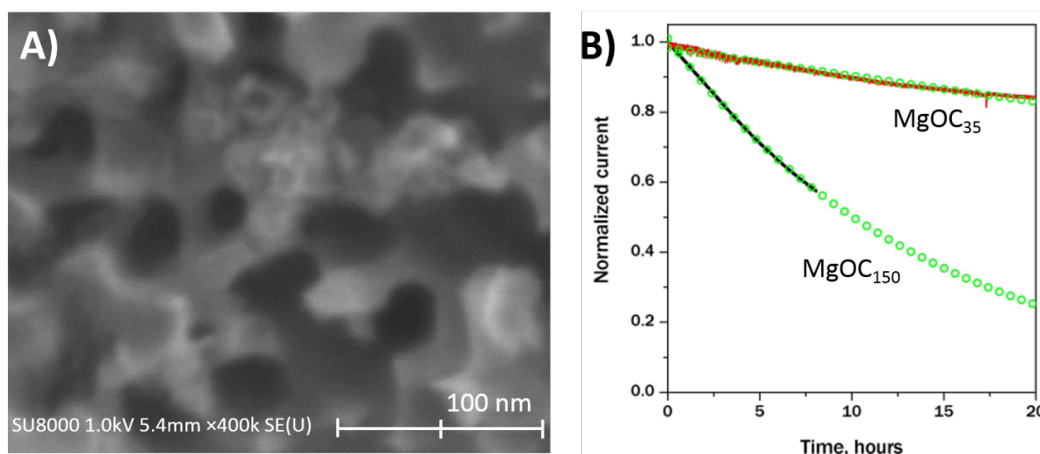


**Figure 13.** A) Field emission scanning electron microscopic images of MgOC<sub>35</sub>. B) Normalized response of *AaHase*-modified (red line) MgOC<sub>35</sub> and (black line) MgOC<sub>150</sub> at 50 °C in pH 7 phosphate buffer (0.1 M). MgOC<sub>35</sub> and MgOC<sub>150</sub> represent a MgO-templated carbon with pore size (diameter) of ca. 35 and ca. 150 nm respectively. Reprinted with permission<sup>347</sup> with modification, Copyright 2018 Elsevier.

The surface properties of electrodes, such as hydrophobicity, surface charge or functionalized groups, can influence the stability of bioelectrodes<sup>406</sup>. *TvLac* adsorbed onto 1-pyrenebutyric acid adamantyl amide functionalized MWCNTs (ADA-MWCNTs) remained 66% of the initial bioelectrocatalytic activity after 1 month<sup>259</sup>. However, *TvLac* on pristine MWCNT exhibited rapid decrease in catalytic currents to less than 5% of the initial value after 20 days (**Figure 14**). In this case, modifier with polycyclic aromatic structure can bind to the active center pocket of the enzymes, diminishing the desorption of the enzyme and reducing the conformational changes of enzymes<sup>259,407,70,408</sup>. A thermostable H<sub>2</sub>/O<sub>2</sub> EFC was assembled with an *AaHase*-based bioanode and a *BpBOD*-based biocathode, which were fabricated by physically adsorbing *AaHase* or *BpBOD* onto 1-pyrenemethylamine hydrochloride functionalized CNT electrodes, retained 95% of the initial power after 17 h continuous operation<sup>67</sup>. These reports suggest that functionalized surfaces of electrodes are likely to improve the stability of bioelectrodes by enhancing intermolecular interaction between enzymes and electrodes as well as reducing the conformational disruption<sup>70,181,257,409-411</sup>. Conformational changes of the enzymes during operation of EFCs is an area that needs investigation.

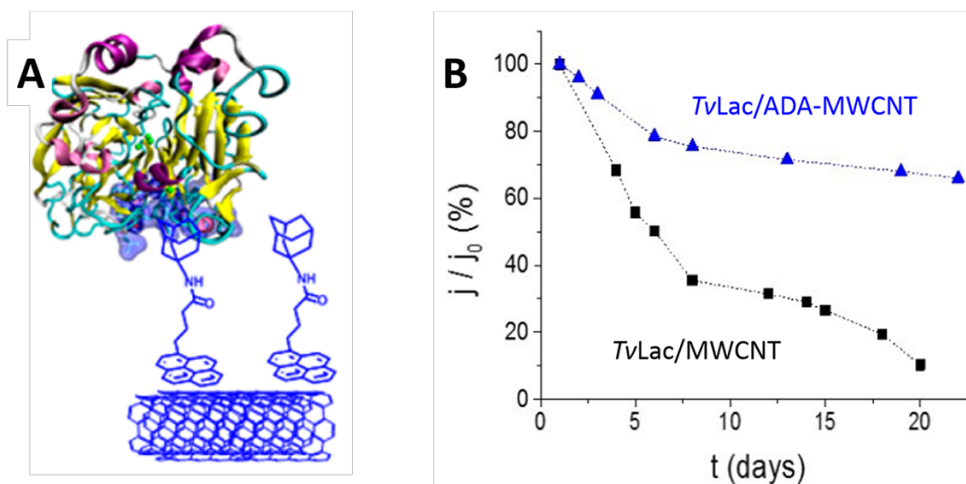


**Figure 14.** A) Schematic of *TvLac* oriented adsorption on 1-pyrenebutyric acid adamantyl amide functionalized MWCNTs (ADA-MWCNT). B) Long-term stability of *TvLAC* at pristine MWCNTs (black) and ADA-MWCNTs (blue). Measurements were carried out by performing a daily 1 h discharge at 0.2 V in stirred oxygen-saturated Mc Ilvaine buffer pH 5. Reprinted with permission<sup>259</sup> with modification. Copyright 2016 American Chemical Society.

Covalent binding is a typical and effective enzyme immobilization method. Peripheral amino or carboxylate groups on enzymes are feasible positions for covalent linkage. One common approach to anchor enzymes onto electrode surfaces is usually based on the formation of amide bonds between carboxylic groups and amino groups<sup>230,234,253,286,412-414</sup>, which are typically mediated by carboxylate activating reagents such as 1-ethyl-3-(3-dimethylaminopropyl)carbodiimide (EDC). With the aid of EDC, the *MvBOD* covalently bound to 6-mercaptohexanoic acid functionalized Au electrode retained more than 80% of the initial current after 4000 s continued measurement, while only 20% of the initial current was remained at the *MvBOD* physically adsorbed 6-mercaptohexanoic acid functionalized Au electrode (without EDC in this case).<sup>234</sup> (Figure 15A, B) The covalent binding between enzymes and electrodes is expected, for example, to prevent the enzyme orientation changes, which, however, affect the interfacial ET and then the lifetime of bioelectrodes. Besides, “click chemistry” is a convenient method to covalently bind redox enzymes to electrode surfaces.<sup>263</sup> A thiol-maleimide click reaction between *MoBOD* variant S362C and maleimide-functionalized MWCNT was employed to construct a stable O<sub>2</sub> bioanode, which retained ca. 95% of the initial current after 3 days storage, with ca. 30% of electrocatalytic current retained after 3 hours storage



for an electrode prepared by simply physical adsorption<sup>415</sup>. (**Figure 15 C, D**) Compared to physical adsorption, covalent binding provides stronger degrees of interaction between the enzymes and the electrode surface, leading to higher stability of the bioelectrodes<sup>416,417</sup>. However, it should be noted that the enzyme activity can decrease to certain extent upon immobilization

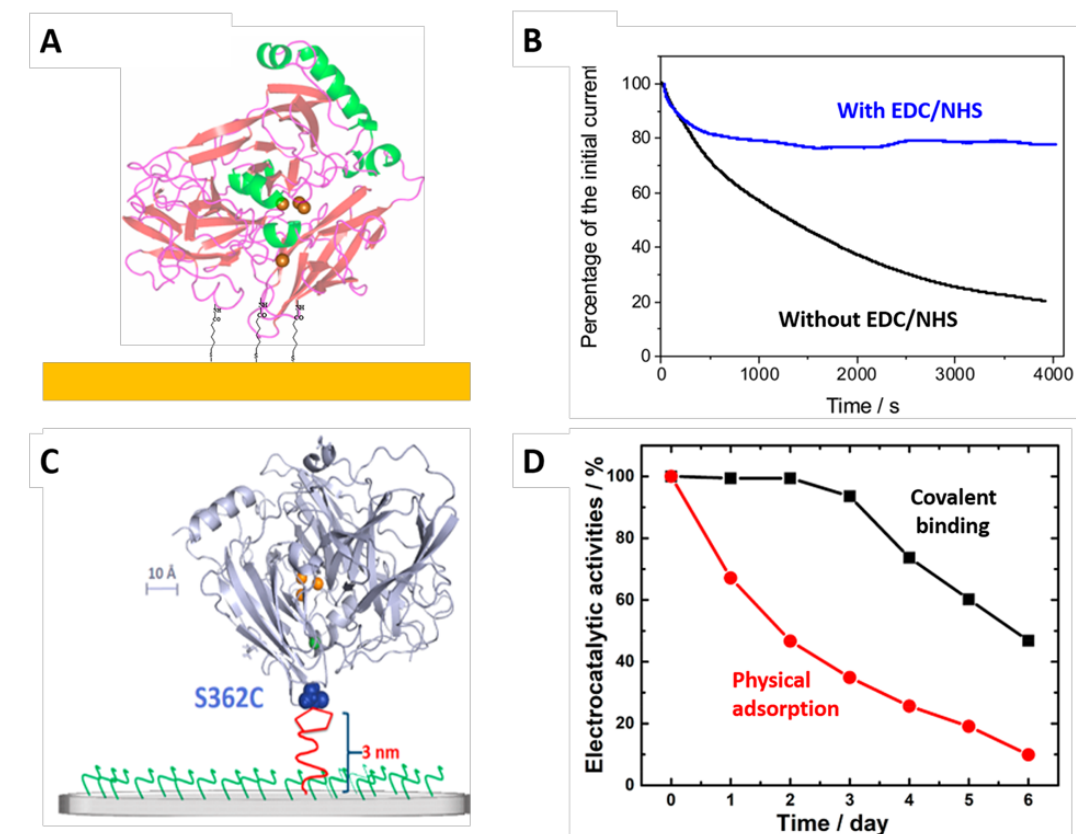


**Figure 15.** A) Scheme of electrode modification with *MvBOD* via an amide bond. B) Chronoamperometry of *MvBOD* at 6-mercaptopentanoic acid functionalized Au electrode with (blue) and without (black) the aid of EDC. C) Scheme of electrode modification with *MoBOD* variant S362C via maleimide/thiol bond; D) Maximum electrocatalytic activities of the maleimide-modified GC/MWCNT electrodes covalently modified with *MoBOD* variant S362C (black line) and adsorbed wild type BOD (red line) as a function of the length of storage. Reprinted with permission<sup>234,415</sup> with modification. Copyright 2016, 2019 American Chemistry Society.

It is a useful method to entrap enzymes into polymer matrices or inorganic frameworks on the electrode surface for enzyme immobilization, which can reduce the amount of leaching while

avoiding denaturation and conformational changes to the enzyme. Sol-gel based methods have been frequently reported to entrap enzymes with high activity and stability<sup>420-424</sup>. Entrapping redox enzymes into membrane-like matrices, such as lipid, agarose and DNA-hydrogel, which can mimic the natural environment of enzymes, retains enzymes in functionally active forms<sup>425-428</sup>. However, such matrices usually suffer from poor conductivity, and cannot be used directly for bioelectrocatalysis. As a result, materials with high conductivity such as CNTs, and redox mediators such as ferricyanide and ABTS, are usually co-encapsulated. A stable current response was obtained at a bioelectrode fabricated by coating a mixture of chitosan, Lac and MWCNT for over 60 days' continuous measurement, with more than 70% of the initial current retained upon storage for six months.<sup>429</sup>

On the other hand, by directly using conductive materials including CNTs as matrices for encapsulation of enzymes, stable bioelectrodes with high electroactivity can be realized.<sup>59,71,430,431</sup> Cosnier and coworkers reported a glucose/O<sub>2</sub> EFC by combining a GOx-based bioanode and Lac-based biocathode, prepared by mixing GOx or Lac with CNT, that showed only a slight (4%) decrease in the maximum power density after 30 days storage in buffer solution (**Figure 16**)<sup>59</sup>. Recently, as novel matrices, metal organic frameworks (MOFs) have been reported to entrap enzymes with long lifetimes<sup>432-436</sup>. A stable O<sub>2</sub> reduction enzyme electrode was prepared by mixing Lac with ABTS, mesoporous Fe(III) trimesate nanoparticle and carbon blacks<sup>433</sup>. With improved operating lifetimes, MOFs-based enzyme-electrodes are potentially of interest in the construction of EFCs.

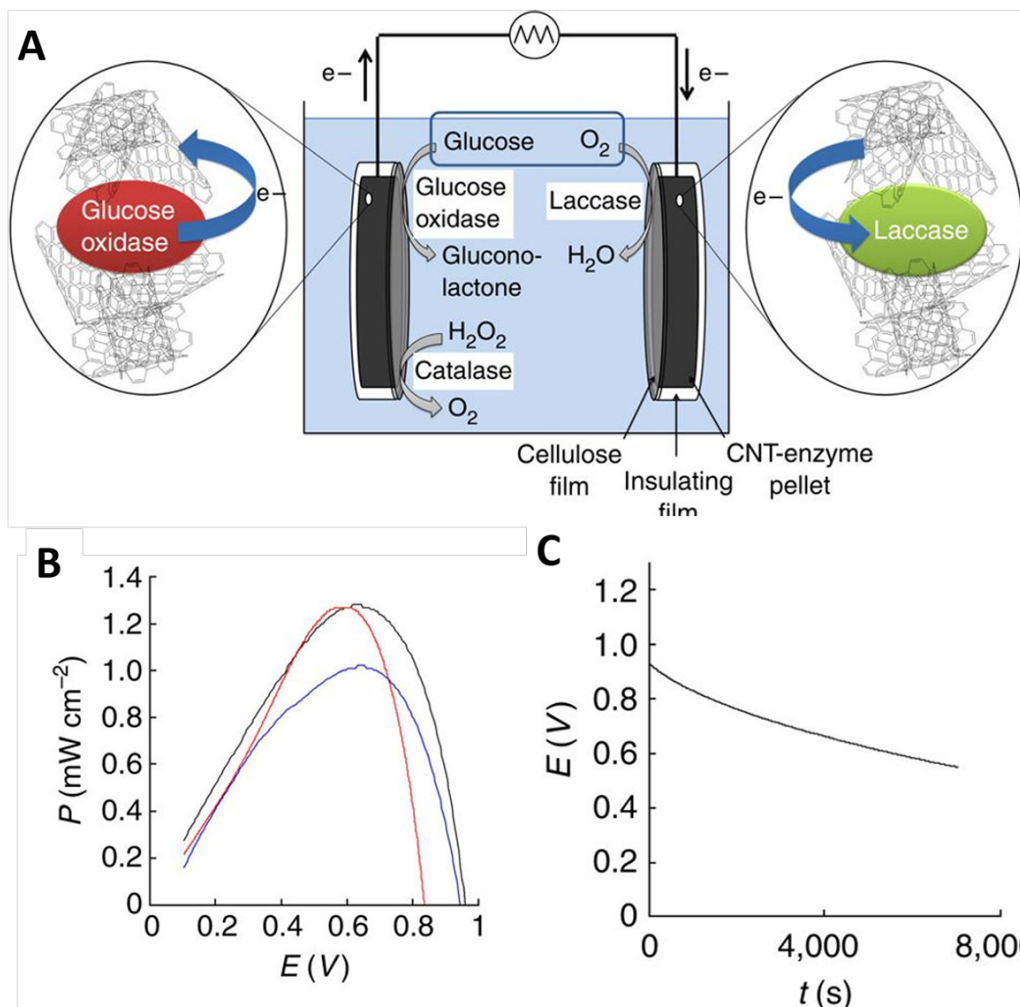


**Figure 16.** A) Schematic of a glucose/O<sub>2</sub> EFC by entrapping GOx and Lac into CNTs covered with cellulose film. B) Dependence of power density on operating voltage in 0.05 mol L<sup>-1</sup> glucose solution before (black) and after one month (red). Blue curve: dependence of power density on operating voltage in  $5 \times 10^{-3}$  mol L<sup>-1</sup> glucose. C) Dependence of voltage on time for continuous discharge under  $200 \mu\text{A cm}^{-2}$  in 0.05 mol L<sup>-1</sup> glucose solution. Experiments carried out in air-saturated phosphate buffer 0.1 mol L<sup>-1</sup>, pH 7.0 (bioanode: catalase/GOx ratio 1:1, biocathode: 20% laccase). Reprinted with permission<sup>59</sup>. Copyright 2011 Nature Publishing Group.

Cross-linking is a simple and effective method to immobilize enzymes on electrode. High stability should be expected because the process is based on bi- or multi-functional reagent ligands, forming rigid enzymatic aggregation, reducing leaching of the enzyme and improving the stability.<sup>437,438</sup> A stable peroxidase layer at ketjen black surface for DET-type bioelectrocatalysis has been reported by using glutaraldehyde as a cross-linker. In the absence of

glutaraldehyde, however, the catalytic current decreased with time and was lower than that in the presence of glutaraldehyde.<sup>439</sup> On the other hand, considering that the enzyme and cross-linking agents can form covalent bonds, the stability of the resultant enzymatic bioelectrodes can be improved<sup>288,440-442</sup>. With the aid of PEGDGE, a MET-type EFC using covalently anchored GOx and BOD, respectively at amino group-derivatized bioanode and biocathode, retained 70% of the initial maximum power after 24 h, while just 10% retention was observed for the EFC based on underivatized graphite<sup>442</sup>. Furthermore, to avoid uncontrollable cross-linking reaction, Schuhmann's group proposed an electrochemically induced cross-linking strategy to improve the operational stability of enzymatic bioelectrodes by locally entrapping enzymes into polymers on electrode surfaces<sup>443-446</sup>. With high stability, reusability as well as high volumetric activities, cross-linking represents an alternative to conventional immobilization approaches on solid surface.<sup>447</sup> However, a heterogeneous enzyme orientation distribution may induce slower ET rates specially in case of the use of cross-linkers.

## **4.2 Tuning enzyme properties**

### **4.2.1 Employing extremophile enzymes**

Biodiversity offers a large variety of microorganisms growing in extreme environments such as extreme pH<sup>18</sup>, high salinity<sup>448</sup> or extreme temperatures. Exploiting enzymes from these microorganisms is still in its infancy in the domain of EFCs, but may enhance the capabilities of EFCs to operate under broader operating conditions, while also potentially improving the stability of the enzymes. The discovery and use of thermostable enzymes from thermophilic microorganisms are of great importance to increase enzyme stability and potentially decrease enzyme production cost by simplifying enzyme purification process and extending enzyme duration in the area of biomanufacturing<sup>449</sup>. In EFCs, the same idea has been adopted to maintain the stability of the enzymatic catalysts and extend the lifetime of the fuel cells. Ohsaka et al. demonstrated the successful application of thermophilic GDH and laccase in EFCs that could be operated at elevated temperatures (76 °C)<sup>450</sup>. Lojou et al. constructed an EFC employing a

hyperthermophilic O<sub>2</sub>-tolerant hydrogenase and a thermostable BOD with a maximum power output of 2.3 mW at 50 °C. The device delivered 15.8 mW h of power after 17 h of continuous operation<sup>67</sup>. An efficient membraneless air-breathing/H<sub>2</sub> EFC was assembled by Cosnier's group relying on the same thermostable enzymes<sup>65,349</sup>. Comparison of two bioanodes constructed with the hyperthermophilic *Aquifex aeolicus* and the mesophilic *Ralstonia eutropha* hydrogenases clearly demonstrated the higher stability of the former not only at elevated temperature but also at room temperature<sup>335</sup>. Another NiFe hydrogenase from the hyperthermophilic bacterium *Pyrococcus furiosus* showed a remaining activity at 80°C upon exposure to O<sub>2</sub>, highlighting combined resistances of these extremophile enzymes<sup>451</sup>. A *Sulfolobus kodaii* alcohol dehydrogenase was investigated for use as a biocatalyst for electrochemical applications by Ohno et al. The constructed bioanode can maintain a high current density at even 80 °C, with a 12-fold increase over that at room temperature<sup>17</sup>. Recently, Zhang's group developed several synthetic enzymatic pathway-catalyzed EFCs comprised of multiple thermostable enzymes cloned from various thermophiles and capable of deeply or completely oxidizing sugar fuels. Such EFCs could be operated at 50 °C and exhibit an 8-fold increase in power density compared to those based on mesophilic enzymes<sup>171,452</sup>.

#### **4.2.2 Protein engineering for better stability**

As discussed in previous sections, protein engineering approaches are mainly used to improve rates of the ET between enzymes and electrodes<sup>453</sup>, tuning the substrate specificity of enzymes<sup>454</sup>, as well as creating scaffolds for enzyme immobilization<sup>105</sup>. General protein engineering strategies for biocatalysts in EFCs have been summarized in detail in two recent reviews<sup>196,455</sup>. More attention here will be paid on increasing the poor stability of EFCs. In detail, protein engineering can enable the stabilization of enzymes, by modifying the enzymes' structures in order to introduce more strong bonds, remove unfavorable steric effects, and remove potential degradation sites<sup>456</sup>. For example, a homodimeric pyrrolquinoline quinone GDH from *Acinetobacter calcoaceticus* was engineered by changing a single amino acid to cysteine, so that the lifetime of the EFC was greatly extended to 152 h, more than 6-fold that of the EFC

employing the wild-type. Enhanced disulfide bond formation of the active enzyme dimer may explain this result <sup>457</sup>. Additional work demonstrated that the thermal stability could be increased by introducing a hydrophobic interaction in the interface of the two subunits in this enzyme through two amino acid substitutions <sup>458</sup>. Direct evolution has been applied to *Saccharomyces cerevisiae* Lac by introducing mutations in the second coordination sphere of T1 to increase the resistance to chloride ions, making it more suitable to be used for EFCs working in physiological fluids <sup>459</sup>. It was also reported that protein oligomerisation is a potential means of increasing the stability of the bioelectrode<sup>460</sup>.

In addition to increasing the stability of engineered enzymes, other studies have focused on replacing expensive nicotinamide-based cofactors (NAD<sup>+</sup> or NADP<sup>+</sup>) required in MET-based EFCs with inexpensive and stable biomimics. In order to use these biomimetic cofactors, the cofactor preference of the respective oxidoreductase has to be altered. For example, Banta et al. engineered an alcohol dehydrogenase from *Pyrococcus furiosus* to utilize the biomimic cofactor nicotinamide mononucleotide (NMN) <sup>461</sup>. Compared to natural cofactors, such biomimic cofactors are smaller with faster rates of diffusion. In addition to increases in stability, gains in the performance of the NMN-mediated EFC were observed possibly due to improved rates of cofactor diffusion, despite a decreased turnover rate of the engineered enzyme. Zhang et al. changed the cofactor specificity of 6-phosphogluconate dehydrogenase from its natural cofactor NADP to NAD through a rational design strategy. The best mutant exhibited a ~60,000-fold reversal of the cofactor selectivity from NADP to NAD, and the associated EFC possessed an increase in power density and enhanced stability at high temperature <sup>462</sup>. Cofactor engineering not only can address the issue of unstable natural cofactors used in EFCs, but can also improve rates of mass transfer and the overall cost of EFCs.

### 4.3 Microbial surface displayed enzymes as biocatalysts to enhance EFCs' stability

#### 4.3.1 Microbial surface display

Microbial surface display refers to the biotechnology of introducing foreign peptides or proteins of interest on the surfaces of microbes by fusing them with appropriate anchoring protein motifs<sup>463,464</sup>, which is capable of maintaining their relatively independent spatial structure and biological activity. The microbial surface display system is usually composed of a passenger protein (target protein), an anchor protein (carrier protein) and host microbes (**Figure 17**). To date, varying anchor proteins such as ice nucleation protein (INP)<sup>465</sup>, Lpp-OmpA<sup>466</sup>, EstA<sup>467</sup>, and OmpC<sup>468</sup>, OmpA<sup>469</sup> have been used. Microbial surface display is classified into phage display, yeast display and bacterial display, which enables foreign peptides or proteins to directly interact with substrate without passing through the outer membrane by means of genetic engineering. Moreover, this strategy can help to improve the stability of displayed proteins due to the immobilization on the surface of biomaterial support<sup>470,471</sup>. So far, microbial surface display has been widely applied in live-vaccines<sup>472</sup>, peptide or protein library screening<sup>473</sup>, bioadsorbents<sup>474</sup>, whole-cell biocatalysts<sup>475</sup> and biosensors<sup>158,476</sup>.





long-term operational stability. Additionally, without the need for enzyme purification, the enzyme-expressing whole-cell based biocatalysts have also been used for the construction of EFCs<sup>477-479</sup>. Alfonta's group displayed GOx on yeast cell surface using a-agglutinin as an anchor motif for EFC construction<sup>477</sup>. The randomly distributed GOx showed interesting advantages over unmodified yeast or purified GOx. Under the same condition, the engineered yeast based EFC showed an increased OCV of ca. 0.88 V in comparison to ca. 0.73 V for purified GOx. The improved performance was probably derived from the synergistic effect of both the GOx on the yeast surface and the immobilization of the metabolic output of the yeast cells for power production. It should be mentioned here that the microbe mainly serves as a stabilizing element<sup>479</sup>, different from MFCs which utilize an entire microorganism (also called electricigens) to convert the chemical energy of organic matter for electricity<sup>480-482</sup>. Recently, dehydrogenases have attracted significant attention as the reactions are not affected by the presence of oxygen. Liu et al. have described a number of reports on dehydrogenases, with xylose dehydrogenase (XDH)<sup>483</sup>, GDH<sup>484,485</sup>, glutamate dehydrogenase<sup>486</sup> and FoDH<sup>487</sup> being successfully displayed on the surface of *E. Coli*. Biosensors<sup>483,486,488-491</sup> and one-compartment biofuel cells<sup>286,492,493</sup> have been prepared using these surface displayed dehydrogenases. Direct energy conversion from xylose was successfully achieved using XDH surface displayed *E. coli* (XDH-bacteria) based EFC, composed of XDH-bacteria immobilized on poly(brilliant cresyl blue)(PBCB)/MWCNTs modified glassy carbon electrode (GCE) (XDH-bacteria/PBCB/MWCNTs/GCE) based bioanode and a free BOD based biocathode<sup>492</sup>. Under optimized condition, a  $P_{\max}$  of  $63 \mu\text{W cm}^{-2}$  at 0.44 V was obtained, 60% higher than that of the free enzyme based EFC<sup>492</sup> (**Figure 18**). It is noteworthy that this EFC could retain 85% of its maximal power after 12 h of continuous operation. A rationally designed XDH mutant NA-1 with improved thermostability was anchored on the bacterial surface<sup>493</sup>. After 12 h operation, 88% of its maximal power was retained<sup>493</sup>. In another report, a bacterial surface displayed GDH mutant (mutant-GDH-bacteria) was immobilized onto MWCNTs as bioanode<sup>286</sup>. This EFC showed a  $P_{\max}$  of  $55.8 \mu\text{W cm}^{-2}$  at 0.45 V and an OCV of 0.80 V in 10 mM glucose. The as-fabricated EFC retained 84% of  $P_{\max}$  even after continuous

operation for 55 h, benefitting from the high stability of the bacterial displayed GDH mutant<sup>286</sup>.

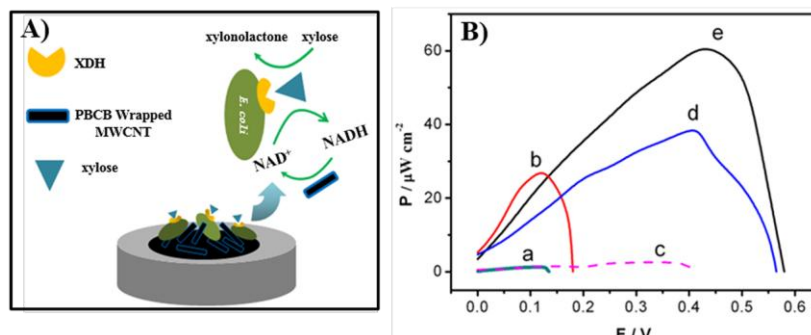


**Figure 18.** A) Schematic illustration of a XDH-bacteria/PBCB/MWCNTs/GCE based bioanode. B) Dependence of the power density on the cell voltage of a free-XDH/PBCB/MWCNTs/GCE bioanode based EFC in the absence (a) and the presence of 30 mM xylose solution (b); free-XDH/PBCB/MWCNTs/GCE bioanode based EFC in the absence (c), and the presence of 30 mM xylose solution (d); and XDH-bacteria/PBCB/MWCNTs/GCE bioanode based EFC in 0.1M PBS quiescent solution containing 30 mM xylose and 10 mM NAD<sup>+</sup> under O<sub>2</sub>-saturated condition (e). Reprinted with permission <sup>492</sup>. Copyright 2013 Elsevier.

Sequential enzymes refer to two or more enzymes involved in catalyzing cascade reactions sequentially and coordinately, for example, glucoamylase (GA)/GOx, ADH/FDH, and GOx/horseradish peroxidase (HRP). Recently, EFCs based on sequential enzymes raised great interests. For instance, a membraneless starch/O<sub>2</sub> EFC based on bioanode by co-immobilizing commercial GA and GOx <sup>494</sup> as well as white rice/O<sub>2</sub> EFC based on the multi-immobilization of GOx, alpha amylase and GA on a carbon paste electrode <sup>495</sup>, was developed. Nevertheless, it is complicated to co-immobilize two or three enzymes at the same time, as the spatial orientation of the enzymes cannot be controlled. Alfonta et al. displayed GA and GOx on yeast surface, respectively, to obtain GA-yeast and GOx-yeast, and then constructed a two-chamber EFC <sup>496</sup>. However, the P<sub>max</sub> was only about 3 μW cm<sup>-2</sup>, probably due to the low catalytic efficiency arising from the spatial barrier between GA and GOx. The same group

further co-expressed ADH and formaldehyde dehydrogenase (FormDH) on yeast cells using cohesin-dockerin interactions<sup>173</sup>. Subsequently, an EFC was fabricated using the displayed ADH/FormDH cascade based bioanodes and copper oxidase based biocathodes, however, a low power density ( $< 3 \mu\text{W cm}^{-2}$ ) was achieved<sup>173</sup> because the surface patterning of the enzymes together with their orientation were not considered. It should be mentioned here that, the controlled co-displayed cascade enzymes should be superior to randomly displayed cascade enzymes as the enzyme cascades assembled on the cell would enable reactants to transfer between active sites of the enzymes efficiently, which makes great sense in biocatalysis and bioelectro-synthesis.

#### 4.4 Strategies for enzyme protection against O<sub>2</sub> and reactive oxygen species (ROS)

While oxygen is the oxidant mainly used as the cathodic substrate in EFCs where it is reduced to water, it can seriously affect the performance of the anode in EFCs if operating in a single compartment configuration. Reactive oxygen species (ROS, such as O<sub>2</sub><sup>-</sup>), produced by the incomplete reduction of O<sub>2</sub>, can seriously affect the activity of enzymes. The majority of sugar/O<sub>2</sub> based EFCs rely on flavoprotein oxidases (e.g. GOx and lactate oxidase (LOx)) carrying a flavin cofactor tethered in the protein that utilizes O<sub>2</sub> as an electron acceptor, producing H<sub>2</sub>O<sub>2</sub> in the process<sup>497,498</sup>. The response of biosensors<sup>499</sup> that rely on DET or MET generally does not detect H<sub>2</sub>O<sub>2</sub> which can have a deleterious effect on the enzymes in the system<sup>500,501</sup>. Scodeller et al. found that exogenous peroxide reduced the electrocatalytic O<sub>2</sub> reduction current at an Os-complex modified polymer mediated *Trametes trogii* Lac biocathode by ca. 20%<sup>502</sup>. H<sub>2</sub>O<sub>2</sub> irreversibly inhibited the activity of a biocathode with immobilized *Myrothecium sp.* BOD, whereas a reversible deleterious effect was found with *TvLac*<sup>503</sup>. The underlying mechanism of inhibition is still unclear.

In the case of implantable EFCs, the generation of H<sub>2</sub>O<sub>2</sub> is also undesirable as it is toxic to the surrounding tissue<sup>3</sup>. Removal of H<sub>2</sub>O<sub>2</sub> can be achieved via catalytic decomposition by catalase<sup>31,34,41,383</sup> on the bioanode. It should be noted that there are EFCs based on H<sub>2</sub>O<sub>2</sub>-reducing

biocathodes<sup>504-507</sup>. For example, GOx can catalyze the oxidation of glucose producing H<sub>2</sub>O<sub>2</sub>, which is electroenzymatically reduced into water by immobilized peroxidases<sup>333</sup>.

Re-engineering of oxygen-sensitive flavoprotein oxidases reduces the effect of oxygen<sup>508</sup>. The conversion of O<sub>2</sub> into H<sub>2</sub>O<sub>2</sub> involves two electrons and two protons transferred from the reduced flavin<sup>509</sup>. The active site binding pocket of *AnGOx* contains Glu412, His516, His559, and FAD<sup>510</sup>. His516 in the active site of native GOx is protonated and positively charged and is likely responsible for the electrostatic stabilization of the transition state for stepwise single-electron transfer between FADH<sup>-</sup> and O<sub>2</sub><sup>511</sup>. The replacement of His516 by alanine by site-directed mutagenesis resulted in a 217-fold decrease in  $k_{cat}/K_M(O_2)$  at pH 5<sup>511</sup>. Gutierrez et al. identified four oxygen/mediator (quinone diimine) activity related positions in *AnGOx*, which were close to the FAD domain and situated at the oxygen entry<sup>512</sup>. Simultaneous site saturation at the four positions by two rounds of directed evolution and ultra high-throughput screening resulted in a 37-fold decreased oxygen dependency, while retaining the catalytic efficiency for redox mediators and thermostability<sup>512</sup>. Sode et al. analyzed an oxygen-binding structural model of *PaGOx* and predicted that eight functional residues were involved in the oxidative half reaction<sup>513</sup>. Mutagenesis analysis by alanine substitution of these residues and subsequent activity assays indicated that the Ser114Ala mutant possessed the highest dehydrogenase performance with a 31 % decrease in oxidase activity<sup>513</sup>. Bimutation at Ser114 and Phe334 in mutated *PaGOx* resulted in a 11-fold decrease in activity towards oxygen in comparison with the wild-type counterpart<sup>514</sup>. To simultaneously decrease the O<sub>2</sub> sensitivity and maintain high activity towards glucose with artificial mediators, a double mutation was performed upon Val564, which is a nonpolar site to guide oxygen binding, and Lys424<sup>515</sup>, which allows enhancement of the electron transfer rate between Os redox polymer and *PaGOx*<sup>516</sup>. The methodology to predict the oxygen access pathway to screen for mutants has been employed with other flavoprotein oxidases. For example, *Aerococcus viridans* lactate oxidase bearing a A96L mutant showed a significant decrease in oxidase activity using molecular oxygen as the electron acceptor, accompanied with a slight increase in activity using ferricyanide as the mediator<sup>517</sup>.

Alternatively, oxygen-insensitive dehydrogenase modified bioanodes can avoid the undesirable issues arising by  $\text{H}_2\text{O}_2$ <sup>84</sup>. NAD-dependent GDH has been widely used for biosensors and EFCs based on the successful reduction of the overpotential for the regeneration of  $\text{NAD}^+$ . However, the cofactor is not tightly bound to the enzyme limiting its application for implantable devices. The utilization of  $\text{NAD}^+$  as a cofactor is also constrained by the complicated electrochemical regeneration of  $\text{NAD}^+$  as the cofactor itself undergoes irreversible oxidation<sup>518</sup>. GDH using PQQ as the bound cofactor holds promise for use in an EFC<sup>221,499,519-522</sup>. DET of PQQ-GDH can be achieved by means of suitable enzyme immobilization<sup>221,520,523</sup>. FAD-dependent GDH (FAD-GDH) has been widely utilized in EFCs<sup>283,524-533</sup>. Milton et al. found that a GOx based membrane-less EFC initially had a higher power density than a FAD-GDH based EFC, while the FAD-GDH based EFC possessed better operating stability (after 24 h continuous operation)<sup>525</sup>. This confirms the negative effects of GOx bioanodes producing  $\text{H}_2\text{O}_2$  on BOD<sup>525</sup> and Lac<sup>530</sup> biocathodes. PDH<sup>266,306,534-537</sup> and CDH are other options for oxygen-inert bioanodes. CDH can catalyze several carbohydrates (glucose, lactose and cellobiose), and is promising as a versatile bioanode catalyst to simultaneously oxidize various fuels<sup>277</sup>. PDH shows a broad substrate specificity including glucose, xylose, galactose etc., and can catalyze the oxidation of sugar anomers at the C-2 and C-3 carbons of the sugar<sup>538</sup>.

Other enzymes are highly sensitive to  $\text{O}_2$  themselves, which is the case of most hydrogenases which are inactivated in the presence of  $\text{O}_2$ , limiting the large-scale development of  $\text{H}_2/\text{O}_2$  EFCs to replace Pt based catalysts suffering from scarcity and inhibition<sup>88</sup>. [NiFe] hydrogenases are the most efficient hydrogenases for  $\text{H}_2$  oxidation. Many studies have been made to produce  $\text{O}_2$ -tolerant mutants, but none of these mutants are sufficiently resistant to be used as bioanodes<sup>88,134,228</sup>. One strategy is to purify oxygen tolerant hydrogenases, such as the membrane-bound [NiFe]-hydrogenases isolated from the bacteria *Ralstonia eutropha*, *E. coli* or *Aquifex aeolicus*<sup>65,67,338</sup>. The tolerance of these hydrogenases has been mainly ascribed to a [4Fe-3S] cluster in close proximity to the active site different from the cluster found in the sensitive hydrogenases, and able to provide the extra electrons required to reduce  $\text{O}_2$  into water as soon as it attacks the

active site. However, even when using these O<sub>2</sub>-tolerant hydrogenases, inactivation by O<sub>2</sub> occurs, although this is a reversible and fast process. A strategy to refill electrons to deactivated hydrogenase was proposed by Armstrong and coworkers, using an additional bioanode<sup>539</sup>. Nevertheless, a membrane separator was necessary to avoid cross diffusion of O<sub>2</sub>, and inactivation of the hydrogenases. Effectively, ROSs formed due to oxygen reduction at the carbon surface held at low potentials were found however to deactivate hydrogenase irreversibly<sup>335</sup>. Upper layers of 3D porous carbon matrix are believed to help to scavenge ROSs before they reach enzymes inside the pores<sup>67</sup>. It found that the hydrogenase encapsulated inside a 3D porous matrix displays 4-6 times more stability against ROS than that on a 2D electrode.

To prevent the oxygen-induced damage on O<sub>2</sub> sensitive hydrogenases, the employment of a “redox hydrogel shield” has been recently proposed by Schuhmann and Lubitz et al. (**Figure 19**)<sup>540</sup>. A specifically designed viologen-based redox polymer with a low potential catalyzes oxygen reduction at the polymer surface, thus preventing the inner enzyme modification layer from O<sub>2</sub> damage and high-potential deactivation. Further, detailed characterization and numerical simulation were applied to reveal the underlying protection mechanism<sup>379</sup>. Protection has been successfully achieved for [NiFe]<sup>540,541</sup>, [FeFe]<sup>542</sup> and [NiFeSe]<sup>444,543</sup> hydrogenases. However, the effect of byproducts such as superoxide and hydrogen peroxide that are derived from partial oxygen reduction should be taken into account<sup>542</sup>. Similar methodologies can be extended to develop a double layered lactose biosensor comprised of an inner CDH and outer GOx layer separately<sup>544</sup>. The outer GOx layer can remove a high concentration of glucose up to 140 mM, that is also the substrate of CDH, enabling the system to operate as a reliable lactose sensor.

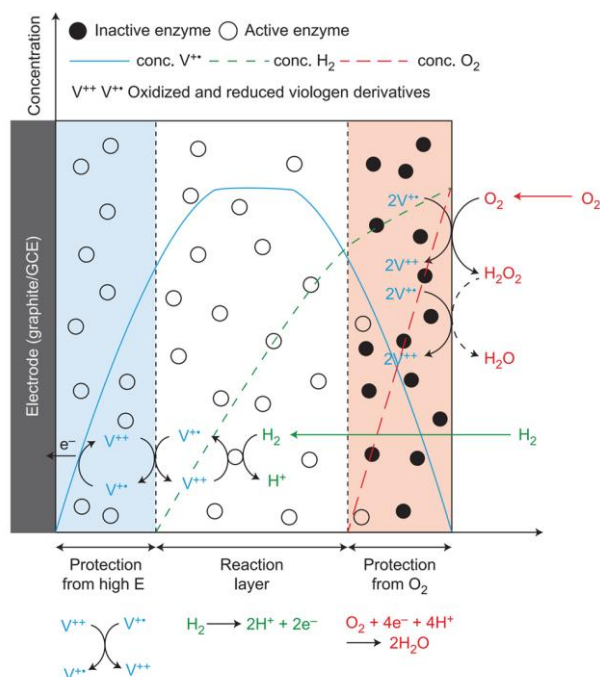


**Figure 19.** Schematic drawing of the double protection of hydrogenases by a viologen based redox hydrogel shield. Active and inactive hydrogenases are indicated by open and filled circles, respectively. Assumed steady-state concentration curves of reduced viologen (blue solid line),  $H_2$  (green dash line) and  $O_2$  (red dash line) are shown. Reprinted with permission<sup>540</sup>. Copyright 2014 Nature Publishing Group.

#### 4.5 Anti-biofouling of implantable glucose/ $O_2$ EFCs

Implantable glucose/ $O_2$  EFCs in blood suffer from biofouling process involving adsorption of layers of proteins and whole cells *etc.* that can impair the rate of diffusion of glucose and thus reduce the power output. Electrodes can be chemically modified with anti-biofouling layers that are hydrophilic (such as ethylene oxide functioning groups) or zwitterionics<sup>545,546</sup>. A range of coating membranes including Nafion®, cellulose acetate, chitosan, fibronectin and poly(styrene-sulphonate)/poly(l-lysine) have been evaluated for their ability to reduce levels of biofouling, using albumin in solution<sup>547</sup>. Fibronectin showed the best anti-biofouling effects with no significant differences in the voltammetric waves of  $[Ru(NH_3)_6]^{3+}$  after exposing to albumin. The use of an anti-biofouling conductive polymer, poly(sulfobetaine-3,4-ethylenedioxythiophene)

(PSBEDOT) which can be used to immobilize GOx is of interest <sup>548</sup>. PSBEDOT bears zwitterionic sulfobetaine side chains, resulting in a significant anti-biofouling electrode with only 8.4% protein adsorption in 100% human blood plasma compared to a control electrode without zwitterionic side chains (PEDOT). The electrochemical response to glucose in human blood plasma at a PSBEDOT-GOx based electrode was twice of a PEDOT-GOx electrode. It should be noted that modifications with anti-biofouling polymers may hinder the rate of ET and the diffusion of the substrate. Alternatively, nanoporous structured electrodes with similar pore sizes to the macromolecules (such as albumin) can repel proteins <sup>549</sup>, leaving the inner pores available for small molecules (such as redox mediators and fuels).

Blood clotting, occurring when placing foreign EFCs in the blood circulation, causes significant disturbance for the glucose transport. It requires the bioelectrodes to be biocompatible causing no inflammatory reactions when implanted in extra-cellular fluids between organs <sup>39</sup>. It's more challenging to make a hemocompatible surface to be implanted in the blood avoiding to destruct blood components <sup>39</sup>. Cosnier's group utilized dialysis bags to wrap carbon-based electrodes to prevent the leakage of immobilized species which were then placed in a Dacron® sleeve to improve biocompatibility <sup>31,34</sup>. However, the employment of dialysis bags requires a large volume EFC. The coating of biocompatible polymer layers, *e.g.* chitosan <sup>550</sup> and collagen, *etc.* is another route <sup>8</sup>. Miyake et al. introduced a 2-methacryloyloxyethyl phosphorylcholine (MPC)-polymer coating to make carbon electrodes biocompatible <sup>341</sup>, without which obvious blood clotting was observed after 2 h immersion in blood. A needle-type glucose/O<sub>2</sub> EFC in a rabbit vein displayed a power output of 0.42 μW at 0.56 V, while the cell without a MPC coating had ca. 40% lower in power <sup>341</sup>. The decreased performance was likely attributed to the presence of blood clots.

Cadet et al. tested Os-complex modified polymer mediated glucose/O<sub>2</sub> EFCs in 30 anonymized and disease-free whole blood samples <sup>273</sup>. A cellulose dialysis bag was placed on the EFCs. Comparison of the faradaic signal from the Os complexes in buffer and in blood showed that



both possessed well-defined redox waves, with a 27 mV larger peak separation in blood. This was explained by interferences caused by endogenous human blood constituents, a reversible process as the electrochemical waves were recovered by transferring the electrodes from blood to buffer. The lower catalytic response of the bioelectrodes in blood was mainly attributed to mass transport limitation as both currents increased with stirring rate. Ascorbate interference<sup>551</sup> upon the biocathode was not observed<sup>273</sup>, which may be explained by the high selectivity of the bioelectrode with the Os-complex modified polymer. Over the course of 6 h continuous operation in blood<sup>273</sup>, the dialysis bag protected both enzymes, retaining twice the response of the unprotected system.

Non-invasive EFCs (**Figure 20**) operating in saliva<sup>552-554</sup>, sweat<sup>48</sup> and tear<sup>142,506</sup> are of interest as activators for wearable medical devices. Unlike implantable EFCs, non-invasive devices do not come into contact with blood and do not involve skin piercing, tissue damage or cause pain. Such biodevices are typically not exposed to the immune system so that tissue inflammatory responses can be avoided. They are also called “wearable EFCs”<sup>47</sup>, can be easily discarded and replaced and generally are flexible structures, with adequate oxygen supply. An interesting example is a contact lens supported microelectronic systems for glucose concentration monitoring in tears that was proposed in 2013<sup>555</sup>. Xiao et al. reported a flexible lactate/O<sub>2</sub> EFC on nanoporous gold electrodes that was mounted onto commercially available contact lenses and produced electricity for more than 5.5 h in a solution of artificial tears<sup>556</sup>. Other examples are tattoo<sup>48</sup> and textile<sup>49</sup> based EFCs producing electricity from human sweat based lactate. However, this approach is still not an effective solution for powering implantable medical devices. Another emerging group of skin borne EFCs are those using solid-state hydrogel electrolytes with preloaded sugars, which can generate biopower when the human subject is not perspiring<sup>50,557-560</sup>.

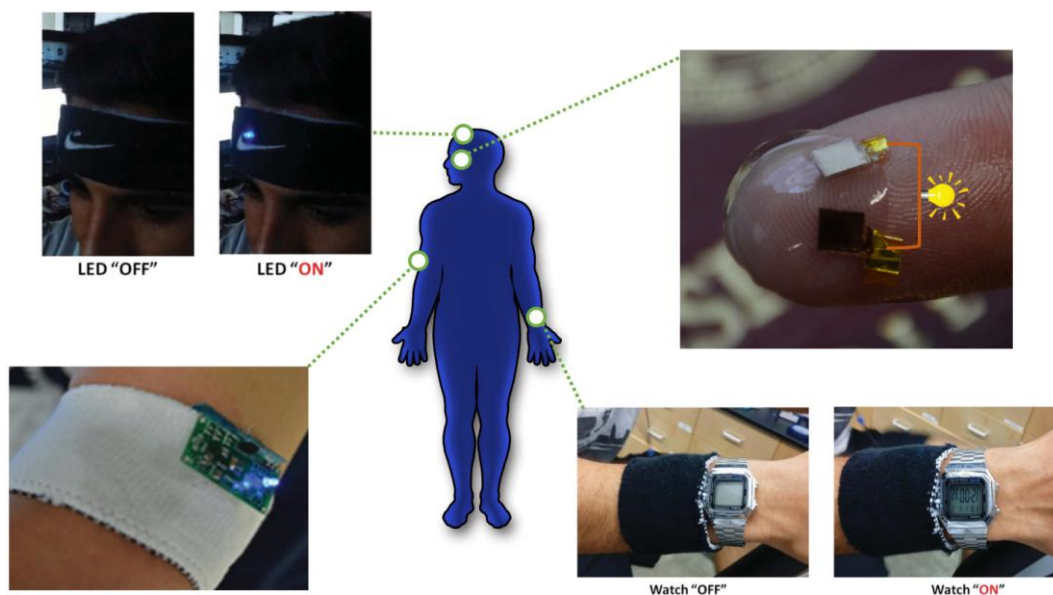


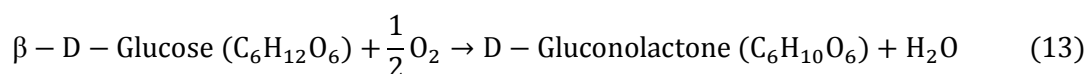
**Figure 20.** Various wearable lactate EFCs that are possible to be fueled with lactate in tears or sweats. Reprinted with permission<sup>49,54,556</sup>. Copyright 2014, 2017 Royal Society of Chemistry; Copyright 2018 American Chemical Society.

## 5. Approaches for the improvement of EFCs' cell voltage

An additional critical challenge of EFCs is that their output voltages are generally incompatible with the values required to operate commercially available microelectronic devices (1-3 V<sup>143,561</sup>), although transistors requiring an operating voltage of 0.5 V and even lower have been developed<sup>562-564</sup>. The OCV of a biofuel cell is limited by the thermodynamic values for the species used as fuel and oxidant. In the standard state, the relationship between the standard Gibbs free energy change  $\Delta G^0$  (kJ mol<sup>-1</sup>) and  $E^0$  (V) can be expressed by the equation<sup>565</sup>:

$$|\Delta G^0| = nFE^0 \quad (12)$$

$|\Delta G^0|$  of biochemical reactants have been summarized by Alberty et al.<sup>566</sup> For example, a glucose/O<sub>2</sub> EFC using GOx or GDH as bioanode catalysts undergoes an overall reaction:



As  $|\Delta G^0|$  for eq. 13 is 227.23 kJ mol<sup>-1</sup> at 25 °C, pH 7 and 0.1 M glucose,  $n = 2$ , the value of  $E^0_{\text{cell}}$  is 1.18 V.

The typical polarization curve of an EFC (**Figure 21B**) presents a wide range of information such as the experimental OCV and maximum cell current/current density. In practice, the registered OCV of an EFC is much lower than  $E^{\circ}$  due to the presence of three types of potential losses, namely kinetic ( $\eta_{act}$ ), ohmic losses ( $I\sum R$ ) and mass transport losses ( $\eta_{diff}$ ), in the system. The relationship between registered OCV and  $E^{\circ}$  can be determined by<sup>11</sup>:

$$OCV = E^{\circ} - \eta_{act} - I\sum R - \eta_{diff} \quad (14)$$

where  $\eta_{act}$  is the overpotential required to overcome energy barriers on the electrode-electrolyte interfaces;  $\eta_{act} = \eta_{act,a} + \eta_{act,c}$ , where the subscripts a and c indicate the anodic and cathodic reactions, respectively;  $\sum R$  is the sum of all resistances associated with current  $I$  that flows through the electrodes, electrolyte and various interconnections;  $\eta_{diff}$  is the mass transport based overpotential due to reactant diffusion limitations. Three characteristic regions, distinguished by the different governing overpotentials ( $\eta_{act}$ ,  $I\sum R$  and  $\eta_{diff}$ ), can be found in a typical polarization curve (**Figure 21B**)<sup>7</sup>.

In region a) governed by  $\eta_{act}$  where the reactants (fuels and oxidants) are abundant and the current is low, the rate of reaction is solely controlled by the rate of heterogenous ET. The current  $I$  can be expressed using the Butler-Volmer equation<sup>567</sup>:

$$I = Ai_0 \left( \exp\left(-\frac{\alpha nF\eta_{act,c}}{RT}\right) - \exp\left(\frac{(1-\alpha)nF\eta_{act,a}}{RT}\right) \right) \quad (15)$$

Where  $i_0$  is the exchange current density.

In the high overpotential region ( $>118/n$  mV), the Butler-Volmer equation can be simplified to the Tafel equation<sup>567</sup>:

$$\eta_{act} = b \log_{10}\left(\frac{i}{i_0}\right) \quad (16)$$

where  $i$  is the current density;  $b$  is the Tafel slope (mV  $\text{dec}^{-1}$ ). Eq. 16 allows the determination of  $i_0$  and  $b$ <sup>568</sup>. Further, the rate of electron transfer rate ( $k_{et}$ ) can be obtained from:

$$i_0 = nFAk_{et}[S] \quad (17)$$

Visually, the measured OCV can be read from the power density profile or the polarization curve (**Figure 21**), which is consistent with the difference between the onset potential for the oxidation of the fuel and the reduction of the oxidant, respectively<sup>7</sup>. Although the term “onset potential” is quite fuzzy due to the difficulties in defining the exact starting points for electrochemical oxidation or reduction<sup>11</sup>, it can be obtained, in practice, by comparing the potential-current profiles of bioelectrodes in the presence and absence of the substrate (**Figure 21A**)<sup>11,569</sup>. Thus, the measured OCV can also be expressed as<sup>80</sup>:

$$OCV = E_c^{onset} - E_a^{onset} - I \sum R_e \quad (18)$$

$$OCV = (E_c - \eta_c) - (E_a - \eta_a) - I \sum R_e \quad (19)$$

where  $R_e$  is the resistance,  $E_c^{onset}$  and  $E_a^{onset}$  are the observed onset potentials for the cathode and anode,  $E_c$  and  $E_a$  are the thermodynamic onset potentials at the cathode and anode, respectively,  $\eta_b$  and  $\eta_a$  are the overpotentials for cathode and anode, respectively. Eqs. 18 and 19 suggest the strategies to maximize OCV of a single EFC via bring the starting potentials of both bioanode and biocathode closer to those of the enzymes/cofactors<sup>4</sup>.

For biocathodes, MCOs based bioelectrodes undergoing DET with low overpotentials are widely adopted. Fungal Lac possesses a much higher redox potential (up to 0.78 V vs. SHE<sup>29</sup>) for the T1 Cu site than that of BOD (ca. 0.67 V vs. SHE<sup>21</sup>). BOD exhibits higher activity at physiological conditions (i.e. neutral pH) and is less sensitive to chloride ions at neutral pH, making it a better candidate for implantable EFCs. Lac is usually inhibited by chloride ions and is active in the pH range 4-5, making it a suitable choice for non-implantable applications. On the bioanode side, NAD-dependent dehydrogenase can present a low onset potential due to the low formal potential of  $NAD^+$  ( $E_{NADH/NAD^+}^{o'}$ : -0.33 V vs. SHE<sup>570</sup>). FAD-dependent dehydrogenases ( $E_{FADH_2/FAD}^{o'}$ : -0.18 V<sup>571</sup>) are preferred over PQQ ( $E_{PQQH_2/PQQ}^{o'}$ : 0.12 V vs. SHE<sup>572</sup>) due to the lower redox potential. While  $O_2$ -sensitive [NiFe] hydrogenases present a very low overpotential for  $H_2$  oxidation, the  $O_2$ -tolerant membrane ones oxidize  $H_2$  at potentials around 150 mV higher.

Nevertheless,  $H_2/O_2$  EFCs based on  $O_2$ -tolerant hydrogenases and BOD possess OCV greater than 1.1 V<sup>88</sup>.

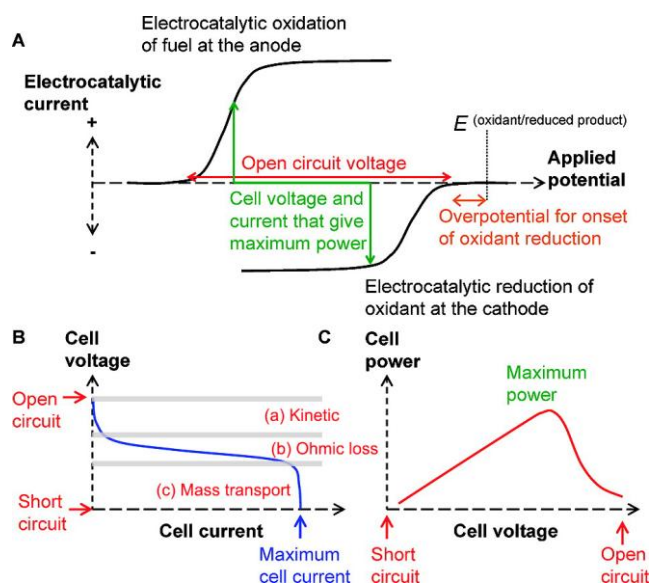


**Figure 21.** (A) Polarisation curves of a bioanode and biocathode. (B) Voltage-current profile (B) and power density-voltage profile of an EFC. Key parameters of an EFC are highlighted. Reprinted with permission<sup>7</sup>. Copyright 2018 American Chemical Society.

## 5.1 Mediator optimization

EFCs based on DET bioelectrocatalysis on both the anode and cathode without the involvement of mediators are promising as they avoid any possible toxicity effects of the mediator, in particular in the use of implantable EFCs<sup>125,573</sup>. They generally display a higher OCV than those based on MET. However, the following examples show that MET can generate higher OCVs. In an example of a FDH modified electrode, the presence of ubiquinone as the mediator with a redox potential in between those of FAD (-0.034 V vs. SHE at pH 5.5) and heme (0.135 V vs. SHE at pH 5.5) enables transfer of electrons directly from FAD directly rather than via the heme<sup>218</sup>. In other words, due to the lower energy barrier to be overcome, the external low-redox-potential mediators substitute the role of the “built-in mediator” (heme) in communicating with FAD catalytic center, leading to lower overpotentials. Similarly, when using an Os redox polymer with a lower potential than that of heme<sup>277</sup>, *MtCDH* modified electrode had

a 150 mV lower onset potential for MET than that of DET. These examples emphasize the importance of engineering the redox potential of mediators for enzymes undergoing MET.

ET between the enzyme and the mediator is driven by the mediator-induced overpotential ( $\Delta E_{et}$ ), i.e. the difference between the redox potential of the enzyme catalytic active center and the mediator <sup>574</sup>. According to Marcus theory, the rate constant ( $k_{et}$ ) between an enzyme and mediator is given by <sup>325</sup>

$$k_{et} = Z \exp\left[-\frac{(\lambda - nF\Delta E_{et})^2}{4\lambda RT}\right] \quad (20)$$

where  $Z$  is the frequency factor,  $\lambda$  is the molecular reorganization free energy,  $R$  is the gas constant,  $T$  is the absolute temperature. Mathematically, the relationship between  $k_{et}$  and  $\Delta E_{et}$  displays a quadratic behaviour, with a region where  $k_{et}$  increases with  $\Delta E_{et}$  (normal region) and an inverted region where  $k_{et}$  decreases with increasing  $\Delta E_{et}$ . Typically, the inverted region is not observed, which is likely due to the fact that at high  $\Delta E_{et}$  the biocatalytic reaction becomes mass-transport limited <sup>574</sup>.  $\Delta E_{et}$  should be as high as possible to enhance the current density, but that can result in higher overpotentials, lowering the OCV. Improvements in the OCV and power density of a mediated EFC are mutually exclusive <sup>64</sup>, thus, the value of  $\Delta E_{et}$  should be optimised to yield both a high current density and a high OCV.

In practice, an efficient combination of redox mediator and enzyme requires optimization experiments <sup>325,575</sup>. The co-immobilization of redox mediator and enzyme is essential for implantable EFCs using MET based bioelectrodes to avoid leakage. Redox polymers introduced by Heller *et al.* <sup>271,576,577</sup> are the most important group of mediators for the construction of EFCs <sup>578</sup>. Redox polymers also act as the host matrix to immobilize enzymes via electrostatic interaction, entrapment and/or chemically cross-linking, resulting in a catalytic film permeable to the fuels and necessary ions <sup>271</sup>. Polymer backbones bearing organometallic groups (*e.g.* Os complex <sup>578</sup>, ferrocene <sup>64,389,579,580</sup>, cobaltocene <sup>581</sup>), organic dyes (*e.g.* viologen <sup>540,581</sup>, phenothiazine <sup>507,582</sup>) and quinone <sup>64,583,584</sup> have been synthesized for mediated bioelectrodes. The

utilization of redox polymers allows electrical connection of multilayered enzymes, irrespective of enzyme orientation, leading to higher current output. The formal potentials of redox polymers (**Figure 22**) are determined primarily by the type and the nature of the covalently bound redox couples,<sup>120,271,585</sup> and redox polymers based bioelectrodes with optimized redox potentials can be fabricated by using the appropriately designed redox species.<sup>580,586-588</sup>

Bartlett and Pratt developed a comprehensive model of the diffusion and kinetic effects within a uniform layer containing both immobilized GOx and mediator on an electrode surface<sup>589</sup>, which can be used to understand the limiting factors in redox-polymer based bioelectrodes. Experimental variables including enzyme loading, film thickness, substrate concentration, mediator concentration and electrode potential can be considered using this approach. The summary case diagrams can be used to predict the electrochemical response of an electrode under specified experimental conditions. It thus important, although difficult, to accurately determine the effective enzyme and mediator concentrations on the electrode.

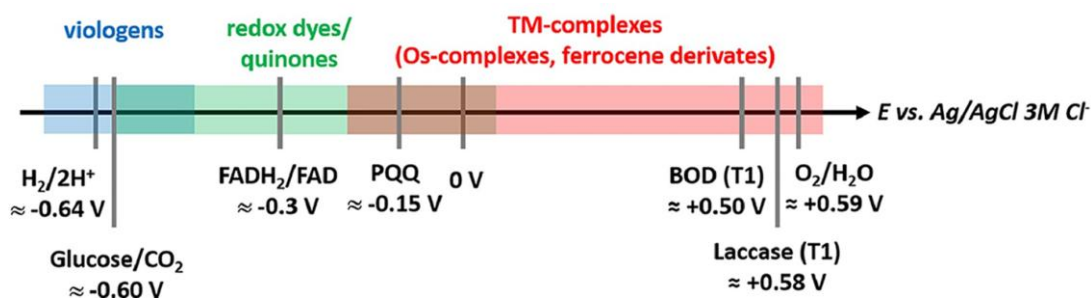


**Figure 22.** The range of redox potentials of enzyme cofactors and common mediators. Reprinted with permission from ref<sup>120</sup>. Copyright 2018 Elsevier.

An example is Os-complex based redox polymers, whose formal potential can be adjusted by using different ligands.<sup>11,586,590,591</sup> Schuhmann's group has reported a series of Os-complex modified polymers with redox potentials, for example, close to 0.2 V vs. SHE.<sup>587,592</sup> Consequently, glucose/O<sub>2</sub> EFCs with OCVs of 0.50 ~ 0.54 V were developed. In addition, EFCs with improved OCVs of 0.6 ~ 0.8 V could be achieved by combination of

phenothiazine- or quinone derivative-modified redox polymer based bioanodes.<sup>64</sup> For more negative redox potentials, viologen based redox polymers can be used, for example with a redox potential of -0.3 vs. SHE (**Figure 23**).<sup>540</sup> H<sub>2</sub>/O<sub>2</sub> EFCs with high OCVs of ~1 V were fabricated by combination of such viologen-based polymer MET-type H<sub>2</sub> bioanodes and DET-type O<sub>2</sub> biocathodes. Various ligands were synthesized to tune the redox potentials of the hydrogels<sup>593</sup>. A similar viologen polymer-modified bioelectrode has been reported by Kano's group for formate oxidation by FDH, and a formate/O<sub>2</sub> EFC with an OCV of 1.2 V was recorded.<sup>15</sup> Compared to the DET-type bioelectrocatalysis and MET-type bioelectrocatalysis using free mediators, redox polymer-based bioelectrocatalysis possess advantages such as rapid rates of ET, low levels of mediators and/or enzyme leakage. From this viewpoint, selection or development of redox polymers with specific properties, for example, low redox potential, high biocompatibility and stability, good permeability for mass transfer of substrate and product through the film (i.e. tunable polymer film thickness), as well as high affinity to enzymes, have significant potential.

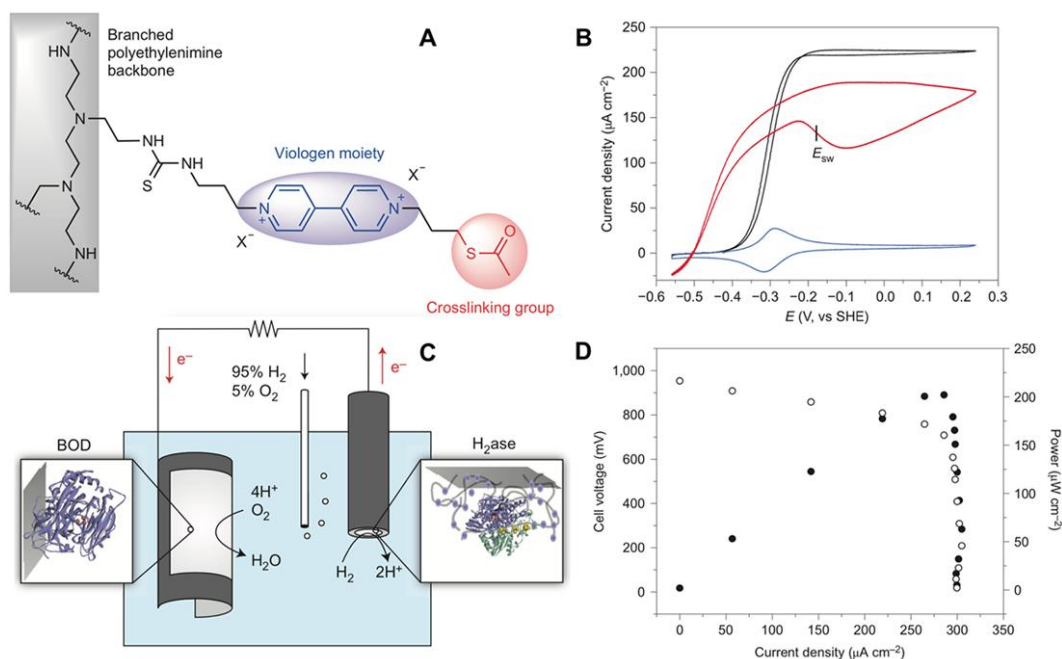


**Figure 23.** Viologen-redox polymer-based H<sub>2</sub>/O<sub>2</sub> biofuel cell. A) Chemical structure of viologen-modified polymer; B) Cyclic voltammograms of a [NiFe] hydrogenase from *Desulfovibrio vulgaris* Miyazaki F/polymer electrode under H<sub>2</sub> (black) and CO (blue) and a covalently modified electrode with the hydrogenase in DET configuration (red). Experimental



conditions: electrode rotation rate of 2,000 rpm, pH 7.0, 40 °C, 1 mV s<sup>-1</sup> and 1 bar of H<sub>2</sub> (black and red traces), 20 mV s<sup>-1</sup> and 1 bar of CO (blue trace). C) Schematic diagram of a single compartment EFC, H<sub>2</sub>/O<sub>2</sub> mixed feed, hydrogenase-coated anode and oversized O<sub>2</sub>-reducing BOD-coated cathode. D) Cell voltage (open circles) and power density (filled circles) versus current density for the H<sub>2</sub>/O<sub>2</sub> EFCs. Reproduced with permission from ref <sup>540</sup>. Copyright 2014 Nature Publishing Group.

Gallaway et al. combined experimental data with numerical modeling to examine the influence of  $\Delta E_{\text{et}}$  of a series of Os redox polymers on *Tv*Lac catalyzed oxygen reduction at pH 4 <sup>574</sup>. When  $\Delta E_{\text{et}}$  was lower than 300 mV, a larger  $\Delta E_{\text{et}}$  significantly enhanced the power output. The optimum  $\Delta E_{\text{et}}$  to obtain maximum power from an EFC using a non-limiting anode with an onset potential of 0 V vs. SHE was 0.17 V. Zafar et al. studied the effects of using five different Os-complex modified polymers with redox potentials over the range -0.07 to +0.36 V vs. SHE on the performance of a mediated *Am*PDH bioanode <sup>535</sup>.  $\Delta E_{\text{et}}$  and the structural properties including flexibility and length of the tether were crucial for the overall performance. The results indicated that an Os-complex modified polymer with a moderately high  $\Delta E_{\text{et}}$ , accompanying with a long tether between the Os complex and the backbone with a greatly enhanced ET collision frequency, gave higher current densities. An Os-complex modified polymer with a redox potential of 0.14 V vs. SHE, that is slightly (ca. 20 mV) higher than that of the bound FAD of *Am*PDH (-0.17 V), was selected to be optimal mediator in terms of high current density and low onset potential <sup>535</sup>. On comparing six different Os-complex modified polymers with redox potentials ranging from -0.02 to 0.49 V vs. SHE for *Glomerella cingulata* FAD-GDH <sup>590</sup>, two Os-complex modified polymers with redox potentials of 0.31 and 0.42 V vs. SHE yielded the highest current densities. The above reports imply that a moderate  $\Delta E_{\text{et}}$  is responsible for the high current density, allowing for optimization of OCV further. Heller suggested a  $\Delta E_{\text{et}}$  of 50 mV for implantable glucose/O<sub>2</sub> EFCs using both mediated bioanodes and biocathode in order to obtain practical OCVs <sup>578</sup>. Based on such a design, Heller's group reported a glucose/O<sub>2</sub> EFC presenting an OCV of ca. 1 V and a  $P_{\text{max}}$  of 350  $\mu\text{W cm}^{-2}$  in an air-saturated 15 mM glucose solution at pH 5 <sup>578</sup>. It consisted of a GOx bioanode mediated by an Os-complex modified polymer with a

13-atom-long flexible tether (ca. 0 V vs. SHE)<sup>594</sup>, and a Lac biocathode with an Os-complex modified polymer bearing 8-atom-long tethers (ca. 0.75 V vs. SHE). It should be noted that O<sub>2</sub> can be reduced at the low-redox-potential Os-complex modified polymer producing H<sub>2</sub>O<sub>2</sub><sup>595</sup> and thus the interference of O<sub>2</sub> on the mediator itself<sup>540</sup> should also be considered.

Minteer et al. compared soluble 1,2- and 1,4- naphthoquinone (NQ) mediated FAD-GDH bioanodes and found that 1,2-NQ derivatives had larger catalytic current densities, which can be explained by the high values of  $\Delta E_{et}$ <sup>64</sup>. The obtained current densities between different NQ species with different structural reorganization or enzymatic affinity effects were not comparable. On grafting 1,2- and 1,4-NQ-epoxy groups onto linear LPEI, the NQ-2-LPEI showed a lower mediated bioelectrocatalytic response in comparison to that of NQ-4-LPEI. The NQ-4-LPEI/GDH-FDH bioanode displayed an onset potential of ca. -0.01 V vs. SHE. In combination with a non-limiting carbon felt/BOD biocathode, the resultant EFC registered an OCV of ca. 0.87 V and a  $P_{max}$  of  $2.3 \pm 0.2$  mW cm<sup>-2</sup> in air-saturated 100 mM glucose at pH 6.5<sup>64</sup>.

## 5.2 Serial connection

Unlike microbial fuel cells which often encounter voltage reversal when stacked, EFCs do not have this issue<sup>596</sup>. Serial assembly of conventional fuel cells can be employed with EFCs to amplify the output voltage, while the connection in parallel can enable increases in current density<sup>182,597</sup>. Sakai reported a carbon fibre based glucose/O<sub>2</sub> EFC with NAD<sup>+</sup>-dependent GDH, BOD and mediators co-immobilized showing a  $P_{max}$  of  $1.45 \pm 0.24$  mW cm<sup>-2</sup> at 0.3 V and a OCV of 0.8 V in the presence of 400 mM glucose<sup>52</sup>. A stacked cell of two individual EFCs allowed the successful operation of a radio-controlled car (16.5 g) and a memory-type Walkman continuously for more than 2 h. A microfluidic biobattery utilizing NAD<sup>+</sup>-dependent ADH and Pt/C at the bioanode and cathode, respectively, generated an OCV of 0.93 V which was increased to 1.44 V on connecting two cells in series<sup>598</sup>. A H<sub>2</sub>/O<sub>2</sub> EFC composed of two stacks of four cells in parallel with OCV and  $P_{max}$  of 2.09 V and 7.84 mW, respectively, was used to power an electronic clock and red LEDs for 8 h with no decrease in light intensity<sup>182</sup>. Miyake et al. reported

a laminated stack of EFCS consisting of fructose oxidizing bioanode fabrics, air-breathing biocathode fabrics and a sandwiched hydrogel layer containing fructose<sup>50</sup>. A triple-layer stack produced an OCV of 2.09 V, a 2.8-fold increase over that of a single set cell (0.74 V) and a  $P_{\max}$  of 0.64 mW at 1.21 V, that was able to power LEDs. Paper based EFCs are cost-effective as disposable devices<sup>19</sup>. A screen-printed circular-type EFC system, composed of a series of 5 individual cells with a single cell OCV of 0.57 V, generated an OCV of 2.65 V and illuminated an LED directly<sup>599</sup>.

The overall performance of interconnected EFC in serial is limited by the weakest EFC. Preparation of the stack needs to be carefully controlled and reproducible, especially with regard to material preparation and to the immobilization of the enzymes. Moreover, the serial-connection of EFCs with metal leads requires that individual EFC be isolated properly to avoid short-circuits introduced by ion-conductive electrolytes. MacVittie et al. prepared a buckypaper supported EFC composed of a PQQ-GDH bioanode and a Lac biocathode achieving an OCV of 0.54 V<sup>33</sup>. Two EFCs implanted in a serial-configuration in separate claws of a lobster showed an OCV of only ca. 0.5–0.6 V. The potential of the serially connected EFCs was limited due to the ionic conductivity in the same body. Serial connection of two lobsters bearing EFCs resulted in a voltage of ca. 1 V. A fluidic system comprised of five EFCs connected in series was able to generate an OCV of ca. 3 V sufficient to activate a pacemaker. Similarly, an implantable glucose/O<sub>2</sub> EFC in a clam registered an OCV of ca. 300–400 mV and the serial connection of 3 “electrified” clams afforded an OCV of ca. 800 mV<sup>36</sup>. Due to the above-mentioned constraint caused by the ionic conductivity, serial configuration has been primarily used for *in vitro* experimentation. As a solution, superhydrophobic surface may help to build ionic isolation between signal cells<sup>597</sup>. Three glucose/O<sub>2</sub> EFCs (OCV: 0.35 V) were series-connected on a fluidic chip and air valves were introduced between cells by a lotus leaf-like superhydrophobic structure. The possible output voltage was ca. 1 V.

### 5.3 Employment of external boost converter

The output voltage of an EFC can be boosted by externally connecting a charge pump as a DC-DC converter<sup>600</sup>. For example, a voltage-doubler operates by charging of two capacitors in parallel separately followed by discharge in series. Many examples in the recent literature illustrate this concept. In 2013, Southcott et al. prepared a fluidic glucose/O<sub>2</sub> EFC with an OCV of 0.47 V in a serum solution that mimick the human blood circulatory system<sup>601</sup>. A single EFC was connected to a combination of a charge pump with a DC-DC converter, which increased the voltage from 0.3 to 2 V and from 2 to 3 V, respectively. The resultant device enabled the continuous operation of a commercial pacemaker<sup>601</sup>. Coupling of a glucose/O<sub>2</sub> biobattery with a charge pump and a capacitor resulted in 1.8 V electric pulses at different intervals determined by the fuel concentration<sup>381</sup>. A commercial BQ25504 boost converter could amplify an input voltage in the range of 0.3-0.5 V up to 3 V<sup>34</sup>. The EFC/boost converter/capacitor assembly enabled a glucose/O<sub>2</sub> EFC implanted in rats with an OCV of 0.57 V to intermittently power a digital thermometer (power consumption: 50  $\mu$ A at 1.5 V) and a LED (4.1 mA at 2.9 V). The output of other reported glucose/O<sub>2</sub> EFCs could be amplified using similar boosting systems (OCV from 0.6 V to 2.3 V) to power a wireless transmitter<sup>323</sup>, from 0.3 V to 1.8 V to power a LED<sup>324</sup> and from 0.145 V to 2.586 V for a glucometer<sup>561</sup>. Those amplified voltage output can be used directly to activate microelectronic devices.

Lactate/O<sub>2</sub> EFCs consuming sweat and tear lactate are of interest to activate wearable medical devices. A power unit composed of an EFC/voltage booster couple can be easily combined into wearable devices. For example, two lactate/O<sub>2</sub> biobatteries with an OCV of 0.67 V in parallel were able to generate 6  $\mu$ W at 0.376 V, which was scaled up to 3.2 V to periodically to illuminate a blue LED bubble requiring 2.5 V and 0.5 mA<sup>49</sup>. A lactate/O<sub>2</sub> EFC with an OCV of 0.87 V was used to provide the operational voltage of an electronic watch (ca. 3 V)<sup>506</sup>. A biobattery using real sweat lactate with an OCV of 0.5 V was coupled with a DC-DC converter/capacitor circuit to produce a 3.5 V pulse with a width of 53 s<sup>54</sup>.

EFCs based on other fuels have also been reported. A lactose/O<sub>2</sub> EFC with an OCV of 0.73 V has been integrated with a voltage amplifier and a capacitor<sup>289</sup>, which was coupled into wireless carbohydrate and oxygen biosensor platforms with a threshold of 44  $\mu$ A and 0.57 V. Three fructose/O<sub>2</sub> EFCs with an OCV of 0.7 V in series generated 2 mW and 2 V, which was integrated with a minipotentiostat containing a DC-DC converter with an output voltage of 4 V<sup>388</sup>. The integrated device enabled an oxygen sensor allowing ten measurements in the pulse mode without any disturbances. A H<sub>2</sub>/O<sub>2</sub> EFC registering an OCV of 1.12 V can be boosted over 6 V to power a wireless device sending data every 25 s in a course of 7 hours continuous operation<sup>382</sup>.

It can be concluded that most reports utilized the DC-DC converter/capacitor junction with a pulse function. Only few reports have claimed that they can power an external device continuously<sup>601</sup>. It should be noted that part of the generated power is consumed by the DC-DC converter as a price of the voltage boost, posing extra demand on EFC's output power<sup>561</sup>. The commercial BQ25504 boost converter requires a net current input from 10 to 100  $\mu$ A<sup>34</sup>, requiring a high-current-density EFC. Otherwise a larger size electrode is required, hindering the miniaturization of the implantable power source. The need for an external circuit increases the size of the devices, making device encapsulation more complex.

## **6. Conclusions and perspectives**

EFCs are expected to be one of the next-generation energy conversion systems because they utilize bioavailable, renewable and diverse biocatalysts and biosourced fuels, operate under mild and safe conditions, and possess high theoretical energy-conversion efficiencies. In this review, we discuss four main obstacles, namely low energy density, power density, stability and output voltage, that hinder the successful development of EFCs and summarize a range of potential solutions. In spite of their high activity, the high specificity of enzymes typically restricts the ability of an enzyme to catalyze just a single reaction, leading to low fuel utilization efficiency and thus low power densities in single-enzyme based EFCs. A rationally designed bioanode

consisting of enzyme cascades or multi-step pathways has been proposed to improve the overall energy density. Additionally, approaches that utilise engineered enzymes to increase their catalytic performance, “wiring” enzyme with favourable orientation to facilitate improved rates of direct electron transfer, utilising nanomaterials to achieve high enzyme loadings, smart design of electrodes and cell for enhanced mass transfer, as well as constructing EFC and biocapacitor hybrid devices, have all been developed for high power density. A range of approaches ranging from enzyme immobilization to biochemical engineering have been investigated to extend the lifetime of EFCs. Microbial surface displayed enzymes, which are anchored on a cell surface mimicking the micro-environment that enzymes function in nature, are expected to provide enzymes with long term operational stability. Improved cell voltages have been realized by well-designed bioelectrode (MET or DET) with low overpotentials, series connection of cells, or external voltage boosters.

It should be noted that these obstacles are identified from the point of view of the measurable performance of EFCs'. Many of the strategies mentioned above can simultaneously address more than one practical issues. For example, enzyme cascades can also be used to improve the power density of an EFC while achieving the complete oxidation of the fuel <sup>124</sup>. Enzyme immobilization also plays a key role in increasing the power density of various DET-type EFCs as it is important to appropriately orient DET-capable enzymes to minimise the distances of electron transfer between enzymes and electrodes <sup>21</sup>. These combined strategies can generate synergistic effects to enhance the performance of EFCs and should be addressed in combination rather than individually.

In addition to increasing performance metrics of EFCs, expanding their functionalities is highly promising to enhance the practicability. As already mentioned, self-powered biosensors employing EFCs to function simultaneously as a power source and as a sensor offer the possibility to fabricate instrument-free (at least potentiostat-free) diagnostic systems <sup>86,151,602</sup>. A self-powered biosensor is generally based on the preparation of an EFC generating power that is

proportional to the concentration of the analyte, which can be the fuel<sup>324,443,507,603,604</sup>, inhibitor<sup>605-607</sup>, activator,<sup>608</sup> biorecognition element<sup>609-611</sup> for enzymes used in the EFC. This type of biosensor is promising due to features of portability, miniaturization and low-cost. Operational stability issue can be overcome by fabricating disposable devices.

Rather than employing EFCs to power existing devices that require high power and voltage, new concepts, i.e. self-power bioelectronics<sup>149</sup>, which utilize EFCs directly to achieve specific functions can be more feasible for practical applications. Unlike batteries requiring careful encapsulation to avoid the direct contact of the battery active materials and the body, EFCs possess the merit of ease-of-miniaturization as the bioelectrodes can be used directly in the body. A recently reported EFC/supercapacitor system can function as a pulse generator to mimic a cardiac pacemaker delivering 10  $\mu$ A pulses for 0.5 ms at a frequency of 0.2 Hz<sup>283</sup>. This is different from previous attempts to use EFCs to power a commercial pacemaker<sup>33</sup>, which required a minimum voltage input of 3 V. EFC based controlled drug release is an emerging area of interest. In preliminary studies, an iontophoretic system using built-in EFCs allowed transdermal release of compounds into the skin<sup>558</sup> and to heal skin wounds<sup>557</sup>. It should be possible to use implantable EFCs to generate electric stimuli to trigger *in vivo* release of drugs<sup>612</sup>. Recent work<sup>613-615</sup> by Katz *et al.* using bioelectrodes for insulin release is of interest.

Enzymatic electrosynthesis<sup>616</sup> in an EFC, or self-powered bioelectrosynthesis, enables simultaneous electrosynthesis of valuable chemicals and energy harvest. Rather than using an external high-power output, self-powered bioelectrosynthesis can enable the production of valuable chemicals circumventing external electricity input<sup>617</sup>. Minteer *et al.* reported the bioelectrocatalytic reduction of N<sub>2</sub> to NH<sub>3</sub> as the biocathode of a H<sub>2</sub>-fuelled EFC<sup>153</sup>. This spontaneous process to produce ammonia is of interest to explore alternatives to the Haber-Bosch process. A H<sub>2</sub>/heptanal EFC reported recently revealed the ability to produce alkanes from aldehydes and alcohols<sup>152</sup>, opening the prospect of using EFCs to prepare renewable biofuels. Zhu *et al.* developed a self-powered system by combining an EFC and an enzymatic

electrosynthesis cell and demonstrated the high-efficient production of l-3,4-dihydroxyphenylalanine powered by glucose oxidation, suggesting that EFCs can be a promising power source for the synthesis of valuable chemicals and pharmaceuticals<sup>618</sup>.

Although there are significant obstacles to the development of EFCs, great opportunities to overcome these issues for practical applications are under investigation. Given that multidisplanar efforts have been taken to this prosperous topic, the time to transfer the lab-scale EFCs to real-life devices is not expected to be far away.

### Acknowledgements

This work was financially supported by National Natural Science Foundation of China (Nos. 81673172, 21475144, 21275152 and 91227116 to A.L., Nos. 21706273, 21878324 to Z.Z.) , Major Program of Shandong Province Natural Science Foundation (ZR2018ZC0125) to A.L., the CAS Pioneer Hundred Talent Program (Type C, reference # 2016-081) to Z.Z., Platform Chimie NanoBio ICMG FR 2607 (PCN-ICMG) to S.C., and ANR (ENZYMOR-ANR-16-CE05- 0024) to E.L.. X.X. acknowledges a Government of Ireland Postgraduate Scholarship (GOIPG/2014/659) and a H. C. Ørsted COFUND fellowship.

### References

- (1) Carrette, L.; Friedrich, K. A.; Stimming, U. Fuel Cells-Fundamentals and Applications. *Fuel Cells* **2001**, *1*, 5-39.
- (2) Windmiller, J. R.; Wang, J. Wearable Electrochemical Sensors and Biosensors: A Review. *Electroanalysis* **2013**, *25*, 29-46.
- (3) Katz, E.; MacVittie, K. Implanted Biofuel Cells Operating *in vivo* - Methods, Applications and Perspectives - Feature Article. *Energy Environ. Sci.* **2013**, *6*, 2791-2803.
- (4) Rasmussen, M.; Abdellaoui, S.; Minteer, S. D. Enzymatic Biofuel Cells: 30 Years of Critical Advancements. *Biosens. Bioelectron.* **2015**, *76*, 91-102.
- (5) Calabrese Barton, S.; Gallaway, J.; Atanassov, P. Enzymatic Biofuel Cells for Implantable and Microscale Devices. *Chem. Rev.* **2004**, *104*, 4867-4886.
- (6) Kim, J.; Jia, H.; Wang, P. Challenges in Biocatalysis for Enzyme-Based Biofuel Cells. *Biotechnol. Adv.* **2006**, *24*, 296-308.
- (7) Cracknell, J. A.; Vincent, K. A.; Armstrong, F. A. Enzymes as Working or Inspirational



- Electrocatalysts for Fuel Cells and Electrolysis. *Chem. Rev.* **2008**, *108*, 2439-2461.
- (8) Cosnier, S.; J. Gross, A.; Le Goff, A.; Holzinger, M. Recent Advances on Enzymatic Glucose/Oxygen and Hydrogen/Oxygen Biofuel Cells: Achievements and Limitations. *J. Power Sources* **2016**, *325*, 252-263.
- (9) Cosnier, S.; Gross, A. J.; Giroud, F.; Holzinger, M. Beyond the Hype Surrounding Biofuel Cells: What's the Future of Enzymatic Fuel Cells? *Curr. Opin. Electrochem.* **2018**, 148-155.
- (10) Yahiro, A. T.; Lee, S. M.; Kimble, D. O. Bioelectrochemistry: I. Enzyme Utilizing Bio-Fuel Cell Studies. *Biochim. Biophys. Acta* **1964**, *88*, 375-383.
- (11) Suzuki, A.; Mano, N.; Tsujimura, S. Lowering the Potential of Electroenzymatic Glucose Oxidation on Redox Hydrogel-Modified Porous Carbon Electrode. *Electrochim. Acta* **2017**, *232*, 581-585.
- (12) Agnès, C.; Reuillard, B.; Le Goff, A.; Holzinger, M.; Cosnier, S. A Double-Walled Carbon Nanotube-Based Glucose/H<sub>2</sub>O<sub>2</sub> Biofuel Cell Operating under Physiological Conditions. *Electrochem. Commun.* **2013**, *34*, 105-108.
- (13) Kamitaka, Y.; Tsujimura, S.; Setoyama, N.; Kajino, T.; Kano, K. Fructose/Dioxygen Biofuel Cell Based on Direct Electron Transfer-Type Bioelectrocatalysis. *Phys. Chem. Chem. Phys.* **2007**, *9*, 1793-1801.
- (14) Ramanavicius, A.; Kausaite, A.; Ramanaviciene, A. Enzymatic Biofuel Cell Based on Anode and Cathode Powered by Ethanol. *Biosens. Bioelectron.* **2008**, *24*, 767-772.
- (15) Sakai, K.; Kitazumi, Y.; Shirai, O.; Takagi, K.; Kano, K. High-Power Formate/Dioxygen Biofuel Cell Based on Mediated Electron Transfer Type Bioelectrocatalysis. *ACS Catal.* **2017**, *7*, 5668-5673.
- (16) Xia, H.-q.; So, K.; Kitazumi, Y.; Shirai, O.; Nishikawa, K.; Higuchi, Y.; Kano, K. Dual Gas-Diffusion Membrane- and Mediatorless Dihydrogen/Air-Breathing Biofuel Cell Operating at Room Temperature. *J. Power Sources* **2016**, *335*, 105-112.
- (17) Kontani, A.; Masuda, M.; Matsumura, H.; Nakamura, N.; Yohda, M.; Ohno, H. A Bioanode Using Thermostable Alcohol Dehydrogenase for an Ethanol Biofuel Cell Operating at High Temperatures. *Electroanalysis* **2014**, *26*, 682-686.
- (18) Wang, X.; Roger, M.; Clement, R.; Lecomte, S.; Biaso, F.; Abriata, L. A.; Mansuelle, P.; Mazurenko, I.; Giudici-Ortoni, M. T.; Lojou, E. *et al.* Electron Transfer in an Acidophilic Bacterium: Interaction between a Diheme Cytochrome and a Cupredoxin. *Chem. Sci.* **2018**, 4879-4891.
- (19) Zhang, L.; Zhou, M.; Wen, D.; Bai, L.; Lou, B.; Dong, S. Small-Size Biofuel Cell on Paper. *Biosens. Bioelectron.* **2012**, *35*, 155-159.
- (20) Ghindilis, A. L.; Atanasov, P.; Wilkins, E. Enzyme-Catalyzed Direct Electron Transfer: Fundamentals and Analytical Applications. *Electroanalysis* **1997**, *9*, 661-674.
- (21) Falk, M.; Blum, Z.; Shleev, S. Direct Electron Transfer Based Enzymatic Fuel Cells. *Electrochim. Acta* **2012**, *82*, 191-202.
- (22) Cass, A. E. G.; Davis, G.; Francis, G. D.; Hill, H. A. O.; Aston, W. J.; Higgins, I. J.; Plotkin, E. V.; Scott, L. D. L.; Turner, A. P. F. Ferrocene-Mediated Enzyme Electrode for Amperometric Determination of Glucose. *Anal. Chem.* **1984**, *56*, 667-671.
- (23) Kano, K.; Ikeda, T. Fundamentals and Practices of Mediated Bioelectrocatalysis. *Anal. Sci.* **2000**, *16*, 1013-1021.
- (24) Vincent, K. A.; Parkin, A.; Armstrong, F. A. Investigating and Exploiting the Electrocatalytic

- Properties of Hydrogenase. *Chem. Rev.* **2007**, *107*, 4366-4413.
- (25) Volbeda, A.; Charon, M.-H.; Piras, C.; Hatachikian, E. C.; Frey, M.; Fontecilla-Camps, J. C. Crystal Structure of Nickel-Iron Hydrogenase from *Desulfovibrio gigas*. *Nature* **1995**, *373*, 580-587.
- (26) Hibino, Y.; Kawai, S.; Kitazumi, Y.; Shirai, O.; Kano, K. Mutation of Heme c Axial Ligands in D-Fructose Dehydrogenase for Investigation of Electron Transfer Pathways and Reduction of Overpotential in Direct Electron Transfer-Type Bioelectrocatalysis. *Electrochem. Commun.* **2016**, *67*, 43-46.
- (27) Kawai, S.; Yakushi, T.; Matsushita, K.; Kitazumi, Y.; Shirai, O.; Kano, K. The Electron Transfer Pathway in Direct Electrochemical Communication of Fructose Dehydrogenase with Electrodes. *Electrochem. Commun.* **2014**, *38*, 28-31.
- (28) Kamitaka, Y.; Tsujimura, S.; Kataoka, K.; Sakurai, T.; Ikeda, T.; Kano, K. Effects of Axial Ligand Mutation of the Type I Copper Site in Bilirubin Oxidase on Direct Electron Transfer-Type Bioelectrocatalytic Reduction of Dioxygen. *J. Electroanal. Chem.* **2007**, *601*, 119-124.
- (29) Shleev, S.; Tkac, J.; Christenson, A.; Ruzgas, T.; Yaropolov, A. I.; Whittaker, J. W.; Gorton, L. Direct Electron Transfer between Copper-Containing Proteins and Electrodes. *Biosens. Bioelectron.* **2005**, *20*, 2517-2554.
- (30) Zebda, A.; Alcaraz, J.-P.; Vadgama, P.; Shleev, S.; Minteer, S. D.; Boucher, F.; Cinquin, P.; Martin, D. K. Challenges for Successful Implantation of Biofuel Cells. *Bioelectrochem.* **2018**, *124*, 57-72.
- (31) Cinquin, P.; Gondran, C.; Giroud, F.; Mazabrard, S.; Pellissier, A.; Boucher, F.; Alcaraz, J.-P.; Gorgy, K.; Lenouvel, F.; Mathé, S. *et al.* A Glucose Biofuel Cell Implanted in Rats. *PLOS ONE* **2010**, *5*, e10476.
- (32) El Ichi, S.; Zebda, A.; Alcaraz, J. P.; Laaroussi, A.; Boucher, F.; Boutonnat, J.; Reverdy-Bruas, N.; Chaussy, D.; Belgacem, M. N.; Cinquin, P. *et al.* Bioelectrodes Modified with Chitosan for Long-Term Energy Supply from the Body. *Energy Environ. Sci.* **2015**, *8*, 1017-1026.
- (33) MacVittie, K.; Halamek, J.; Halamkova, L.; Southcott, M.; Jemison, W. D.; Lobel, R.; Katz, E. From "Cyborg" Lobsters to a Pacemaker Powered by Implantable Biofuel Cells. *Energy Environ. Sci.* **2013**, *6*, 81-86.
- (34) Zebda, A.; Cosnier, S.; Alcaraz, J.-P.; Holzinger, M.; Le Goff, A.; Gondran, C.; Boucher, F.; Giroud, F.; Gorgy, K.; Lamraoui, H. Single Glucose Biofuel Cells Implanted in Rats Power Electronic Devices. *Sci. Rep.* **2013**, *3*, 1516.
- (35) Shoji, K.; Akiyama, Y.; Suzuki, M.; Nakamura, N.; Ohno, H.; Morishima, K. Biofuel Cell Backpack Insect and Its Application to Wireless Sensing. *Biosens. Bioelectron.* **2016**, *78*, 390-395.
- (36) Szczupak, A.; Halamek, J.; Halamkova, L.; Bocharova, V.; Alfonta, L.; Katz, E. Living Battery-Biofuel Cells Operating *in vivo* in Clams. *Energy Environ. Sci.* **2012**, *5*, 8891-8895.
- (37) Rasmussen, M.; Ritzmann, R. E.; Lee, I.; Pollack, A. J.; Scherson, D. An Implantable Biofuel Cell for a Live Insect. *J. Am. Chem. Soc.* **2012**, *134*, 1458-1460.
- (38) Castorena-Gonzalez, J. A.; Foote, C.; MacVittie, K.; Halánek, J.; Halámková, L.; Martínez-Lemus, L. A.; Katz, E. Biofuel Cell Operating *in vivo* in Rat. *Electroanalysis* **2013**, *25*, 1579-1584.
- (39) Cosnier, S.; Le Goff, A.; Holzinger, M. Towards Glucose Biofuel Cells Implanted in Human Body for Powering Artificial Organs: Review. *Electrochem. Commun.* **2014**, *38*, 19-23.
- (40) Babadi, A. A.; Bagheri, S.; Hamid, S. B. Progress on Implantable Biofuel Cell: Nano-Carbon

- Functionalization for Enzyme Immobilization Enhancement. *Biosens. Bioelectron.* **2016**, *79*, 850-860.
- (41) Reuillard, B.; Le Goff, A.; Agnes, C.; Holzinger, M.; Zebda, A.; Gondran, C.; Elouarzaki, K.; Cosnier, S. High Power Enzymatic Biofuel Cell Based on Naphthoquinone-Mediated Oxidation of Glucose by Glucose Oxidase in a Carbon Nanotube 3D Matrix. *Phys. Chem. Chem. Phys.* **2013**, *15*, 4892-4896.
- (42) Zhu, Z.; Kin Tam, T.; Sun, F.; You, C.; Percival Zhang, Y. H. A High-Energy-Density Sugar Biobattery Based on a Synthetic Enzymatic Pathway. *Nat. Commun.* **2014**, *5*, 3026.
- (43) Kang, Z.; Jiao, K.; Cheng, J.; Peng, R.; Jiao, S.; Hu, Z. A Novel Three-Dimensional Carbonized PANI1600@CNTs Network for Enhanced Enzymatic Biofuel Cell. *Biosens. Bioelectron.* **2018**, *101*, 60-65.
- (44) Gamella, M.; Koushanpour, A.; Katz, E. Biofuel Cells-Activation of Micro- and Macro-Electronic Devices. *Bioelectrochem.* **2018**, *119*, 33-42.
- (45) Bandodkar, A. J.; Wang, J. Wearable Biofuel Cells: A Review. *Electroanalysis* **2016**, *28*, 1188-1200.
- (46) Yu, Y.; Zhai, J.; Xia, Y.; Dong, S. Single Wearable Sensing Energy Device Based on Photoelectric Biofuel Cells for Simultaneous Analysis of Perspiration and Illuminance. *Nanoscale* **2017**, *9*, 11846-11850.
- (47) Bandodkar, A. J. Review—Wearable Biofuel Cells: Past, Present and Future. *J. Electrochem. Soc.* **2017**, *164*, H3007-H3014.
- (48) Jia, W.; Valdés-Ramírez, G.; Bandodkar, A. J.; Windmiller, J. R.; Wang, J. Epidermal Biofuel Cells: Energy Harvesting from Human Perspiration. *Angew. Chem. Int. Ed.* **2013**, *52*, 7233-7236.
- (49) Jia, W.; Wang, X.; Imani, S.; Bandodkar, A. J.; Ramirez, J.; Mercier, P. P.; Wang, J. Wearable Textile Biofuel Cells for Powering Electronics. *J. Mater. Chem. A* **2014**, *2*, 18184-18189.
- (50) Miyake, T.; Haneda, K.; Yoshino, S.; Nishizawa, M. Flexible, Layered Biofuel Cells. *Biosens. Bioelectron.* **2013**, *40*, 45-49.
- (51) Desmaële, D.; Renaud, L.; Tingry, S. A Wireless Sensor Powered by a Flexible Stack of Membraneless Enzymatic Biofuel Cells. *Sens. Actuat. B: Chem.* **2015**, *220*, 583-589.
- (52) Sakai, H.; Nakagawa, T.; Tokita, Y.; Hatazawa, T.; Ikeda, T.; Tsujimura, S.; Kano, K. A High-Power Glucose/Oxygen Biofuel Cell Operating under Quiescent Conditions. *Energy Environ. Sci.* **2009**, *2*, 133-138.
- (53) Majdecka, D.; Draminska, S.; Janusek, D.; Krysinski, P.; Bilewicz, R. A Self-Powered Biosensing Device with an Integrated Hybrid Biofuel Cell for Intermittent Monitoring of Analytes. *Biosens. Bioelectron.* **2018**, *102*, 383-388.
- (54) Bandodkar, A. J.; You, J.-M.; Kim, N.-H.; Gu, Y.; Kumar, R.; Mohan, A. M. V.; Kurniawan, J.; Imani, S.; Nakagawa, T.; Parish, B. *et al.* Soft, Stretchable, High Power Density Electronic Skin-Based Biofuel Cells for Scavenging Energy from Human Sweat. *Energy Environ. Sci.* **2017**, *10*, 1581-1589.
- (55) Zhu, Z.; Tam, T.; Zhang, Y. H. P. In *Fundamentals and Application of New Bioproduction Systems*; Zeng, A.-P., Ed.; Springer Berlin Heidelberg, 2013; Vol. 137.
- (56) Sokic-Lazic, D.; Arechederra, R. L.; Treu, B. L.; Minter, S. D. Oxidation of Biofuels: Fuel Diversity and Effectiveness of Fuel Oxidation through Multiple Enzyme Cascades. *Electroanalysis* **2010**, *22*, 757-764.
- (57) Pinyou, P.; Conzuelo, F.; Sliozberg, K.; Vivekananthan, J.; Contin, A.; Pöller, S.; Plumeré, N.;

- Schuhmann, W. Coupling of an Enzymatic Biofuel Cell to an Electrochemical Cell for Self-Powered Glucose Sensing with Optical Readout. *Bioelectrochem.* **2015**, *106*, 22-27.
- (58) Merle, G.; Brunel, L.; Tingry, S.; Cretin, M.; Rolland, M.; Servat, K.; Jolival, C.; Innocent, C.; Seta, P. Electrode Biomaterials Based on Immobilized Laccase. Application for Enzymatic Reduction of Dioxygen. *Mater. Sci. Eng. C* **2008**, *28*, 932-938.
- (59) Zebda, A.; Gondran, C.; Le Goff, A.; Holzinger, M.; Cinquin, P.; Cosnier, S. Mediatorless High-Power Glucose Biofuel Cells Based on Compressed Carbon Nanotube-Enzyme Electrodes. *Nat. Commun.* **2011**, *2*, 370.
- (60) Shleev, S. *Quo Vadis*, Implanted Fuel Cell? *ChemPlusChem* **2017**, *82*, 522-539.
- (61) Tokita, Y.; Nakagawa, T.; Sakai, H.; Sugiyama, T.; Matsumoto, R.; Hatazawa, T. Sony's Biofuel Cell. *ECS Trans.* **2008**, *13*, 89-97.
- (62) Kwon, C. H.; Lee, S.-H.; Choi, Y.-B.; Lee, J. A.; Kim, S. H.; Kim, H.-H.; Spinks, G. M.; Wallace, G. G.; Lima, M. D.; Kozlov, M. E. *et al.* High-Power Biofuel Cell Textiles from Woven Biscrolled Carbon Nanotube Yarns. *Nat. Commun.* **2014**, *5*, 3928.
- (63) Fujita, S.; Yamanoi, S.; Murata, K.; Mita, H.; Samukawa, T.; Nakagawa, T.; Sakai, H.; Tokita, Y. A Repeatedly Refuelable Mediated Biofuel Cell Based on a Hierarchical Porous Carbon Electrode. *Sci. Rep.* **2014**, *4*, 4937.
- (64) Aquino Neto, S.; Hickey, D. P.; Milton, R. D.; De Andrade, A. R.; Minter, S. D. High Current Density PQQ-Dependent Alcohol and Aldehyde Dehydrogenase Bioanodes. *Biosens. Bioelectron.* **2015**, *72*, 247-254.
- (65) de Poulpiquet, A.; Ciaccafava, A.; Gadiou, R.; Gounel, S.; Giudici-Ortoni, M. T.; Mano, N.; Lojou, E. Design of a H<sub>2</sub>/O<sub>2</sub> Biofuel Cell Based on Thermostable Enzymes. *Electrochem. Commun.* **2014**, *42*, 72-74.
- (66) Xu, L.; Armstrong, F. A. Optimizing the Power of Enzyme-Based Membrane-Less Hydrogen Fuel Cells for Hydrogen-Rich H<sub>2</sub>-Air Mixtures. *Energy Environ. Sci.* **2013**, *6*, 2166-2171.
- (67) Mazurenko, I.; Monsalve, K.; Infossi, P.; Giudici-Ortoni, M.-T.; Topin, F.; Mano, N.; Lojou, E. Impact of Substrate Diffusion and Enzyme Distribution in 3D-Porous Electrodes: A Combined Electrochemical and Modelling Study of a Thermostable H<sub>2</sub>/O<sub>2</sub> Enzymatic Fuel Cell. *Energy Environ. Sci.* **2017**, *10*, 1966-1982.
- (68) So, K.; Kitazumi, Y.; Shirai, O.; Nishikawa, K.; Higuchi, Y.; Kano, K. Direct Electron Transfer-Type Dual Gas Diffusion H<sub>2</sub>/O<sub>2</sub> Biofuel Cells. *J. Mater. Chem. A* **2016**, *4*, 8742-8749.
- (69) Szczesny, J.; Marković, N.; Conzuelo, F.; Zacarias, S.; Pereira, I. A. C.; Lubitz, W.; Plumeré, N.; Schuhmann, W.; Ruff, A. A Gas Breathing Hydrogen/Air Biofuel Cell Comprising a Redox Polymer/Hydrogenase-Based Bioanode. *Nat. Commun.* **2018**, *9*, 4715.
- (70) So, K.; Kawai, S.; Hamano, Y.; Kitazumi, Y.; Shirai, O.; Hibi, M.; Ogawa, J.; Kano, K. Improvement of a Direct Electron Transfer-Type Fructose/Dioxygen Biofuel Cell with a Substrate-Modified Biocathode. *Phys. Chem. Chem. Phys.* **2014**, *16*, 4823-4829.
- (71) Miyake, T.; Yoshino, S.; Yamada, T.; Hata, K.; Nishizawa, M. Self-Regulating Enzyme-Nanotube Ensemble Films and Their Application as Flexible Electrodes for Biofuel Cells. *J. Am. Chem. Soc.* **2011**, *133*, 5129-5134.
- (72) Kizling, M.; Stolarczyk, K.; Tammela, P.; Wang, Z.; Nyholm, L.; Golimowski, J.; Bilewicz, R. Bioelectrodes Based on Pseudocapacitive Cellulose/Polypyrrole Composite Improve Performance of

- Biofuel cell. *Bioelectrochem.* **2016**, *112*, 184-190.
- (73) Gai, P.; Ji, Y.; Chen, Y.; Zhu, C.; Zhang, J.; Zhu, J.-J. A Nitrogen-Doped Graphene/Gold Nanoparticle/Formate Dehydrogenase Bioanode for High Power Output Membrane-Less Formic Acid/O<sub>2</sub> Biofuel Cells. *Analyst* **2015**, *140*, 1822-1826.
- (74) Handa, Y.; Yamagiwa, K.; Ikeda, Y.; Yanagisawa, Y.; Watanabe, S.; Yabuuchi, N.; Komaba, S. Fabrication of Carbon-Felt-Based Multi-Enzyme Immobilized Anodes to Oxidize Sucrose for Biofuel Cells. *ChemPhysChem* **2014**, *15*, 2145-2151.
- (75) Deng, L.; Shang, L.; Wen, D.; Zhai, J.; Dong, S. A Membraneless Biofuel Cell Powered by Ethanol and Alcoholic Beverage. *Biosens. Bioelectron.* **2010**, *26*, 70-73.
- (76) Selloum, D.; Tingry, S.; Techer, V.; Renaud, L.; Innocent, C.; Zouaoui, A. Optimized Electrode Arrangement and Activation of Bioelectrodes Activity by Carbon Nanoparticles for Efficient Ethanol Microfluidic Biofuel Cells. *J. Power Sources* **2014**, *269*, 834-840.
- (77) Masa, J.; Schuhmann, W. Electrocatalysis and Bioelectrocatalysis – Distinction without a Difference. *Nano Energy* **2016**, *29*, 466-475.
- (78) Saboe, P. O.; Conte, E.; Farrell, M.; Bazan, G. C.; Kumar, M. Biomimetic and Bioinspired Approaches for Wiring Enzymes to Electrode Interfaces. *Energy Environ. Sci.* **2016**, *10*, 14-41.
- (79) Moehlenbrock, M. J.; Minteer, S. D. Extended Lifetime Biofuel Cells. *Chem. Soc. Rev.* **2008**, *37*, 1188-1196.
- (80) Luz, R. A.; Pereira, A. R.; de Souza, J. C.; Sales, F. C.; Crespilho, F. N. Enzyme Biofuel Cells: Thermodynamics, Kinetics and Challenges in Applicability. *ChemElectroChem* **2014**, *1*, 1751-1777.
- (81) Pereira, A. R.; de Souza, J. C. P.; Iost, R. M.; Sales, F. C. P. F.; Crespilho, F. N. Application of Carbon Fibers to Flexible Enzyme Electrodes. *J. Electroanal. Chem.* **2016**, *780*, 396-406.
- (82) Cooney, M. J.; Svoboda, V.; Lau, C.; Martin, G.; Minteer, S. D. Enzyme Catalysed Biofuel Cells. *Energy Environ. Sci.* **2008**, *1*, 320-337.
- (83) Ha, S.; Wee, Y.; Kim, J. Nanobiocatalysis for Enzymatic Biofuel Cells. *Top. Catal.* **2012**, *55*, 1181-1200.
- (84) Leech, D.; Kavanagh, P.; Schuhmann, W. Enzymatic Fuel Cells: Recent Progress. *Electrochim. Acta* **2012**, *84*, 223-234.
- (85) Zhou, M.; Wang, J. Biofuel Cells for Self-Powered Electrochemical Biosensing and Logic Biosensing: A Review. *Carbon* **2012**, *24*, 197-209.
- (86) Zhou, M. Recent Progress on the Development of Biofuel Cells for Self-Powered Electrochemical Biosensing and Logic Biosensing: A Review. *Electroanalysis* **2015**, *27*, 1786-1810.
- (87) Zhao, C.-e.; Gai, P.; Song, R.; Chen, Y.; Zhang, J.; Zhu, J.-J. Nanostructured Material-Based Biofuel Cells: Recent Advances and Future Prospects. *Chem. Soc. Rev.* **2017**, *46*, 1545-1564.
- (88) Mazurenko, I.; Wang, X.; de Poulpiquet, A.; Lojou, E. H<sub>2</sub>/O<sub>2</sub> Enzymatic Fuel Cells: From Proof-of-Concept to Powerful Devices. *Sustainable Energy Fuels* **2017**, *1*, 1475-1501.
- (89) Cosnier, S.; Holzinger, M.; Le Goff, A. Recent Advances in Carbon Nanotube-Based Enzymatic Fuel Cells. *Front. Bioeng. Biotechnol.* **2014**, *2*, 45.
- (90) de Poulpiquet, A.; Ciaccafava, A.; Lojou, E. New Trends in Enzyme Immobilization at Nanostructured Interfaces for Efficient Electrocatalysis in Biofuel Cells. *Electrochim. Acta* **2014**, *126*, 104-114.
- (91) Holade, Y.; Tingry, S.; Servat, K.; Napporn, T.; Cornu, D.; Kokoh, K. Nanostructured Inorganic

- Materials at Work in Electrochemical Sensing and Biofuel Cells. *Catalysts* **2017**, *7*, 31.
- (92) Wen, D.; Eychmüller, A. Enzymatic Biofuel Cells on Porous Nanostructures. *Small* **2016**, *12*, 4649-4661.
- (93) Karimi, A.; Othman, A.; Uzunoglu, A.; Stanciu, L.; Andreescu, S. Graphene Based Enzymatic Bioelectrodes and Biofuel Cells. *Nanoscale* **2015**, *7*, 6909-6923.
- (94) Liu, Y.; Du, Y.; Li, C. M. Direct Electrochemistry Based Biosensors and Biofuel Cells Enabled with Nanostructured Materials. *Electroanalysis* **2013**, *25*, 815-831.
- (95) Qiu, H. J.; Guan, Y.; Luo, P.; Wang, Y. Recent Advance in Fabricating Monolithic 3D Porous Graphene and Their Applications in Biosensing and Biofuel Cells. *Biosens. Bioelectron.* **2017**, *89*, 85-95.
- (96) Yang, X.-Y.; Tian, G.; Jiang, N.; Su, B.-L. Immobilization Technology: A Sustainable Solution for Biofuel Cell Design. *Energy Environ. Sci.* **2012**, *5*, 5540-5563.
- (97) Ammam, M. Electrochemical and Electrophoretic Deposition of Enzymes: Principles, Differences and Application in Miniaturized Biosensor and Biofuel Cell Electrodes. *Biosens. Bioelectron.* **2014**, *58*, 121-131.
- (98) Yates, N. D. J.; Fascione, M. A.; Parkin, A. Methodologies for “Wiring” Redox Proteins/Enzymes to Electrode Surfaces. *Chem. Eur. J.* **2018**, *24*, 12164-12182.
- (99) Le Goff, A.; Holzinger, M.; Cosnier, S. Recent Progress in Oxygen-Reducing Laccase Biocathodes for Enzymatic Biofuel Cells. *Cell Mol Life Sci.* **2015**, *72*, 941-952.
- (100) Meredith, M. T.; Minteer, S. D. Biofuel Cells: Enhanced Enzymatic Bioelectrocatalysis. *Annu. Rev. Anal. Chem.* **2012**, *5*, 157-179.
- (101) Betancor, L.; Johnson, G. R.; Luckarift, H. R. Stabilized Laccases as Heterogeneous Bioelectrocatalysts. *ChemCatChem* **2013**, *5*, 46-60.
- (102) So, K.; Sakai, K.; Kano, K. Gas Diffusion Bioelectrodes. *Curr. Opin. Electrochem.* **2017**, *5*, 173-182.
- (103) Catalano, P. N.; Wolosiuk, A.; Soler-Illia, G. J. A. A.; Bellino, M. G. Wired Enzymes in Mesoporous Materials: A Benchmark for Fabricating Biofuel Cells. *Bioelectrochem.* **2015**, *106*, 14-21.
- (104) Mostafavi, S. M. 3D Graphene Biocatalysts for Development of Enzymatic Biofuel Cells: A Short Review. *J. Nanoanalysis* **2015**, *2*, 57-62.
- (105) Milton, R. D.; Wang, T.; Knoche, K. L.; Minteer, S. D. Tailoring Biointerfaces for Electrocatalysis. *Langmuir* **2016**, *32*, 2291-2301.
- (106) Katz, E. Magneto-Switchable Electrodes and Electrochemical Systems. *Electroanalysis* **2016**, *28*, 904-919.
- (107) Desmet, C.; Marquette, C. A.; Blum, L. J.; Doumèche, B. Paper Electrodes for Bioelectrochemistry: Biosensors and Biofuel Cells. *Biosens. Bioelectron.* **2016**, *76*, 145-163.
- (108) Xiao, X.; Si, P.; Magner, E. An Overview of Dealloyed Nanoporous Gold in Bioelectrochemistry. *Bioelectrochem.* **2016**, *109*, 117-126.
- (109) Tello, A.; Cao, R.; Marchant, M. J.; Gomez, H. Conformational Changes of Enzymes and Aptamers Immobilized on Electrodes. *Bioconjugate Chem.* **2016**, *27*, 2581-2591.
- (110) Kückler, A.; Yoshimoto, M.; Luginbühl, S.; Mavelli, F.; Walde, P. Enzymatic Reactions in Confined Environments. *Nat. Nanotechnol.* **2016**, *11*, 409.
- (111)Huong Le, T. X.; Bechelany, M.; Cretin, M. Carbon Felt Based-Electrodes for Energy and

- Environmental Applications: A Review. *Carbon* **2017**, *122*, 564-591.
- (112) Kim, J.; Kumar, R.; Bandodkar, A. J.; Wang, J. Advanced Materials for Printed Wearable Electrochemical Devices: A Review. *Adv. Electron. Mater.* **2017**, *3*, 1600260.
- (113) Stine, K. J. Enzyme Immobilization on Nanoporous Gold: A Review. *Biochem. Insights* **2017**, *10*, 1178626417748607.
- (114) Mazurenko, I.; de Poulpiquet, A.; Lojou, E. Recent Developments in High Surface Area Bioelectrodes for Enzymatic Fuel Cells. *Curr. Opin. Electrochem.* **2017**, *5*, 74-84.
- (115) Adeel, M.; Bilal, M.; Rasheed, T.; Sharma, A.; Iqbal, H. M. N. Graphene and Graphene Oxide: Functionalization and Nano-Bio-Catalytic System for Enzyme. *Int. J. Biol. Macromol.* **2018**, *120*, 1430-1440.
- (116) Le Goff, A.; Holzinger, M. Molecular Engineering of the Bio/Nano-Interface for Enzymatic Electrocatalysis in Fuel Cells. *Sustainable Energy Fuels* **2018**, *2*, 2555-2566.
- (117) Gross, A. J.; Holzinger, M.; Cosnier, S. Buckypaper Bioelectrodes: Emerging Materials for Implantable and Wearable Biofuel Cells. *Energy Environ. Sci.* **2018**, *11*, 1670-1687.
- (118) Janczuk-Richter, M.; Marinović, I.; Niedziółka-Jönsson, J.; Szot-Karpińska, K. Recent Applications of Bacteriophage-Based Electrodes: A Mini-Review. *Electrochem. Commun.* **2019**, *99*, 11-15.
- (119) Casado, N.; Hernández, G.; Sardon, H.; Mecerreyes, D. Current Trends in Redox Polymers for Energy and Medicine. *Prog. Polym. Sci.* **2016**, *52*, 107-135.
- (120) Ruff, A. Redox Polymers in Bioelectrochemistry: Common Playgrounds and Novel Concepts. *Curr. Opin. Electrochem.* **2017**, *5*, 66-73.
- (121) Horst, A. E. W.; Mangold, K.-M.; Holtmann, D. Application of Gas Diffusion Electrodes in Bioelectrochemical Syntheses and Energy Conversion. *Biotechnol. Bioeng.* **2016**, *113*, 260-267.
- (122) Renner, J. N.; Minteer, S. D. The Use of Engineered Protein Materials in Electrochemical Devices. *Exp. Biol. Med.* **2016**, *241*, 980-985.
- (123) Minteer, S. D. Oxidative Bioelectrocatalysis: From Natural Metabolic Pathways to Synthetic Metabolons and Minimal Enzyme Cascades. *Biochim. Biophys. Acta Bioenerg.* **2016**, *1857*, 621-624.
- (124) Macazo, F. C.; Minteer, S. D. Enzyme Cascades in Biofuel Cells. *Curr. Opin. Electrochem.* **2017**, *5*, 114-120.
- (125) Milton, R. D.; Minteer, S. D. Direct Enzymatic Bioelectrocatalysis: Differentiating between Myth and Reality. *J. R. Soc. Interface* **2017**, *14*, 20170253.
- (126) Rajendran, L.; Kirthiga, M.; Laborda, E. Mathematical Modeling of Nonlinear Reaction-Diffusion Processes in Enzymatic Biofuel Cells. *Curr. Opin. Electrochem.* **2017**, *1*, 121-132.
- (127) Bostick, C. D.; Mukhopadhyay, S.; Pecht, I.; Sheves, M.; Cahen, D.; Lederman, D. Protein Bioelectronics: A Review of What We Do and Do Not Know. *Rep. Prog. Phys.* **2018**, *81*, 026601.
- (128) Hitaishi, V.; Clement, R.; Bourassin, N.; Baaden, M.; de Poulpiquet, A.; Sacquin-Mora, S.; Ciaccafava, A.; Lojou, E. Controlling Redox Enzyme Orientation at Planar Electrodes. *Catalysts* **2018**, *8*, 192.
- (129) Jenner, L. P.; Butt, J. N. Electrochemistry of Surface-Confined Enzymes: Inspiration, Insight and Opportunity for Sustainable Biotechnology. *Curr. Opin. Electrochem.* **2018**, *8*, 81-88.
- (130) Ma, S.; Ludwig, R. Direct Electron Transfer of Enzymes Facilitated by Cytochromes. *ChemElectroChem* **2019**, *6*, 958-975.

- (131) Yamashita, Y.; Lee, I.; Loew, N.; Sode, K. Direct Electron Transfer (DET) Mechanism of FAD Dependent Dehydrogenase Complexes ~From the Elucidation of Intra- and Inter-Molecular Electron Transfer Pathway to the Construction of Engineered DET Enzyme Complexes~. *Curr. Opin. Electrochem.* **2018**, *12*, 92-100.
- (132) Bollella, P.; Gorton, L.; Antiochia, R. Direct Electron Transfer of Dehydrogenases for Development of 3rd Generation Biosensors and Enzymatic Fuel Cells. *Sensors* **2018**, *18*, 1319.
- (133) Armstrong, F. A.; Evans, R. M.; Hexter, S. V.; Murphy, B. J.; Roessler, M. M.; Wulff, P. Guiding Principles of Hydrogenase Catalysis Instigated and Clarified by Protein Film Electrochemistry. *Acc. Chem. Res.* **2016**, *49*, 884-892.
- (134) Sensi, M.; del Barrio, M.; Baffert, C.; Fourmond, V.; Léger, C. New Perspectives in Hydrogenase Direct Electrochemistry. *Curr. Opin. Electrochem.* **2017**, *5*, 135-145.
- (135) Shleev, S.; Andoralov, V.; Pankratov, D.; Falk, M.; Aleksejeva, O.; Blum, Z. Oxygen Electroreduction Versus Bioelectroreduction: Direct Electron Transfer Approach. *Electroanalysis* **2016**, *28*, 2270-2287.
- (136) Mate, D. M.; Alcalde, M. Laccase: A Multi-Purpose Biocatalyst at the Forefront of Biotechnology. *Microb. Biotechnol.* **2017**, *10*, 1457-1467.
- (137) Mano, N.; de Poulpiquet, A. O<sub>2</sub> Reduction in Enzymatic Biofuel Cells. *Chem. Rev.* **2017**, *118*, 2392-2468.
- (138) Zhang, Y.; Lv, Z.; Zhou, J.; Xin, F.; Ma, J.; Wu, H.; Fang, Y.; Jiang, M.; Dong, W. Application of Eukaryotic and Prokaryotic Laccases in Biosensor and Biofuel Cells: Recent Advances and Electrochemical Aspects. *Appl. Microbiol. Biotechnol.* **2018**, *102*, 10409-10423.
- (139) Sode, K.; Yamazaki, T.; Lee, I.; Hanashi, T.; Tsugawa, W. BioCapacitor: A Novel Principle for Biosensors. *Biosens. Bioelectron.* **2016**, *76*, 20-28.
- (140) Shleev, S.; González-Arribas, E.; Falk, M. Biosupercapacitors. *Curr. Opin. Electrochem.* **2017**, *5*, 226-233.
- (141) Yang, Y.; Liu, T.; Tao, K.; Chang, H. Generating Electricity on Chips: Microfluidic Biofuel Cells in Perspective. *Ind. Eng. Chem. Res.* **2018**, *57*, 2746-2758.
- (142) Pankratov, D.; González-Arribas, E.; Blum, Z.; Shleev, S. Tear Based Bioelectronics. *Electroanalysis* **2016**, *28*, 1250-1266.
- (143) Shi, B.; Li, Z.; Fan, Y. Implantable Energy-Harvesting Devices. *Adv. Mater.* **2018**, *0*, 1801511.
- (144) Kim, J.; Jeerapan, I.; Sempionatto, J. R.; Barfidokht, A.; Mishra, R. K.; Campbell, A. S.; Hubble, L. J.; Wang, J. Wearable Bioelectronics: Enzyme-Based Body-Worn Electronic Devices. *Acc. Chem. Res.* **2018**, *51*, 2820-2828.
- (145) Huang, X.; Zhang, L.; Zhang, Z.; Guo, S.; Shang, H.; Li, Y.; Liu, J. Wearable Biofuel Cells Based on the Classification of Enzyme for High Power Outputs and Lifetimes. *Biosens. Bioelectron.* **2019**, *124-125*, 40-52.
- (146) Dagdeviren, C.; Li, Z.; Wang, Z. L. Energy Harvesting from the Animal/Human Body for Self-Powered Electronics. *Annu. Rev. Biomed. Eng.* **2017**, *19*, 85-108.
- (147) Fu, L.; Liu, J.; Hu, Z.; Zhou, M. Recent Advances in the Construction of Biofuel Cells Based Self-powered Electrochemical Biosensors: A Review. *Electroanalysis* **2018**, *30*, 2535-2550.
- (148) Niitsu, K. Energy-Autonomous Biosensing Platform Using Supply-Sensing CMOS



Integrated Sensor and Biofuel Cell for Next-Generation Healthcare Internet of Things. *Jpn. J. Appl. Phys.* **2018**, *57*, 1002A1005.

(149) Conzuelo, F.; Ruff, A.; Schuhmann, W. Self-Powered Bioelectrochemical Devices. *Curr. Opin. Electrochem.* **2018**, 156-163.

(150) Gonzalez-Solino, C.; Lorenzo, D. M. Enzymatic Fuel Cells: Towards Self-Powered Implantable and Wearable Diagnostics. *Biosensors* **2018**, *8*.

(151) Grattieri, M.; Minteer, S. D. Self-Powered Biosensors. *ACS Sens.* **2018**, *3*, 44-53.

(152) Abdellaoui, S.; Macazo Florika, C.; Cai, R.; De Lacey Antonio, L.; Pita, M.; Minteer Shelley, D. Enzymatic Electrosynthesis of Alkanes by Bioelectrocatalytic Decarbonylation of Fatty Aldehydes. *Angew. Chem. Int. Ed.* **2017**, *57*, 2404-2408.

(153) Milton, R. D.; Cai, R.; Abdellaoui, S.; Leech, D.; De Lacey, A. L.; Pita, M.; Minteer, S. D. Bioelectrochemical Haber–Bosch Process: An Ammonia-Producing H<sub>2</sub>/N<sub>2</sub> Fuel Cell. *Angew. Chem. Int. Ed.* **2017**, *56*, 2680-2683.

(154) Gentil, S.; Che Mansor, S. M.; Jamet, H.; Cosnier, S.; Cavazza, C.; Le Goff, A. Oriented Immobilization of [NiFeSe] Hydrogenases on Covalently and Noncovalently Functionalized Carbon Nanotubes for H<sub>2</sub>/Air Enzymatic Fuel Cells. *ACS Catal.* **2018**, *8*, 3957-3964.

(155) Palmore, G. T. R.; Bertschy, H.; Bergens, S. H.; Whitesides, G. M. A Methanol/Dioxygen Biofuel Cell that Uses NAD(+)-Dependent Dehydrogenases as Catalysts: Application of an Electro-Enzymatic Method to Regenerate Nicotinamide Adenine Dinucleotide at Low Overpotentials. *J. Electroanal. Chem.* **1998**, *443*, 155-161.

(156) Arechederra, R. L.; Minteer, S. D. Complete Oxidation of Glycerol in an Enzymatic Biofuel Cell. *Fuel Cells* **2009**, *9*, 63-69.

(157) Sokic-Lazic, D.; Minteer, S. D. Pyruvate/Air Enzymatic Biofuel Cell Capable of Complete Oxidation. *Electrochem. Solid-State Lett.* **2009**, *12*, F26-F28.

(158) Li, L.; Liang, B.; Li, F.; Shi, J.; Mascini, M.; Lang, Q.; Liu, A. Co-Immobilization of Glucose Oxidase and Xylose Dehydrogenase Displayed Whole Cell on Multiwalled Carbon Nanotube Nanocomposite Films Modified Electrode for Simultaneous Voltammetric Detection of D-Glucose and D-Xylose. *Biosens. Bioelectron.* **2013**, *42*, 156-162.

(159) Zhu, Z.; Wang, Y.; Minteer, S. D.; Percival Zhang, Y. H. Maltodextrin-Powered Enzymatic Fuel Cell Through a Non-Natural Enzymatic Pathway. *J. Power Sources* **2011**, *196*, 7505-7509.

(160) Sokic-Lazic, D.; Minteer, S. D. Citric Acid Cycle Biomimic on a Carbon Electrode. *Biosens. Bioelectron.* **2008**, *24*, 939-944.

(161) Akers, N. L.; Moore, C. M.; Minteer, S. D. Development of Alcohol/O<sub>2</sub> Biofuel Cells Using Salt-Extracted Tetrabutylammonium Bromide/Nafion Membranes to Immobilize Dehydrogenase Enzymes. *Electrochim. Acta* **2005**, *50*, 2521-2525.

(162) Arechederra, R. L.; Boehm, K.; Minteer, S. D. Mitochondrial Bioelectrocatalysis for Biofuel Cell Applications. *Electrochim. Acta* **2009**, *54*, 7268-7273.

(163) Addo, P. K.; Arechederra, R. L.; Minteer, S. D. Evaluating Enzyme Cascades for Methanol/Air Biofuel Cells Based on NAD<sup>+</sup>-Dependent Enzymes. *Electroanal* **2010**, *22*, 807-812.

(164) Kim, Y. H.; Campbell, E.; Yu, J.; Minteer, S. D.; Banta, S. Complete Oxidation of Methanol in Biobattery Devices Using a Hydrogel Created from Three Modified Dehydrogenases. *Angew. Chem. Int. Ed.* **2013**, *52*, 1437-1440.

- (165) Wang, H. B.; Thia, L.; Li, N.; Ge, X. M.; Liu, Z. L.; Wang, X. Pd Nanoparticles on Carbon Nitride-Graphene for the Selective Electro-Oxidation of Glycerol in Alkaline Solution. *ACS Catal.* **2015**, *5*, 3174-3180.
- (166) Hickey, D. P.; McCammant, M. S.; Giroud, F.; Sigman, M. S.; Minteer, S. D. Hybrid Enzymatic and Organic Electrocatalytic Cascade for the Complete Oxidation of Glycerol. *J. Am. Chem. Soc.* **2014**, *136*, 15917-15920.
- (167) Zhu, Z.; Ma, C.; Percival Zhang, Y. H. Co-Utilization of Mixed Sugars in an Enzymatic Fuel Cell Based on an *in vitro* Enzymatic Pathway. *Electrochim. Acta* **2018**, *263*, 184-191.
- (168) Cosnier, S.; Shan, D.; Ding, S. N. An Easy Compartment-Less Biofuel Cell Construction Based on the Physical Co-Inclusion of Enzyme and Mediator Redox within Pressed Graphite Discs. *Electrochem. Commun.* **2010**, *12*, 266-269.
- (169) Tasca, F.; Gorton, L.; Kujawa, M.; Patel, I.; Harreither, W.; Peterbauer, C. K.; Ludwig, R.; Nöll, G. Increasing the Coulombic Efficiency of Glucose Biofuel Cell Anodes by Combination of Redox Enzymes. *Biosens. Bioelectron.* **2010**, *25*, 1710-1716.
- (170) Xu, S.; Minteer, S. D. Enzymatic Biofuel Cell for Oxidation of Glucose to CO<sub>2</sub>. *ACS Catal.* **2011**, *2*, 91-94.
- (171) Zhu, Z. G.; Sun, F. F.; Zhang, X. Z.; Zhang, Y. H. P. Deep Oxidation of Glucose in Enzymatic Fuel Cells Through a Synthetic Enzymatic Pathway Containing a Cascade of Two Thermostable Dehydrogenases. *Biosens. Bioelectron.* **2012**, *36*, 110-115.
- (172) Wu, R.; Ma, C.; Zhang, Y. H. P.; Zhu, Z. Complete Oxidation of Xylose for Bioelectricity Generation by Reconstructing a Bacterial Xylose Utilization Pathway *in vitro*. *ChemCatChem* **2018**, *10*, 1-7.
- (173) Szczupak, A.; Aizik, D.; Moraïs, S.; Vazana, Y.; Barak, Y.; Bayer, E. A.; Alfonta, L. The Electrosome: A Surface-Displayed Enzymatic Cascade in a Biofuel Cell's Anode and a High-Density Surface-Displayed Biocathodic Enzyme. *Nanomaterials* **2017**, *7*, 153.
- (174) Wheeldon, I.; Minteer, S.; Banta, S.; Barton, S.; Atanassov, P.; Sigman, M. Substrate Channelling as an Approach to Cascade Reactions. *Nat. Chem.* **2016**, *8*, 299-309.
- (175) Liu, Y. C.; Hickey, D. P.; Guo, J. Y.; Earl, E.; Abdellaoui, S.; Milton, R. D.; Sigman, M. S.; Minteer, S. D.; Barton, S. C. Substrate Channeling in an Artificial Metabolon: A Molecular Dynamics Blueprint for an Experimental Peptide Bridge. *ACS Catal.* **2017**, *7*, 2486-2493.
- (176) Xia, L.; Nguyen, K. V.; Holade, Y.; Han, H.; Dooley, K.; Atanassov, P.; Banta, S.; Minteer, S. D. Improving the Performance of Methanol Biofuel Cells Utilizing an Enzyme Cascade Bioanode with DNA-Bridged Substrate Channeling. *ACS Energy Lett.* **2017**, *2*, 1435-1438.
- (177) Moehlenbrock, M. J.; Toby, T. K.; Waheed, A.; Minteer, S. D. Metabolon Catalyzed Pyruvate/Air Biofuel Cell. *J. Am. Chem. Soc.* **2010**, *132*, 6288-6289.
- (178) de Souza, J. C. P.; Silva, W. O.; Lima, F. H. B.; Crespilho, F. N. Enzyme Activity Evaluation by Differential Electrochemical Mass Spectrometry. *Chem. Commun.* **2017**, *53*, 8400-8402.
- (179) Zhao, F.; Slade, R. C. T.; Varcoe, J. R. Techniques for the study and development of microbial fuel cells: an electrochemical perspective. *Chem. Soc. Rev.* **2009**, *38*, 1926-1939.
- (180) Trifonov, A.; Tel-Vered, R.; Fadeev, M.; Willner, I. Electrically Contacted Bienzyme-Functionalized Mesoporous Carbon Nanoparticle Electrodes: Applications for the Development of Dual Amperometric Biosensors and Multifuel-Driven Biofuel Cells. *Adv. Energy*

*Mater.* **2015**, *5*, 1401853.

- (181) Meredith, M. T.; Minson, M.; Hickey, D.; Artyushkova, K.; Glatzhofer, D. T.; Minter, S. D. Anthracene-Modified Multi-Walled Carbon Nanotubes as Direct Electron Transfer Scaffolds for Enzymatic Oxygen Reduction. *ACS Catal.* **2011**, *1*, 1683-1690.
- (182) Xu, L.; Armstrong, F. A. Pushing the Limits for Enzyme-Based Membrane-Less Hydrogen Fuel Cells - Achieving Useful Power and Stability. *RSC Adv.* **2015**, *5*, 3649-3656.
- (183) Kizling, M.; Dzwonek, M.; Olszewski, B.; Baçal, P.; Tymecki, Ł.; Więckowska, A.; Stolarczyk, K.; Bilewicz, R. Reticulated Vitreous Carbon as a Scaffold for Enzymatic Fuel Cell Designing. *Biosens. Bioelectron.* **2017**, *95*, 1-7.
- (184) Fadzillah, D. M.; Kamarudin, S. K.; Zainoodin, M. A.; Masdar, M. S. Critical Challenges in the System Development of Direct Alcohol Fuel Cells as Portable Power Supplies: An Overview. *Int. J. Hydrogen Energy* **2019**, *44*, 3031-3054.
- (185) Gross, A. J.; Chen, X.; Giroud, F.; Abreu, C.; Le Goff, A.; Holzinger, M.; Cosnier, S. A High Power Buckypaper Biofuel Cell: Exploiting 1,10-Phenanthroline-5,6-Dione with FAD-Dependent Dehydrogenase for Catalytically-Powerful Glucose Oxidation. *ACS Catal.* **2017**, *7*, 4408-4416.
- (186) Campbell, A. S.; Jeong, Y. J.; Geier, S. M.; Koepsel, R. R.; Russell, A. J.; Islam, M. F. Membrane/Mediator-Free Rechargeable Enzymatic Biofuel Cell Utilizing Graphene/Single-Wall Carbon Nanotube Cogel Electrodes. *ACS Appl. Mater. Interfaces* **2015**, *7*, 4056-4065.
- (187) Shao, B. B.; Liu, Z. F.; Zeng, G. M.; Liu, Y.; Yang, X.; Zhou, C. Y.; Chen, M.; Liu, Y. J.; Jiang, Y. L.; Yan, M. Immobilization of Laccase on Hollow Mesoporous Carbon Nanospheres: Noteworthy Immobilization, Excellent Stability and Efficacious for Antibiotic Contaminants Removal. *J. Hazard. Mater.* **2019**, *362*, 318-326.
- (188) Sadeghi, S.; Fooladi, E.; Malekaneh, M. A New Amperometric Biosensor Based on Fe<sub>3</sub>O<sub>4</sub>/Polyaniline/Laccase/Chitosan Biocomposite-Modified Carbon Paste Electrode for Determination of Catechol in Tea Leaves. *Appl. Biochem. Biotechnol.* **2015**, *175*, 1603-1616.
- (189) Itoh, T.; Shibuya, Y.; Yamaguchi, A.; Hoshikawa, Y.; Tanaike, O.; Tsunoda, T.; Hanaoka, T. A.; Hamakawa, S.; Mizukami, F.; Hayashi, A. *et al.* High-Performance Bioelectrocatalysts Created by Immobilization of an Enzyme into Carbon-Coated Composite Membranes with Nano-Tailored Structures. *J. Mater. Chem. A* **2017**, *5*, 20244-20251.
- (190) Campbell, A. S.; Jose, M. V.; Marx, S.; Cornelius, S.; Koepsel, R. R.; Islam, M. F.; Russell, A. J. Improved Power Density of an Enzymatic Biofuel Cell with Fibrous Supports of High Curvature. *RSC Adv.* **2016**, *6*, 10150-10158.
- (191) Shukla, A.; Suresh, P.; Berchmans, S.; Rajendran, A. Biological Fuel Cells and Their Applications. *Curr. Sci.* **2004**, *87*, 455-468.
- (192) Michaelis, L.; Menten, M. L. The Kinetics of the Inversion Effect. *Biochem. Z.* **1913**, *49*, 333-369.
- (193) Bisswanger, H. Enzyme Assays. *Perspect. Sci.* **2014**, *1*, 41-55.
- (194) Koshland, D. E. The Application and Usefulness of the Ratio  $k_{cat}/K_M$ . *Bioorg. Chem.* **2002**, *30*, 211-213.
- (195) Laidler, K. J. Symbolism and Terminology in Chemical Kinetics. *Pure Appl. Chem.* **1981**, *53*, 753-771.
- (196) Güven, G.; Prodanovic, R.; Schwaneberg, U. Protein Engineering—An Option for Enzymatic

- Biofuel Cell Design. *Electroanalysis* **2010**, *22*, 765-775.
- (197) Zhu, Z.; Momeu, C.; Zakhartsev, M.; Schwaneberg, U. Making Glucose Oxidase Fit for Biofuel Cell Applications by Directed Protein Evolution. *Biosens. Bioelectron.* **2006**, *21*, 2046-2051.
- (198) Zhu, Z.; Wang, M.; Gautam, A.; Nazor, J.; Momeu, C.; Prodanovic, R.; Schwaneberg, U. Directed Evolution of Glucose Oxidase from *Aspergillus niger* for Ferrocenemethanol-Mediated Electron Transfer. *Biotechnol. J.* **2007**, *2*, 241-248.
- (199) Mano, N. A 280  $\mu\text{W cm}^{-2}$  Biofuel Cell Operating at Low Glucose Concentration. *Chem. Commun.* **2008**, *0*, 2221-2223.
- (200) Courjean, O.; Mano, N. Recombinant Glucose Oxidase from *Penicillium amagasakiense* for Efficient Bioelectrochemical Applications in Physiological Conditions. *J. Biotechnol.* **2011**, *151*, 122-129.
- (201) PrévotEAU, A.; Courjean, O.; Mano, N. Deglycosylation of Glucose Oxidase to Improve Biosensors and Biofuel Cells. *Electrochem. Commun.* **2010**, *12*, 213-215.
- (202) Marcus, R. A. Electron Transfer Reactions in Chemistry: Theory and Experiment (Nobel Lecture). *Angew. Chem. Int. Ed.* **1993**, *32*, 1111-1121.
- (203) Mayo, S. L.; Ellis, W. R.; Crutchley, R. J.; Gray, H. B. Long-Range Electron Transfer in Heme Proteins. *Science* **1986**, *233*, 948-952.
- (204) Page, C. C.; Moser, C. C.; Chen, X.; Dutton, P. L. Natural Engineering Principles of Electron Tunnelling in Biological Oxidation-Reduction. *Nature* **1999**, *402*, 47-52.
- (205) Wang, J. Electrochemical Glucose Biosensors. *Chem. Rev.* **2008**, *108*, 814-825.
- (206) Sucheta, A.; Cammack, R.; Weiner, J.; Armstrong, F. A. Reversible Electrochemistry of Fumarate Reductase Immobilized on an Electrode Surface. Direct Voltammetric Observations of Redox Centers and Their Participation in Rapid Catalytic Electron Transport. *Biochemistry* **1993**, *32*, 5455-5465.
- (207) Armstrong, F. A. Recent Developments in Dynamic Electrochemical Studies of Adsorbed Enzymes and Their Active Sites. *Curr. Opin. Chem. Biol.* **2005**, *9*, 110-117.
- (208) Léger, C.; Bertrand, P. Direct Electrochemistry of Redox Enzymes as a Tool for Mechanistic Studies. *Chem. Rev.* **2008**, *108*, 2379-2438.
- (209) Laviron, E. General Expression of the Linear Potential Sweep Voltammogram in the Case of Diffusionless Electrochemical Systems. *J. Electroanal. Chem. Interfacial Electrochem.* **1979**, *101*, 19-28.
- (210) Léger, C.; Jones, A. K.; Albracht, S. P. J.; Armstrong, F. A. Effect of a Dispersion of Interfacial Electron Transfer Rates on Steady State Catalytic Electron Transport in [NiFe]-hydrogenase and Other Enzymes. *J. Phys. Chem. B* **2002**, *106*, 13058-13063.
- (211) Zayats, M.; Katz, E.; Willner, I. Electrical Contacting of Flavoenzymes and NAD(P)<sup>+</sup>-Dependent Enzymes by Reconstitution and Affinity Interactions on Phenylboronic Acid Monolayers Associated with Au-Electrodes. *J. Am. Chem. Soc.* **2002**, *124*, 14724-14735.
- (212) Agip, A.-N. A.; Blaza, J. N.; Fedor, J. G.; Hirst, J. Mammalian Respiratory Complex I Through the Lens of Cryo-EM. *Annu. Rev. Biophys.* **2019**, *48*, 165-184.
- (213) Burrows, A. L.; Guo, L. H.; Hill, H. A.; McLendon, G.; Sherman, F. Direct Electrochemistry of Proteins. Investigations of Yeast Cytochrome c Mutants and Their Complexes with Cytochrome b<sub>5</sub>

*Eur. J. Biochem.* **1991**, *202*, 543-549.

- (214) Ludwig, R.; Harreither, W.; Tasca, F.; Gorton, L. Cellobiose Dehydrogenase: A Versatile Catalyst for Electrochemical Applications. *ChemPhysChem* **2010**, *11*, 2674-2697.
- (215) Ludwig, R.; Ortiz, R.; Schulz, C.; Harreither, W.; Sygmund, C.; Gorton, L. Cellobiose Dehydrogenase Modified Electrodes: Advances by Materials Science and Biochemical Engineering. *Anal. Bioanal. Chem.* **2013**, *405*, 3637-3658.
- (216) Ameyama, M.; Shinagawa, E.; Matsushita, K.; Adachi, O. *D*-Fructose Dehydrogenase of *Gluconobacter Industrius*: Purification, Characterization, and Application to Enzymatic Microdetermination of *D*-Fructose. *J. Bacteriol.* **1981**, *145*, 814-823.
- (217) Xia, H.-q.; Hibino, Y.; Kitazumi, Y.; Shirai, O.; Kano, K. Interaction between *D*-Fructose Dehydrogenase and Methoxy-Substituent-Functionalized Carbon Surface to Increase Productive Orientations. *Electrochim. Acta* **2016**, *218*, 41-46.
- (218) Kizling, M.; Bilewicz, R. Fructose Dehydrogenase Electron Transfer Pathway in Bioelectrocatalytic Reactions. *ChemElectroChem* **2017**, *5*, 166-174.
- (219) Yamashita, Y.; Ferri, S.; Huynh, M. L.; Shimizu, H.; Yamaoka, H.; Sode, K. Direct Electron Transfer Type Disposable Sensor Strip for Glucose Sensing Employing an Engineered FAD Glucose Dehydrogenase. *Enzyme Microb. Technol.* **2013**, *52*, 123-128.
- (220) Shiota, M.; Yamazaki, T.; Yoshimatsu, K.; Kojima, K.; Tsugawa, W.; Ferri, S.; Sode, K. An Fe-S Cluster in the Conserved Cys-Rich Region in the Catalytic Subunit of FAD-Dependent Dehydrogenase Complexes. *Bioelectrochemistry* **2016**, *112*, 178-183.
- (221) Babanova, S.; Matanovic, I.; Chavez, M. S.; Atanassov, P. Role of Quinones in Electron Transfer of PQQ-Glucose Dehydrogenase Anodes—Mediation or Orientation Effect. *J. Am. Chem. Soc.* **2015**, *137*, 7754-7762.
- (222) Ivnitski, D.; Atanassov, P.; Apblett, C. Direct Bioelectrocatalysis of PQQ-Dependent Glucose Dehydrogenase. *Electroanalysis* **2007**, *19*, 1562-1568.
- (223) Torimura, M.; Kano, K.; Ikeda, T.; Ueda, T. Spectroelectrochemical Characterization of Quinohemoprotein Alcohol Dehydrogenase from *Gluconobacter suboxydans*. *Chem. Lett.* **1997**, *26*, 525-526.
- (224) Treu, B. L.; Minteer, S. D. Isolation and Purification of PQQ-Dependent Lactate Dehydrogenase from *Gluconobacter* and Use for Direct Electron Transfer at Carbon and Gold Electrodes. *Bioelectrochemistry* **2008**, *74*, 73-77.
- (225) Laurinavicius, V.; Razumiene, J.; Ramanavicius, A.; Ryabov, A. D. Wiring of PQQ-Dehydrogenases. *Biosens. Bioelectron.* **2004**, *20*, 1217-1222.
- (226) Okuda, J.; Sode, K. PQQ Glucose Dehydrogenase with Novel Electron Transfer Ability. *Biochem. Biophys. Res. Commun.* **2004**, *314*, 793-797.
- (227) Ito, K.; Okuda-Shimazaki, J.; Mori, K.; Kojima, K.; Tsugawa, W.; Ikebukuro, K.; Lin, C.-E.; La Belle, J.; Yoshida, H.; Sode, K. Designer Fungus FAD Glucose Dehydrogenase Capable of Direct Electron Transfer. *Biosens. Bioelectron.* **2019**, *123*, 114-123.
- (228) Lubitz, W.; Ogata, H.; Rüdiger, O.; Reijerse, E. Hydrogenases. *Chem. Rev.* **2014**, *114*, 4081-4148.
- (229) Lojou, É.; Luo, X.; Brugna, M.; Candoni, N.; Dementin, S.; Giudici-Orticoni, M. T. Biocatalysts for Fuel Cells: Efficient Hydrogenase Orientation for H<sub>2</sub> Oxidation at Electrodes

- Mmodified with Carbon Nanotubes. *J. Biol. Inorg. Chem.* **2008**, *13*, 1157-1167.
- (230) Gutiérrez-Sánchez, C.; Pita, M.; Vaz-Domínguez, C.; Shleev, S.; De Lacey, A. L. Gold Nanoparticles as Electronic Bridges for Laccase-Based Biocathodes. *J. Am. Chem. Soc.* **2012**, *134*, 17212-17220.
- (231) Solomon, E. I.; Augustine, A. J.; Yoon, J. O<sub>2</sub> Reduction to H<sub>2</sub>O by the multicopper oxidases. *Dalton Trans.* **2008**, *0*, 3921-3932.
- (232) Quintanar, L.; Stoj, C.; Taylor, A. B.; Hart, P. J.; Kosman, D. J.; Solomon, E. I. Shall We Dance? How A Multicopper Oxidase Chooses Its Electron Transfer Partner. *Acc. Chem. Res.* **2007**, *40*, 445-452.
- (233) Sakurai, T.; Kataoka, K. Basic and Applied Features of Multicopper Oxidases, CueO, Bilirubin Oxidase, and Laccase. *Chem. Rec.* **2007**, *7*, 220-229.
- (234) Gutierrez-Sanchez, C.; Ciaccafava, A.; Blanchard, P. Y.; Monsalve, K.; Giudici-Ortoni, M. T.; Lecomte, S.; Lojou, E. Efficiency of Enzymatic O<sub>2</sub> Reduction by *Myrothecium Verrucaria* Bilirubin Oxidase Probed by Surface Plasmon Resonance, PMIRRAS, and Electrochemistry. *ACS Catal.* **2016**, *6*, 5482-5492.
- (235) Karyakin, A. A. Principles of Direct (Mediator Free) Bioelectrocatalysis. *Bioelectrochemistry* **2012**, *88*, 70-75.
- (236) Mazurenko, I.; Monsalve, K.; Rouhana, J.; Parent, P.; Laffon, C.; Goff, A. L.; Szunerits, S.; Boukherroub, R.; Giudici-Ortoni, M.-T.; Mano, N.*et al.* How the Intricate Interactions between Carbon Nanotubes and Two Bilirubin Oxidases Control Direct and Mediated O<sub>2</sub> Reduction. *ACS Appl. Mater. Interfaces* **2016**, *8*, 23074-23085.
- (237) Oteri, F.; Ciaccafava, A.; Poulpiquet, A. d.; Baaden, M.; Lojou, E.; Sacquin-Mora, S. The Weak, Fluctuating, Dipole Moment of Membrane-Bound Hydrogenase from *Aquifex aeolicus* Accounts for Its Adaptability to Charged Electrodes. *Phys. Chem. Chem. Phys.* **2014**, *16*, 11318-11322.
- (238) Pankratov, D.; Sotres, J.; Barrantes, A.; Arnebrant, T.; Shleev, S. Interfacial Behavior and Activity of Laccase and Bilirubin Oxidase on Bare Gold Surfaces. *Langmuir* **2014**, *30*, 2943-2951.
- (239) Hitaishi, V. P.; Mazurenko, I.; Harb, M.; Clément, R.; Taris, M.; Castano, S.; Duché, D.; Lecomte, S.; Ilbert, M.; de Poulpiquet, A.*et al.* Electrostatic-Driven Activity, Loading, Dynamics, and Stability of a Redox Enzyme on Functionalized-Gold Electrodes for Bioelectrocatalysis. *ACS Catal.* **2018**, *8*, 12004-12014.
- (240) Nam, D. H.; Zhang, J. Z.; Andrei, V.; Kornienko, N.; Heidary, N.; Wagner, A.; Nakanishi, K.; Sokol, K. P.; Slater, B.; Zebger, I.*et al.* Solar Water Splitting with a Hydrogenase Integrated in Photoelectrochemical Tandem Cells. *Angew. Chem. Int. Ed.* **2018**, *57*, 10595-10599.
- (241) Singh, K.; McArdle, T.; Sullivan, P. R.; Blanford, C. F. Sources of Activity Loss in the Fuel Cell Enzyme Bilirubin Oxidase. *Energy Environ. Sci.* **2013**, *6*, 2460-2464.
- (242) Ciaccafava, A.; Infossi, P.; Ilbert, M.; Guiral, M.; Lecomte, S.; Giudici-Ortoni, M. T.; Lojou, E. Electrochemistry, AFM, and PM-IRRA Spectroscopy of Immobilized Hydrogenase: Role of a Hydrophobic Helix in Enzyme Orientation for Efficient H<sub>2</sub> Oxidation. *Angew. Chem. Int. Ed.* **2012**, *51*, 953-956.
- (243) Dagys, M.; Laurynėnas, A.; Ratautas, D.; Kulys, J.; Vidžiūnaitė, R.; Talaikis, M.; Niaura, G.; Marcinkevičienė, L.; Meškys, R.; Shleev, S. Oxygen Electroreduction Catalysed by Laccase Wired to Gold Nanoparticles via the Trinuclear Copper Cluster. *Energy Environ. Sci.* **2017**, *10*, 498-502.

- (244) Heidary, N.; Utesch, T.; Zerball, M.; Horch, M.; Millo, D.; Fritsch, J.; Lenz, O.; von Klitzing, R.; Hildebrandt, P.; Fischer, A. *et al.* Orientation-Controlled Electrocatalytic Efficiency of an Adsorbed Oxygen-Tolerant Hydrogenase. *PLOS ONE* **2015**, *10*, e0143101.
- (245) Olejnik, P.; Palys, B.; Kowalczyk, A.; Nowicka, A. M. Orientation of Laccase on Charged Surfaces. Mediatorless Oxygen Reduction on Amino- and Carboxyl-Ended Ethylphenyl Groups. *J. Phys. Chem. C* **2012**, *116*, 25911-25918.
- (246) Olejnik, P.; Pawłowska, A.; Palys, B. Application of Polarization Modulated Infrared Reflection Absorption Spectroscopy for Electrocatalytic Activity Studies of Laccase Adsorbed on Modified Gold Electrodes. *Electrochim. Acta* **2013**, *110*, 105-111.
- (247) Hao, X.; Zhang, J.; Christensen, H. E. M.; Wang, H.; Ulstrup, J. Electrochemical Single-Molecule AFM of the Redox Metalloenzyme Copper Nitrite Reductase in Action. *ChemPhysChem* **2012**, *13*, 2919-2924.
- (248) Gutiérrez-Sánchez, C.; Olea, D.; Marques, M.; Fernández, V. M.; Pereira, I. A. C.; Vélez, M.; De Lacey, A. L. Oriented Immobilization of a Membrane-Bound Hydrogenase onto an Electrode for Direct Electron Transfer. *Langmuir* **2011**, *27*, 6449-6457.
- (249) Gutiérrez-Sanz, Ó.; Natale, P.; Márquez, I.; Marques, M. C.; Zacarias, S.; Pita, M.; Pereira, I. A. C.; López-Montero, I.; De Lacey, A. L.; Vélez, M. H<sub>2</sub>-Fueled ATP Synthesis on an Electrode: Mimicking Cellular Respiration. *Angew. Chem. Int. Ed.* **2016**, *55*, 6216-6220.
- (250) Harada, H.; Onoda, A.; Uchihashi, T.; Watanabe, H.; Sunagawa, N.; Samejima, M.; Igarashi, K.; Hayashi, T. Interdomain Flip-Flop Motion Visualized in Flavocytochrome Cellobiose Dehydrogenase using High-Speed Atomic Force Microscopy During Catalysis. *Chem. Sci.* **2017**, *8*, 6561-6565.
- (251) Cracknell, J. A.; McNamara, T. P.; Lowe, E. D.; Blanford, C. F. Bilirubin Oxidase from *Myrothecium verrucaria*: X-Ray Determination of the Complete Crystal Structure and a Rational Surface Modification for Enhanced Electrocatalytic O<sub>2</sub> Reduction. *Dalton Trans.* **2011**, *40*, 6668-6675.
- (252) Lalaoui, N.; Le Goff, A.; Holzinger, M.; Cosnier, S. Fully Oriented Bilirubin Oxidase on Porphyrin-Functionalized Carbon Nanotube Electrodes for Electrocatalytic Oxygen Reduction. *Chem. Eur. J.* **2015**, *21*, 16868-16873.
- (253) Vaz-Dominguez, C.; Campuzano, S.; Rüdiger, O.; Pita, M.; Gorbacheva, M.; Shleev, S.; Fernandez, V. M.; De Lacey, A. L. Laccase Electrode for Direct Electrocatalytic Reduction of O<sub>2</sub> to H<sub>2</sub>O with High-Operational Stability and Resistance to Chloride Inhibition. *Biosens. Bioelectron.* **2008**, *24*, 531-537.
- (254) Krishnan, S.; Armstrong, F. A. Order-of-Magnitude Enhancement of an Enzymatic Hydrogen-Air Fuel Cell based on Pyrenyl Carbon Nanostructures. *Chem. Sci.* **2012**, *3*, 1015-1023.
- (255) Di Bari, C.; Goñi-Urtiaga, A.; Pita, M.; Shleev, S.; Toscano, M. D.; Sainz, R.; De Lacey, A. L. Fabrication of High Surface Area Graphene Electrodes with High Performance Towards Enzymatic Oxygen Reduction. *Electrochim. Acta* **2016**, *191*, 500-509.
- (256) Gentil, S.; Carriere, M.; Cosnier, S.; Gounel, S.; Mano, N.; Le Goff, A. Direct Electrochemistry of Bilirubin Oxidase from *Magnaporthe oryzae* on Covalently-Functionalized MWCNT for the Design of High-Performance Oxygen-Reducing Biocathodes. *Chem. Eur. J.* **2018**, *24*, 8404-8408.
- (257) Blanford, C. F.; Heath, R. S.; Armstrong, F. A. A Stable Electrode for High-Potential,

Electrocatalytic O<sub>2</sub> Reduction Based on Rational Attachment of a Blue Copper Oxidase to a Graphite Surface. *Chem. Commun.* **2007**, *0*, 1710-1712.

(258) Blanford, C. F.; Foster, C. E.; Heath, R. S.; Armstrong, F. A. Efficient Electrocatalytic Oxygen Reduction by the 'Blue' Copper Oxidase, Laccase, Directly Attached to Chemically Modified Carbons. *Faraday Discuss.* **2009**, *140*, 319-335.

(259) Lalaoui, N.; David, R.; Jamet, H.; Holzinger, M.; Le Goff, A.; Cosnier, S. Hosting Adamantane in the Substrate Pocket of Laccase: Direct Bioelectrocatalytic Reduction of O<sub>2</sub> on Functionalized Carbon Nanotubes. *ACS Catal.* **2016**, *6*, 4259-4264.

(260) Lalaoui, N.; Rousselot-Pailley, P.; Robert, V.; Mekmouche, Y.; Villalonga, R.; Holzinger, M.; Cosnier, S.; Tron, T.; Le Goff, A. Direct Electron Transfer between a Site-Specific Pyrene-Modified Laccase and Carbon Nanotube/Gold Nanoparticle Supramolecular Assemblies for Bioelectrocatalytic Dioxygen Reduction. *ACS Catal.* **2016**, *6*, 1894-1900.

(261) Guan, D.; Kurra, Y.; Liu, W.; Chen, Z. A Click Chemistry Approach to Site-Specific Immobilization of a Small Laccase Enables Efficient Direct Electron Transfer in a Biocathode. *Chem. Commun.* **2015**, *51*, 2522-2525.

(262) Schlesinger, O.; Pasi, M.; Dandela, R.; Meijler, M. M.; Alfonta, L. Electron Transfer Rate Analysis of a Site-Specifically Wired Copper Oxidase. *Phys. Chem. Chem. Phys.* **2018**, *20*, 6159-6166.

(263) Al-Lolage, F. A.; Meneghello, M.; Ma, S.; Ludwig, R.; Bartlett, P. N. A Flexible Method for the Stable, Covalent Immobilization of Enzymes at Electrode Surfaces. *ChemElectroChem* **2017**, *4*, 1528-1534.

(264) Kalisz, H. M.; Hecht, H.-J.; Schomburg, D.; Schmid, R. D. Crystallization and Preliminary X-ray Diffraction Studies of a Deglycosylated Glucose Oxidase from *Aspergillus niger*. *J. Mol. Biol.* **1990**, *213*, 207-209.

(265) Courjean, O.; Gao, F.; Mano, N. Deglycosylation of Glucose Oxidase for Direct and Efficient Glucose Electrooxidation on a Glassy Carbon Electrode. *Angew. Chem. Int. Ed.* **2009**, *48*, 5897-5899.

(266) Yakovleva, M. E.; Killyéni, A.; Ortiz, R.; Schulz, C.; MacAodha, D.; Conghaile, P. Ó.; Leech, D.; Popescu, I. C.; Gonaus, C.; Peterbauer, C. K. *et al.* Recombinant Pyranose Dehydrogenase—A Versatile Enzyme Possessing Both Mediated and Direct Electron Transfer. *Electrochem. Commun.* **2012**, *24*, 120-122.

(267) Bartlett, P. N.; Al-Lolage, F. A. There is No Evidence to Support Literature Claims of Direct Electron Transfer (DET) for Native Glucose Oxidase (GOx) at Carbon Nanotubes or Graphene. *J. Electroanal. Chem.* **2018**, *819*, 26-37.

(268) Wilson, G. S. Native Glucose Oxidase Does Not Undergo Direct Electron Transfer. *Biosens. Bioelectron.* **2016**, *82*, vii-viii.

(269) Wooten, M.; Karra, S.; Zhang, M.; Gorski, W. On the Direct Electron Transfer, Sensing, and Enzyme Activity in the Glucose Oxidase/Carbon Nanotubes System. *Anal. Chem.* **2014**, *86*, 752-757.

(270) Adachi, T.; Kitazumi, Y.; Shirai, O.; Kano, K. Construction of a Bioelectrochemical Formate Generating System from Carbon Dioxide and Dihydrogen. *Electrochem. Commun.* **2018**, *97*, 73-76.

(271) Heller, A. Electron-Conducting Redox Hydrogels: Design, Characteristics and Synthesis. *Curr. Opin. Chem. Biol.* **2006**, *10*, 664-672.

(272) Cosnier, S.; Holzinger, M. Electrosynthesized Polymers for Biosensing. *Chem. Soc. Rev.*



**2011**, *40*, 2146-2156.

(273) Cadet, M.; Gounel, S.; Stines-Chaumeil, C.; Brilland, X.; Rouhana, J.; Louerat, F.; Mano, N. An Enzymatic Glucose/O<sub>2</sub> Biofuel Cell Operating in Human Blood. *Biosens. Bioelectron.* **2016**, *83*, 60-67.

(274) van Rijt, S. H.; Sadler, P. J. Current Applications and Future Potential for Bioinorganic Chemistry in the Development of Anticancer Drugs. *Drug Discov. Today* **2009**, *14*, 1089-1097.

(275) Gross, A. J.; Chen, X.; Giroud, F.; Travelet, C.; Borsali, R.; Cosnier, S. Redox-Active Glyconanoparticles as Electron Shuttles for Mediated Electron Transfer with Bilirubin Oxidase in Solution. *J. Am. Chem. Soc.* **2017**, *139*, 16076-16079.

(276) Hammond, J. H.; Gross, A. J.; Giroud, F.; Travelet, C.; Redouane, B.; Cosnier, S. Solubilized Enzymatic Fuel Cell (SEFC) for Quasi-Continuous Operation Exploiting Carbohydrate Block Copolymer Glyconanoparticle Mediators. *ACS Energy Lett.* **2019**, *4*, 142-148.

(277) Tasca, F.; Gorton, L.; Harreither, W.; Haltrich, D.; Ludwig, R.; Nöll, G. Highly Efficient and Versatile Anodes for Biofuel Cells Based on Cellobiose Dehydrogenase from *Myriococcum thermophilum*. *J. Phys. Chem. C* **2008**, *112*, 13668-13673.

(278) Hodak, J.; Etchenique, R.; Calvo, E. J.; Singhal, K.; Bartlett, P. N. Layer-by-Layer Self-Assembly of Glucose Oxidase with a Poly(allylamine)ferrocene Redox Mediator. *Langmuir* **1997**, *13*, 2708-2716.

(279) Flexer, V.; Calvo, E. J.; Bartlett, P. N. The Application of the Relaxation and Simplex Method to the Analysis of Data for Glucose Electrodes Based on Glucose Oxidase Immobilised in an Osmium Redox Polymer. *J. Electroanal. Chem.* **2010**, *646*, 24-32.

(280) Godman, N. P.; DeLuca, J. L.; McCollum, S. R.; Schmidtke, D. W.; Glatzhofer, D. T. Electrochemical Characterization of Layer-By-Layer Assembled Ferrocene-Modified Linear Poly(ethylenimine)/Enzyme Bioanodes for Glucose Sensor and Biofuel Cell Applications. *Langmuir* **2016**, *32*, 3541-3551.

(281) Elouarzaki, K.; Cheng, D.; Fisher, A. C.; Lee, J.-M. Coupling Orientation and Mediation Strategies for Efficient Electron Transfer in Hybrid Biofuel Cells. *Nat. Energy* **2018**, *3*, 574-581.

(282) Siepenkoetter, T.; Salaj-Kosla, U.; Xiao, X.; Belochapkine, S.; Magner, E. Nanoporous Gold Electrodes with Tuneable Pore Sizes for Bioelectrochemical Applications. *Electroanalysis* **2016**, *28*, 2415-2423.

(283) Siepenkoetter, T.; Salaj-Kosla, U.; Xiao, X.; Conghaile, P. Ó.; Pita, M.; Ludwig, R.; Magner, E. Immobilization of Redox Enzymes on Nanoporous Gold Electrodes: Applications in Biofuel Cells. *ChemPlusChem* **2017**, *82*, 553-560.

(284) Scanlon, M. D.; Salaj-Kosla, U.; Belochapkine, S.; MacAodha, D.; Leech, D.; Ding, Y.; Magner, E. Characterization of Nanoporous Gold Electrodes for Bioelectrochemical Applications. *Langmuir* **2011**, *28*, 2251-2261.

(285) Ding, Y.; Kim, Y. J.; Erlebacher, J. Nanoporous Gold Leaf: "Ancient Technology"/Advanced Material. *Adv. Mater.* **2004**, *16*, 1897-1900.

(286) Hou, C.; Yang, D.; Liang, B.; Liu, A. Enhanced Performance of a Glucose/O<sub>2</sub> Biofuel Cell Assembled with Laccase-Covalently Immobilized Three-Dimensional Macroporous Gold Film-Based Biocathode and Bacterial Surface Displayed Glucose Dehydrogenase-Based Bioanode. *Anal. Chem.*

**2014**, *86*, 6057-6063.

(287) Murata, K.; Kajiya, K.; Nakamura, N.; Ohno, H. Direct Electrochemistry of Bilirubin Oxidase on Three-Dimensional Gold Nanoparticle Electrodes and Its Application in a Biofuel Cell. *Energy Environ. Sci.* **2009**, *2*, 1280-1285.

(288) Wang, X.; Falk, M.; Ortiz, R.; Matsumura, H.; Bobacka, J.; Ludwig, R.; Bergelin, M.; Gorton, L.; Shleev, S. Mediatorless Sugar/Oxygen Enzymatic Fuel Cells Based on Gold Nanoparticle-Modified Electrodes. *Biosens. Bioelectron.* **2012**, *31*, 219-225.

(289) Falk, M.; Alcalde, M.; Bartlett, P. N.; De Lacey, A. L.; Gorton, L.; Gutierrez-Sanchez, C.; Haddad, R.; Kilburn, J.; Leech, D.; Ludwig, R. *et al.* Self-Powered Wireless Carbohydrate/Oxygen Sensitive Biodevice Based on Radio Signal Transmission. *PLOS ONE* **2014**, *9*, e109104.

(290) Nishio, K.; Masuda, H. Anodization of Gold in Oxalate Solution to Form a Nanoporous Black Film. *Angew. Chem. Int. Ed.* **2011**, *50*, 1603-1607.

(291) R. Szamocki; S. Reculosa; S. Ravaine; P. N. Bartlett; A. Kuhn; R. Hempelmann. Tailored Messtructuring and Biofunctionalization of Gold for Increased Electroactivity. *Angew. Chem. Int. Ed.* **2006**, *45*, 1317-1321.

(292) Karajić, A.; Reculosa, S.; Heim, M.; Garrigue, P.; Ravaine, S.; Mano, N.; Kuhn, A. Bottom-up Generation of Miniaturized Coaxial Double Electrodes with Tunable Porosity. *Adv. Mater. Interfaces* **2015**, *2*, 1500192.

(293) Boland, S.; Leech, D. A Glucose/Oxygen Enzymatic Fuel Cell Based on Redox Polymer and Enzyme Immobilisation at Highly-Ordered Macroporous Gold Electrodes. *Analyst* **2012**, *137*, 113-117.

(294) du Toit, H.; Di Lorenzo, M. Continuous Power Generation from Glucose with Two Different Miniature Flow-Through Enzymatic Biofuel Cells. *Biosens. Bioelectron.* **2015**, *69*, 199-205.

(295) Xiao, X.; Li, H.; Zhang, K.; Si, P. Examining the Effects of Self-Assembled Monolayers on Nanoporous Gold Based Amperometric Glucose Biosensors. *Analyst* **2014**, *139*, 488-494.

(296) Pita, M.; Gutierrez-Sanchez, C.; Toscano, M. D.; Shleev, S.; De Lacey, A. L. Oxygen Biosensor Based on Bilirubin Oxidase Immobilized on a Nanostructured Gold Electrode. *Bioelectrochemistry* **2013**, *94*, 69-74.

(297) Siepenkoetter, T.; Salaj-Kosla, U.; Magner, E. The Immobilization of Fructose Dehydrogenase on Nanoporous Gold Electrodes for the Detection of Fructose. *ChemElectroChem* **2017**, *4*, 905-912.

(298) Gao, Z.; Binyamin, G.; Kim, H. H.; Barton, S. C.; Zhang, Y.; Heller, A. Electrodeposition of Redox Polymers and Co-Electrodeposition of Enzymes by Coordinative Crosslinking. *Angew. Chem. Int. Ed.* **2002**, *41*, 810-813.

(299) Xiao, X.; Wang, M. e.; Li, H.; Si, P. One-Step Fabrication of Bio-Functionalized Nanoporous Gold/Poly (3, 4-Ethylenedioxythiophene) Hybrid Electrodes for Amperometric Glucose Sensing. *Talanta* **2013**, *115*, 1054-1059.

(300) Salaj-Kosla, U.; Scanlon, M. D.; Baumeister, T.; Zahma, K.; Ludwig, R.; Conghaile, P. Ó.; MacAodha, D.; Leech, D.; Magner, E. Mediated Electron Transfer of Cellobiose Dehydrogenase and Glucose Oxidase at Osmium Polymer-Modified Nanoporous Gold Electrodes. *Anal. Bioanal. Chem.* **2013**, *405*, 3823-3830.

(301) Deng, L.; Wang, F.; Chen, H.; Shang, L.; Wang, L.; Wang, T.; Dong, S. A Biofuel Cell with

Enhanced Performance by Multilayer Biocatalyst Immobilized on Highly Ordered Macroporous Electrode. *Biosens. Bioelectron.* **2008**, *24*, 329-333.

(302) Chen, L. Y.; Fujita, T.; Chen, M. W. Biofunctionalized Nanoporous Gold for Electrochemical Biosensors. *Electrochim. Acta* **2012**, *67*, 1-5.

(303) Hou, C.; Liu, A. An Integrated Device of Enzymatic Biofuel Cells and Supercapacitor for Both Efficient Electric Energy Conversion and Storage. *Electrochim. Acta* **2017**, *245*, 303-308.

(304) Yu, Y.; Han, Y.; Xu, M.; Zhang, L.; Dong, S. Automatic Illumination Compensation Device Based on a Photoelectrochemical Biofuel Cell Driven by Visible Light. *Nanoscale* **2016**, *8*, 9004-9008.

(305) Reid, R. C.; Jones, S. R.; Hickey, D. P.; Minter, S. D.; Gale, B. K. Modeling Carbon Nanotube Connectivity and Surface Activity in a Contact Lens Biofuel Cell. *Electrochim. Acta* **2016**, *203*, 30-40.

(306) Ó Conghaile, P.; Falk, M.; MacAodha, D.; Yakovleva, M. E.; Gonaus, C.; Peterbauer, C. K.; Gorton, L.; Shleev, S.; Leech, D. Fully Enzymatic Membraneless Glucose/Oxygen Fuel Cell That Provides 0.275 mA cm<sup>-2</sup> in 5 mM Glucose, Operates in Human Physiological Solutions, and Powers Transmission of Sensing Data. *Anal. Chem.* **2016**, *88*, 2156-2163.

(307) Giroud, F.; Sawada, K.; Taya, M.; Cosnier, S. 5,5-Dithiobis(2-Nitrobenzoic Acid) Pyrene Derivative-Carbon Nanotube Electrodes for NADH Electrooxidation and Oriented Immobilization of Multicopper Oxidases for the Development of Glucose/O<sub>2</sub> Biofuel Cells. *Biosens. Bioelectron.* **2017**, *87*, 957-963.

(308) Yoshino, S.; Miyake, T.; Yamada, T.; Hata, K.; Nishizawa, M. Molecularly Ordered Bioelectrocatalytic Composite Inside a Film of Aligned Carbon Nanotubes. *Adv. Energy Mater.* **2013**, *3*, 60-64.

(309) Muguruma, H.; Iwasa, H.; Hidaka, H.; Hiratsuka, A.; Uzawa, H. Mediatorless Direct Electron Transfer between Flavin Adenine Dinucleotide-Dependent Glucose Dehydrogenase and Single-Walled Carbon Nanotubes. *ACS Catal.* **2017**, *7*, 725-734.

(310) Holzinger, M.; Le Goff, A.; Cosnier, S. Carbon Nanotube/Enzyme Biofuel Cells. *Electrochim. Acta* **2012**, *82*, 179-190.

(311) Zhong, Z.; Qian, L.; Tan, Y.; Wang, G.; Yang, L.; Hou, C.; Liu, A. A High-Performance Glucose/Oxygen Biofuel Cell Based on Multi-Walled Carbon Nanotube Films with Electrophoretic Deposition. *J. Electroanal. Chem.* **2018**, *823*, 723-729.

(312) Xia, H. Q.; Kitazumi, Y.; Shirai, O.; Ozawa, H.; Onizuka, M.; Komukai, T.; Kano, K. Factors Affecting the Interaction Between Carbon Nanotubes and Redox Enzymes in Direct Electron Transfer-Type Bioelectrocatalysis. *Bioelectrochem.* **2017**, *118*, 70-74.

(313) Bai, L.; Jin, L.; Han, L.; Dong, S. Self-Powered Fluorescence Controlled Wwitch Systems Based on Biofuel Cells. *Energy Environ. Sci.* **2013**, *6*, 3015-3021.

(314) Gumeci, C.; Do, D.; Barton, S. C. Electrospun Carbon Nanofibers as Supports for Bioelectrodes. *Electrocatalysis* **2017**, *8*, 321-328.

(315) Komori, K.; Huang, J.; Mizushima, N.; Ko, S.; Tatsuma, T.; Sakai, Y. Controlled Direct Electron Transfer Kinetics of Fructose Dehydrogenase at Cup-Stacked Carbon Nanofibers. *Phys. Chem. Chem. Phys.* **2017**, *19*, 27795-27800.

(316) Senthamizhan, A.; Balusamy, B.; Uyar, T. Glucose Sensors Based on Electrospun Nanofibers: A Review. *Anal. Bioanal. Chem.* **2016**, *408*, 1285-1306.

- (317) Bourourou, M.; Holzinger, M.; Elouarzaki, K.; Le Goff, A.; Bossard, F.; Rossignol, C.; Djurado, E.; Martin, V.; Curtil, D.; Chaussy, D. *et al.* Laccase Wiring on Free-Standing Electrospun Carbon Nanofibres Using a Mediator Plug. *Chem. Commun.* **2015**, *51*, 14574-14577.
- (318) Sim, H. J.; Lee, D. Y.; Kim, H.; Choi, Y.-B.; Kim, H.-H.; Baughman, R. H.; Kim, S. J. Stretchable Fiber Biofuel Cell by Rewrapping Multiwalled Carbon Nanotube Sheets. *Nano Lett.* **2018**, *18*, 5272-5278.
- (319) Filip, J.; Tkac, J. Is Graphene Worth Using in Biofuel Cells? *Electrochim. Acta* **2014**, *136*, 340-354.
- (320) Tsujimura, S.; Murata, K.; Akatsuka, W. Exceptionally High Glucose Current on a Hierarchically Structured Porous Carbon Electrode with “Wired” Flavin Adenine Dinucleotide-Dependent Glucose Dehydrogenase. *J. Am. Chem. Soc.* **2014**, *136*, 14432-14437.
- (321) Funabashi, H.; Takeuchi, S.; Tsujimura, S. Hierarchical Meso/Macro-Porous Carbon Fabricated from Dual MgO Templates for Direct Electron Transfer Enzymatic Electrodes. *Sci. Rep.* **2017**, *7*, 45147.
- (322) Wu, G.; Gao, Y.; Zhao, D.; Ling, P.; Gao, F. Methanol/Oxygen Enzymatic Biofuel Cell Using Laccase and NAD<sup>+</sup>-Dependent Dehydrogenase Cascades as Biocatalysts on Carbon Nanodots Electrodes. *ACS Appl. Mater. Interfaces* **2017**, *9*, 40978-40986.
- (323) MacVittie, K.; Conlon, T.; Katz, E. A Wireless Transmission System Powered by an Enzyme Biofuel Cell Implanted in an Orange. *Bioelectrochemistry* **2015**, *106*, 28-33.
- (324) Slaughter, G.; Kulkarni, T. A Self-Powered Glucose Biosensing System. *Biosens. Bioelectron.* **2016**, *78*, 45-50.
- (325) Hickey, D. P.; Milton, R. D.; Rasmussen, M.; Abdellaoui, S.; Nguyen, K.; Minteer, S. D. In *Electrochemistry*; The Royal Society of Chemistry, 2016; Vol. 13.
- (326) Koushanpour, A.; Guz, N.; Gamella, M.; Katz, E. Biofuel Cell Based on Carbon Fiber Electrodes Functionalized with Graphene Nanosheets. *ECS J. Solid State Sci. Technol.* **2016**, *5*, M3037-M3040.
- (327) Ouyang, J.; Liu, Z.; Han, Y.; Zeng, K.; Sheng, J.; Deng, L.; Liu, Y.-N. Fabrication of Surface Protein-Imprinted Biofuel Cell for Sensitive Self-Powered Glycoprotein Detection. *ACS Appl. Mater. Interfaces* **2016**, *8*, 35004-35011.
- (328) Poulpiquet, A. d.; Marques-Knopf, H.; Wernert, V.; Giudici-Ortoni, M. T.; Gadiou, R.; Lojou, E. Carbon Nanofiber Mesoporous Films: Efficient Platforms for Bio-Hydrogen Oxidation in Biofuel Cells. *Phys. Chem. Chem. Phys.* **2014**, *16*, 1366-1378.
- (329) Song, Y.; Chen, C.; Wang, C. Graphene/Enzyme-Encrusted Three-Dimensional Carbon Micropillar Arrays for Mediatorless Micro-Biofuel Cells. *Nanoscale* **2015**, *7*, 7084-7090.
- (330) Lalaoui, N.; Holzinger, M.; Le Goff, A.; Cosnier, S. Diazonium Functionalisation of Carbon Nanotubes for Specific Orientation of Multicopper Oxidases: Controlling Electron Entry Points and Oxygen Diffusion to the Enzyme. *Chem. Eur. J.* **2016**, *22*, 10494-10500.
- (331) Sosna, M.; Stoica, L.; Wright, E.; Kilburn, J. D.; Schuhmann, W.; Bartlett, P. N. Mass Transport Controlled Oxygen Reduction at Anthraquinone Modified 3D-CNT Electrodes with Immobilized *Trametes hirsuta* Laccase. *Phys. Chem. Chem. Phys.* **2012**, *14*, 11882-11885.
- (332) Ghanem, M. A.; Kocak, I.; Al-Mayouf, A.; AlHoshan, M.; Bartlett, P. N. Covalent Modification of Carbon Nanotubes with Anthraquinone by Electrochemical Grafting and Solid Phase

Synthesis. *Electrochim. Acta* **2012**, *68*, 74-80.

(333) Elouarzaki, K.; Bourourou, M.; Holzinger, M.; Le Goff, A.; Marks, R. S.; Cosnier, S. Freestanding HRP-GOx Redox Buckypaper as an Oxygen-Reducing Biocathode for Biofuel Cell Applications. *Energy Environ. Sci.* **2015**, *8*, 2069-2074.

(334) Habermüller, K.; Ramanavicius, A.; Laurinavicius, V.; Schuhmann, W. An Oxygen-Insensitive Reagentless Glucose Biosensor Based on Osmium-Complex Modified Polypyrrole. *Electroanalysis* **2000**, *12*, 1383-1389.

(335) Monsalve, K.; Mazurenko, I.; Gutierrez-Sanchez, C.; Ilbert, M.; Infossi, P.; Frielingsdorf, S.; Giudici-Ortoni, M. T.; Lenz, O.; Lojou, E. Impact of Carbon Nanotube Surface Chemistry on Hydrogen Oxidation by Membrane-Bound Oxygen-Tolerant Hydrogenases. *ChemElectroChem* **2016**, *3*, 2179-2188.

(336) Trohalaki, S.; Pachter, R.; Luckarift, H. R.; Johnson, G. R. Immobilization of the Laccases from *Trametes versicolor* and *Streptomyces coelicolor* on Single-Wall Carbon Nanotube Electrodes: A Molecular Dynamics Study. *Fuel Cells* **2012**, *12*, 656-664.

(337) Singh, M.; Holzinger, M.; Biloivan, O.; Cosnier, S. 3D-Nanostructured Scaffold Electrodes Based on Single-Walled Carbon Nanotubes and Nanodiamonds for High Performance Biosensors. *Carbon* **2013**, *61*, 349-356.

(338) Ciaccafava, A.; De Poulpiquet, A.; Techer, V.; Giudici-Ortoni, M. T.; Tingry, S.; Innocent, C.; Lojou, E. An Innovative Powerful and Mediatorless H<sub>2</sub>O<sub>2</sub> Biofuel Cell Based on an Outstanding Bioanode. *Electrochem. Commun.* **2012**, *23*, 25-28.

(339) Chen, T.; Barton, S. C.; Binyamin, G.; Gao, Z.; Zhang, Y.; Kim, H.-H.; Heller, A. A Miniature Biofuel Cell. *J. Am. Chem. Soc.* **2001**, *123*, 8630-8631.

(340) Mano, N.; Mao, F.; Heller, A. Characteristics of a Miniature Compartment-less Glucose-O<sub>2</sub> Biofuel Cell and Its Operation in a Living Plant. *J. Am. Chem. Soc.* **2003**, *125*, 6588-6594.

(341) Miyake, T.; Haneda, K.; Nagai, N.; Yatagawa, Y.; Onami, H.; Yoshino, S.; Abe, T.; Nishizawa, M. Enzymatic Biofuel Cells Designed for Direct Power Generation from Biofluids in Living Organisms. *Energy Environ. Sci.* **2011**, *4*, 5008-5012.

(342) Sales, F. C. P. F.; Iost, R. M.; Martins, M. V. A.; Almeida, M. C.; Crespilho, F. N. An Intravenous Implantable Glucose/Dioxygen Biofuel Cell with Modified Flexible Carbon Fiber Electrodes. *Lab Chip* **2013**, *13*, 468-474.

(343) Orecchioni, M.; Ménard-Moyon, C.; Delogu, L. G.; Bianco, A. Graphene and the Immune System: Challenges and Potentiality. *Adv. Drug Deliv. Rev.* **2016**, *105*, 163-175.

(344) Magrez, A.; Kasas, S.; Salicio, V.; Pasquier, N.; Seo, J. W.; Celio, M.; Catsicas, S.; Schwaller, B.; Forró, L. Cellular Toxicity of Carbon-Based Nanomaterials. *Nano Lett.* **2006**, *6*, 1121-1125.

(345) Du, J.; Wang, S.; You, H.; Zhao, X. Understanding the Toxicity of Carbon Nanotubes in the Environment is Crucial to the Control of Nanomaterials in Producing and Processing and the Assessment of Health Risk for Human: A Review. *Environ. Toxicol. Pharmacol.* **2013**, *36*, 451-462.

(346) Flexer, V.; Brun, N.; Backov, R.; Mano, N. Designing Highly Efficient Enzyme-Based Carbonaceous Foams Electrodes for Biofuel Cells. *Energy Environ. Sci.* **2010**, *3*, 1302-1306.

(347) Mazurenko, I.; Clément, R.; Byrne-Kodjabachian, D.; de Poulpiquet, A.; Tsujimura, S.; Lojou, E. Pore Size Effect of MgO-Templated Carbon on Enzymatic H<sub>2</sub> Oxidation by the Hyperthermophilic Hydrogenase from *Aquifex aeolicus*. *J. Electroanal. Chem.* **2018**, *812*, 221-226.

- (348) Kontani, R.; Tsujimura, S.; Kano, K. Air Diffusion Biocathode with CueO as Electrocatalyst Adsorbed on Carbon Particle-Modified Electrodes. *Bioelectrochemistry* **2009**, *76*, 10-13.
- (349) Lalaoui, N.; de Poulpiquet, A.; Haddad, R.; Le Goff, A.; Holzinger, M.; Gounel, S.; Mermoux, M.; Infossi, P.; Mano, N.; Lojou, E. *et al.* A membraneless air-breathing hydrogen biofuel cell based on direct wiring of thermostable enzymes on carbon nanotube electrodes. *Chem. Commun.* **2015**, *51*, 7447-7450.
- (350) Shleev, S.; Shumakovich, G.; Morozova, O.; Yaropolov, A. Stable 'Floating' Air Diffusion Biocathode Based on Direct Electron Transfer Reactions Between Carbon Particles and High Redox Potential Laccase. *Fuel Cells* **2010**, *10*, 726-733.
- (351) Nakagawa, T.; Mita, H.; Kumita, H.; Sakai, H.; Tokita, Y.; Tsujimura, S. Water-Repellent-Treated Enzymatic Electrode for Passive Air-Breathing Biocathodic Reduction of Oxygen. *Electrochem. Commun.* **2013**, *36*, 46-49.
- (352) So, K.; Onizuka, M.; Komukai, T.; Kitazumi, Y.; Shirai, O.; Kano, K. Binder/Surfactant-Free Biocathode with Bilirubin Oxidase for Gas-Diffusion-Type System. *Electrochem. Commun.* **2016**, *66*, 58-61.
- (353) Tarasevich, M. R.; Bogdanovskaya, V. A.; Kapustin, A. V. Nanocomposite Material Laccase/Dispersed Carbon Carrier for Oxygen Electrode. *Electrochem. Commun.* **2003**, *5*, 491-496.
- (354) Gupta, G.; Lau, C.; Rajendran, V.; Colon, F.; Branch, B.; Ivnitski, D.; Atanassov, P. Direct Electron Transfer Catalyzed by Bilirubin Oxidase for Air Breathing Gas-Diffusion Electrodes. *Electrochem. Commun.* **2011**, *13*, 247-249.
- (355) Gupta, G.; Lau, C.; Branch, B.; Rajendran, V.; Ivnitski, D.; Atanassov, P. Direct Bio-Electrocatalysis by Multi-Copper Oxidases: Gas-Diffusion Laccase-Catalyzed Cathodes for Biofuel Cells. *Electrochim. Acta* **2011**, *56*, 10767-10771.
- (356) Rincón, R. A.; Lau, C.; Luckarift, H. R.; Garcia, K. E.; Adkins, E.; Johnson, G. R.; Atanassov, P. Enzymatic Fuel Cells: Integrating Flow-Through Anode and Air-Breathing Cathode into a Membrane-Less Biofuel Cell Design. *Biosens. Bioelectron.* **2011**, *27*, 132-136.
- (357) Higgins, S. R.; Lau, C.; Atanassov, P.; Minteer, S. D.; Cooney, M. J. Hybrid Biofuel Cell: Microbial Fuel Cell with an Enzymatic Air-Breathing Cathode. *ACS Catal.* **2011**, *1*, 994-997.
- (358) Lau, C.; Adkins, E. R.; Ramasamy, R. P.; Luckarift, H. R.; Johnson, G. R.; Atanassov, P. Design of Carbon Nanotube-Based Gas-Diffusion Cathode for O<sub>2</sub> Reduction by Multicopper Oxidases. *Adv. Energy Mater.* **2012**, *2*, 162-168.
- (359) So, K.; Kitazumi, Y.; Shirai, O.; Kurita, K.; Nishihara, H.; Higuchi, Y.; Kano, K. Gas-Diffusion and Direct-Electron-Transfer-Type Bioanode for Hydrogen Oxidation with Oxygen-Tolerant [NiFe]-Hydrogenase as an Electrocatalyst. *Chem. Lett.* **2014**, *43*, 1575-1577.
- (360) Sakai, K.; Kitazumi, Y.; Shirai, O.; Takagi, K.; Kano, K. Efficient Bioelectrocatalytic CO<sub>2</sub> Reduction on Gas-Diffusion-Type Biocathode with Tungsten-Containing Formate Dehydrogenase. *Electrochem. Commun.* **2016**, *73*, 85-88.
- (361) Ciniciato, G. P. M. K.; Lau, C.; Cochrane, A.; Sibbett, S. S.; Gonzalez, E. R.; Atanassov, P. Development of Paper Based Electrodes: From Air-Breathing to Paintable Enzymatic Cathodes. *Electrochim. Acta* **2012**, *82*, 208-213.
- (362) Narváez Villarrubia, C. W.; Lau, C.; Ciniciato, G. P. M. K.; Garcia, S. O.; Sibbett, S. S.; Petsev, D. N.; Babanova, S.; Gupta, G.; Atanassov, P. Practical Electricity Generation from a Paper

Based Biofuel Cell Powered by Glucose in Ubiquitous Liquids. *Electrochem. Commun.* **2014**, *45*, 44-47.

(363) Lau, C.; Moehlenbrock, M. J.; Arechederra, R. L.; Falase, A.; Garcia, K.; Rincon, R.; Minteer, S. D.; Banta, S.; Gupta, G.; Babanova, S. *et al.* Paper Based Biofuel Cells: Incorporating Enzymatic Cascades for Ethanol and Methanol Oxidation. *Int. J. Hydrogen Energy* **2015**, *40*, 14661-14666.

(364) Narvaez Villarrubia, C. W.; Soavi, F.; Santoro, C.; Arbizzani, C.; Serov, A.; Rojas-Carbonell, S.; Gupta, G.; Atanassov, P. Self-Feeding Paper Based Biofuel Cell/Self-Powered Hybrid  $\mu$ -Supercapacitor Integrated System. *Biosens. Bioelectron.* **2016**, *86*, 459-465.

(365) Mi, L.; Yu, J.; He, F.; Jiang, L.; Wu, Y.; Yang, L.; Han, X.; Li, Y.; Liu, A.; Wei, W. *et al.* Boosting Gas Involved Reactions at Nanochannel Reactor with Joint Gas-Solid-Liquid Interfaces and Controlled Wettability. *J. Am. Chem. Soc.* **2017**, *139*, 10441-10446.

(366) Moore, C. M.; Minteer, S. D.; Martin, R. S. Microchip-Based Ethanol/Oxygen Biofuel Cell. *Lab Chip* **2005**, *5*, 218-225.

(367) Lim, K. G.; Palmore, G. T. R. Microfluidic Biofuel Cells: The Influence of Electrode Diffusion Layer on Performance. *Biosens. Bioelectron.* **2007**, *22*, 941-947.

(368) Zebda, A.; Renaud, L.; Cretin, M.; Innocent, C.; Pichot, F.; Ferrigno, R.; Tingry, S. Electrochemical Performance of a Glucose/Oxygen Microfluidic Biofuel Cell. *J. Power Sources* **2009**, *193*, 602-606.

(369) Zebda, A.; Renaud, L.; Cretin, M.; Innocent, C.; Ferrigno, R.; Tingry, S. Membraneless microchannel glucose biofuel cell with improved electrical performances. *Sens. Actuat. B: Chem.* **2010**, *149*, 44-50.

(370) Togo, M.; Takamura, A.; Asai, T.; Kaji, H.; Nishizawa, M. An Enzyme-Based Microfluidic Biofuel Cell Using Vitamin K<sub>3</sub>-Mediated Glucose Oxidation. *Electrochim. Acta* **2007**, *52*, 4669-4674.

(371) Beneyton, T.; Wijaya, I. P. M.; Salem, C. B.; Griffiths, A. D.; Taly, V. Membraneless Glucose/O<sub>2</sub> Microfluidic Biofuel Cells Using Covalently Bound Enzymes. *Chem. Commun.* **2013**, *49*, 1094-1096.

(372) Abreu, C.; Nedellec, Y.; Ondel, O.; Buret, F.; Cosnier, S.; Le Goff, A.; Holzinger, M. Glucose Oxidase Bioanodes for Glucose Conversion and H<sub>2</sub>O<sub>2</sub> Production for Horseradish Peroxidase Biocathodes in a Flow Through Glucose Biofuel Cell Design. *J. Power Sources* **2018**, *392*, 176-180.

(373) Abreu, C.; Nedellec, Y.; Gross, A. J.; Ondel, O.; Buret, F.; Goff, A. L.; Holzinger, M.; Cosnier, S. Assembly and Stacking of Flow-Through Enzymatic Bioelectrodes for High Power Glucose Fuel Cells. *ACS Appl. Mater. Interfaces* **2017**, *9*, 23836-23842.

(374) Gonzalez-Guerrero, M. J.; Esquivel, J. P.; Sanchez-Molas, D.; Godignon, P.; Munoz, F. X.; del Campo, F. J.; Giroud, F.; Minteer, S. D.; Sabate, N. Membraneless Glucose/O<sub>2</sub> Microfluidic Enzymatic Biofuel Cell Using Pyrolyzed Photoresist Film Electrodes. *Lab Chip* **2013**, *13*, 2972-2979.

(375) Dector, A.; Escalona-Villalpando, R. A.; Dector, D.; Vallejo-Becerra, V.; Chávez-Ramírez, A. U.; Arriaga, L. G.; Ledesma-García, J. Perspective Use of Direct Human Blood as an Energy Source in Air-Breathing Hybrid Microfluidic Fuel Cells. *J. Power Sources* **2015**, *288*, 70-75.

(376) Escalona-Villalpando, R. A.; Reid, R. C.; Milton, R. D.; Arriaga, L. G.; Minteer, S. D.; Ledesma-García, J. Improving the Performance of Lactate/Oxygen Biofuel Cells Using a Microfluidic Design. *J. Power Sources* **2017**, *342*, 546-552.

- (377) Desmaële, D.; Nguyen-Boisse, T. T.; Renaud, L.; Tingry, S. Integration of Cantilevered Porous Electrodes into Microfluidic Co-Laminar Enzymatic Biofuel Cells: Toward Higher Enzyme Loadings for Enhanced Performance. *Microelectron. Eng.* **2016**, *165*, 23-26.
- (378) Pankratov, D.; Ohlsson, L.; Gudmundsson, P.; Halak, S.; Ljunggren, L.; Blum, Z.; Shleev, S. *Ex vivo* Electric Power Generation in Human Blood Using an Enzymatic Fuel Cell in a Vein Replica. *RSC Adv.* **2016**, *6*, 70215-70220.
- (379) Winter, M.; Brodd, R. J. What Are Batteries, Fuel Cells, and Supercapacitors? *Chem. Rev.* **2004**, *104*, 4245-4270.
- (380) Skunik-Nuckowska, M.; Grzejszczyk, K.; Stolarczyk, K.; Bilewicz, R.; Kulesza, P. J. Integration of Supercapacitors with Enzymatic Biobatteries toward More Effective Pulse-Powered Use in Small-Scale Energy Harvesting Devices. *J. Appl. Electrochem.* **2014**, *44*, 497-507.
- (381) Hanashi, T.; Yamazaki, T.; Tsugawa, W.; Ferri, S.; Nakayama, D.; Tomiyama, M.; Ikebukuro, K.; Sode, K. BioCapacitor—A Novel Category of Biosensor. *Biosens. Bioelectron.* **2009**, *24*, 1837-1842.
- (382) Monsalve, K.; Mazurenko, I.; Lalaoui, N.; Le Goff, A.; Holzinger, M.; Infossi, P.; Nitsche, S.; Lojou, J. Y.; Giudici-Ortoni, M. T.; Cosnier, S. *et al.* A H<sub>2</sub>/O<sub>2</sub> Enzymatic Fuel Cell as a Sustainable Power for a Wireless Device. *Electrochem. Commun.* **2015**, *60*, 216-220.
- (383) Agnes, C.; Holzinger, M.; Le Goff, A.; Reuillard, B.; Elouarzaki, K.; Tingry, S.; Cosnier, S. Supercapacitor/Biofuel Cell Hybrids Based on Wired Enzymes on Carbon Nanotube Matrices: Autonomous Reloading after High Power Pulses in Neutral Buffered Glucose Solutions. *Energy Environ. Sci.* **2014**, *7*, 1884-1888.
- (384) Pankratov, D.; Blum, Z.; Suyatin, D. B.; Popov, V. O.; Shleev, S. Self-Charging Electrochemical Biocapacitor. *ChemElectroChem* **2014**, *1*, 343-346.
- (385) Pankratov, D.; Blum, Z.; Shleev, S. Hybrid Electric Power Biodevices. *ChemElectroChem* **2014**, *1*, 1798-1807.
- (386) Santoro, C.; Soavi, F.; Serov, A.; Arbizzani, C.; Atanassov, P. Self-Powered Supercapacitive Microbial Fuel Cell: The Ultimate Way of Boosting and Harvesting Power. *Biosens. Bioelectron.* **2016**, *78*, 229-235.
- (387) Kizling, M.; Stolarczyk, K.; Kiat, J. S. S.; Tammela, P.; Wang, Z.; Nyholm, L.; Bilewicz, R. Pseudocapacitive Polypyrrole–Nanocellulose Composite for Sugar–Air Enzymatic Fuel Cells. *Electrochem. Commun.* **2015**, *50*, 55-59.
- (388) Kizling, M.; Draminska, S.; Stolarczyk, K.; Tammela, P.; Wang, Z.; Nyholm, L.; Bilewicz, R. Biosupercapacitors for Powering Oxygen Sensing Devices. *Bioelectrochemistry* **2015**, *106*, Part A, 34-40.
- (389) Knoche, K. L.; Hickey, D. P.; Milton, R. D.; Curchoe, C. L.; Minteer, S. D. Hybrid Glucose/O<sub>2</sub> Biobattery and Supercapacitor Utilizing a Pseudocapacitive Dimethylferrocene Redox Polymer at the Bioanode. *ACS Energy Lett.* **2016**, *1*, 380-385.
- (390) Alsaoub, S.; Ruff, A.; Conzuelo, F.; Ventosa, E.; Ludwig, R.; Shleev, S.; Schuhmann, W. An Intrinsic Self-Charging Biosupercapacitor Comprised of a High-Potential Bioanode and a Low-Potential Biocathode. *ChemPlusChem* **2017**, *82*, 576-583.
- (391) Mosa, I. M.; Pattammattel, A.; Kadimisetty, K.; Pande, P.; El-Kady, M. F.; Bishop, G. W.; Novak, M.; Kaner, R. B.; Basu, A. K.; Kumar, C. V. *et al.* Ultrathin Graphene–Protein Supercapacitors



- for Miniaturized Bioelectronics. *Adv. Energy Mater.* **2017**, *7*, 1700358.
- (392) Xiao, X.; Conghaile, P. Ó.; Leech, D.; Ludwig, R.; Magner, E. A Symmetric Supercapacitor/Biofuel Cell Hybrid Device Based on Enzyme-Modified Nanoporous Gold: An Autonomous Pulse Generator. *Biosens. Bioelectron.* **2017**, *90*, 96-102.
- (393) Shen, F.; Pankratov, D.; Pankratova, G.; Toscano, M. D.; Zhang, J.; Ulstrup, J.; Chi, Q.; Gorton, L. Supercapacitor/Biofuel Cell Hybrid Device Employing Biomolecules for Energy Conversion and Charge Storage. *Bioelectrochem.* **2019**, *128*, 94-99.
- (394) Ahmad, R.; Sardar, M. Enzyme Immobilization: An Overview on Nanoparticles as Immobilization Matrix. *Biochem. Anal. Biochem.* **2015**, *4*, 1000178.
- (395) Mateo, C.; Palomo, J. M.; Fernandez-Lorente, G.; Guisan, J. M.; Fernandez-Lafuente, R. Improvement of Enzyme Activity, Stability and Selectivity via Immobilization Techniques. *Enzyme Microb. Technol.* **2007**, *40*, 1451-1463.
- (396) Lojou, E. Hydrogenases as Catalysts for Fuel Cells: Strategies for Efficient Immobilization at Electrode Interfaces. *Electrochim. Acta* **2011**, *56*, 10385-10397.
- (397) Climent, V.; Zhang, J.; Friis, E. P.; Østergaard, L. H.; Ulstrup, J. Voltammetry and Single-Molecule in Situ Scanning Tunneling Microscopy of Laccases and Bilirubin Oxidase in Electrocatalytic Dioxygen Reduction on Au(111) Single-Crystal Electrodes. *J. Phys. Chem. C* **2011**, *116*, 1232-1243.
- (398) Sugimoto, Y.; Kitazumi, Y.; Tsujimura, S.; Shirai, O.; Yamamoto, M.; Kano, K. Electrostatic Interaction between an Enzyme and Electrodes in the Electric Double Layer Examined in a View of Direct Electron Transfer-Type Bioelectrocatalysis. *Biosens. Bioelectron.* **2015**, *63*, 138-144.
- (399) Salaj-Kosla, U.; Poller, S.; Schuhmann, W.; Shleev, S.; Magner, E. Direct Electron Transfer of *Trametes hirsuta* Laccase Adsorbed at Unmodified Nanoporous Gold Electrodes. *Bioelectrochemistry* **2013**, *91*, 15-20.
- (400) Krikstolaityte, V.; Barrantes, A.; Ramanavicius, A.; Arnebrant, T.; Shleev, S.; Ruzgas, T. Bioelectrocatalytic Reduction of Oxygen at Gold Nanoparticles Modified with Laccase. *Bioelectrochemistry* **2014**, *95*, 1-6.
- (401) Dagens, M.; Haberska, K.; Shleev, S.; Arnebrant, T.; Kulys, J.; Ruzgas, T. Laccase-Gold Nanoparticle Assisted Bioelectrocatalytic Reduction of Oxygen. *Electrochem. Commun.* **2010**, *12*, 933-935.
- (402) Qiu, H.; Xu, C.; Huang, X.; Ding, Y.; Qu, Y.; Gao, P. Adsorption of Laccase on the Surface of Nanoporous Gold and Direct Electron Transfer between Them. *J. Phys. Chem. C* **2008**, *112*, 14781-14785.
- (403) Bellino, M. G.; Soler-Illia, G. J. A. A. Nano-Designed Enzyme-Functionalized Hierarchical Metal-Oxide Mesoporous Thin Films: En Route to Versatile Biofuel Cells. *Small* **2014**, *10*, 2834-2839.
- (404) Funabashi, H.; Murata, K.; Tsujimura, S. Effect of Pore Size of MgO-Templated Carbon on the Direct Electrochemistry of *D*-Fructose Dehydrogenase. *Electrochemistry* **2015**, *83*, 372-375.
- (405) Takahashi, H.; Li, B.; Sasaki, T.; Miyazaki, C.; Kajino, T.; Inagaki, S. Catalytic Activity in Organic Solvents and Stability of Immobilized Enzymes Depend on the Pore Size and Surface Characteristics of Mesoporous Silica. *Chem. Mater.* **2000**, *12*, 3301-3305.
- (406) Lamberg, P.; Hamit-Eminovski, J.; Toscano, M. D.; Eicher-Lorka, O.; Niaura, G.; Arnebrant, T.; Shleev, S.; Ruzgas, T. Electrical Activity of Cellobiose Dehydrogenase Adsorbed on Thiols:

- Influence of Charge and Hydrophobicity. *Bioelectrochemistry* **2017**, *115*, 26-32.
- (407) Bourourou, M.; Elouarzaki, K.; Lalaoui, N.; Agnes, C.; Le Goff, A.; Holzinger, M.; Maaref, A.; Cosnier, S. Supramolecular Immobilization of Laccase on Carbon Nanotube Electrodes Functionalized with (Methylpyrenylaminomethyl)Anthraquinone for Direct Electron Reduction of Oxygen. *Chemistry* **2013**, *19*, 9371-9375.
- (408) Xia, H.-q.; Kitazumi, Y.; Shirai, O.; Kano, K. Enhanced Direct Electron Transfer-Type Bioelectrocatalysis of Bilirubin Oxidase on Negatively Charged Aromatic Compound-Modified Carbon Electrode. *J. Electroanal. Chem.* **2016**, *763*, 104-109.
- (409) Matanovic, I.; Babanova, S.; Chavez, M. S.; Atanassov, P. Protein-Support Interactions for Rationally Designed Bilirubin Oxidase Based Cathode: A Computational Study. *J. Phys. Chem. B* **2016**, *120*, 3634-3641.
- (410) Tasca, F.; Harreither, W.; Ludwig, R.; Gooding, J. J.; Gorton, L. Cellobiose Dehydrogenase Aryl Diazonium Modified Single Walled Carbon Nanotubes: Enhanced Direct Electron Transfer through a Positively Charged Surface. *Anal. Chem.* **2011**, *83*, 3042-3049.
- (411) Minson, M.; Meredith, M. T.; Shrier, A.; Giroud, F.; Hickey, D.; Glatzhofer, D. T.; Minteer, S. D. High Performance Glucose/O<sub>2</sub> Biofuel Cell: Effect of Utilizing Purified Laccase with Anthracene-Modified Multi-Walled Carbon Nanotubes. *J. Electrochem. Soc.* **2012**, *159*, G166-G170.
- (412) Pellissier, M.; Barrière, F.; Downard, A. J.; Leech, D. Improved Stability of Redox Enzyme Layers on Glassy Carbon Electrodes via Covalent Grafting. *Electrochem. Commun.* **2008**, *10*, 835-838.
- (413) Shim, J.; Kim, G.-Y.; Moon, S.-H. Covalent Co-Immobilization of Glucose Oxidase and Ferrocenedicarboxylic Acid for an Enzymatic Biofuel Cell. *J. Electroanal. Chem.* **2011**, *653*, 14-20.
- (414) Di Bari, C.; Shleev, S.; De Lacey, A. L.; Pita, M. Laccase-Modified Gold Nanorods for Electrocatalytic Reduction of Oxygen. *Bioelectrochemistry* **2016**, *107*, 30-36.
- (415) Al-Lolage, F. A.; Bartlett, P. N.; Gounel, S.; Staigre, P.; Mano, N. Site-Directed Immobilization of Bilirubin Oxidase for Electrocatalytic Oxygen Reduction. *ACS Catal.* **2019**, *9*, 2068-2078.
- (416) Soozanipour, A.; Taheri-Kafrani, A.; Landarani Isfahani, A. Covalent Attachment of Xylanase on Functionalized Magnetic Nanoparticles and Determination of Its Activity and Stability. *Chem. Eng. J.* **2015**, *270*, 235-243.
- (417) Balistreri, N.; Gaboriau, D.; Jolival, C.; Launay, F. Covalent Immobilization of Glucose Oxidase on Mesocellular Silica Foams: Characterization and Stability Towards Temperature and Organic Solvents. *J. Mol. Catal. B: Enzym.* **2016**, *127*, 26-33.
- (418) Ghanem, M. A.; Chrétien, J.-M.; Pinczewska, A.; Kilburn, J. D.; Bartlett, P. N. Covalent Modification of Glassy Carbon Surface with Organic Redox Probes through Diamine Linkers Using Electrochemical and Solid-Phase Synthesis Methodologies. *J. Mater. Chem.* **2008**, *18*, 4917-4927.
- (419) Sosna, M.; Boer, H.; Bartlett, P. N. A His-Tagged *Melanocarpus albomyces* Laccase and its Electrochemistry upon Immobilisation on NTA-Modified Electrodes and in Conducting Polymer Films. *ChemPhysChem* **2013**, *14*, 2225-2231.
- (420) Choi, O.; Kim, B. C.; An, J. H.; Min, K.; Kim, Y. H.; Um, Y.; Oh, M. K.; Sang, B. I. A Biosensor Based on the Self-Entrapment of Glucose Oxidase within Biomimetic Silica Nanoparticles Induced by a Fusion Enzyme. *Enzyme Microb. Technol.* **2011**, *49*, 441-445.
- (421) Naik, R. R.; Tomczak, M. M.; Luckarift, H. R.; Spain, J. C.; Stone, M. O. Entrapment of

Enzymes and Nanoparticles Using Biomimetically Synthesized Silica. *Chem. Commun.* **2004**, *0*, 1684-1685.

(422) Liu, C.; Alwarappan, S.; Chen, Z.; Kong, X.; Li, C. Z. Membraneless Enzymatic Biofuel Cells Based on Graphene Nanosheets. *Biosens. Bioelectron.* **2010**, *25*, 1829-1833.

(423) Ivnitski, D.; Artyushkova, K.; Rincon, R. A.; Atanassov, P.; Luckarift, H. R.; Johnson, G. R. Entrapment of Enzymes and Carbon Nanotubes in Biologically Synthesized Silica: Glucose Oxidase-catalyzed Direct Electron Transfer. *Small* **2008**, *4*, 357-364.

(424) Franco, A.; Cebrian-Garcia, S.; Rodriguez-Padron, D.; Puente-Santiago, A. R.; Munoz-Batista, M. J.; Caballero, A.; Balu, A.; Romero, A.; Luque, R. Encapsulated Laccases As Effective Electrocatalysts for Oxygen Reduction Reactions. *ACS Sustainable Chem. Eng.* **2018**, *6*, 11058.

(425) Grippo, V.; Pawłowska, J.; Biernat, J. F.; Bilewicz, R. Synergic Effect of Naphthylated Carbon Nanotubes and Gold Nanoparticles on Catalytic Performance of Hybrid Films Containing Bilirubin Oxidase for the Dioxygen Reduction. *Electroanalysis* **2017**, *29*, 103-109.

(426) Wu, G.; Yao, Z.; Fei, B.; Gao, F. An Enzymatic Ethanol Biosensor and Ethanol/Air Biofuel Cell Using Liquid-Crystalline Cubic Phases as Hosting Matrices to Co-Entrap Enzymes and Mediators. *J. Electrochem. Soc.* **2017**, *164*, G82-G86.

(427) Wang, S.-F.; Chen, T.; Zhang, Z.-L.; Pang, D.-W.; Wong, K.-Y. Effects of Hydrophilic Room-Temperature Ionic Liquid 1-Butyl-3-Methylimidazolium Tetrafluoroborate on Direct Electrochemistry and Bioelectrocatalysis of Heme Proteins Entrapped in Agarose Hydrogel Films. *Electrochem. Commun.* **2007**, *9*, 1709-1714.

(428) Nguyen, K. V.; Minter, S. D. Investigating DNA Hydrogels as a New Biomaterial for Enzyme Immobilization in Biobatteries. *Chem. Commun.* **2015**, *51*, 13071-13073.

(429) El Ichi, S.; Zebda, A.; Laaroussi, A.; Reverdy-Bruas, N.; Chaussy, D.; Naceur Belgacem, M.; Cinquin, P.; Martin, D. K. Chitosan Improves Stability of Carbon Nanotube Biocathodes for Glucose Biofuel Cells. *Chem. Commun.* **2014**, *50*, 14535-14538.

(430) Reuillard, B.; Abreu, C.; Lalaoui, N.; Le Goff, A.; Holzinger, M.; Ondel, O.; Buret, F.; Cosnier, S. One-Year Stability for a Glucose/Oxygen Biofuel Cell Combined with pH Reactivation of the Laccase/Carbon Nanotube Biocathode. *Bioelectrochemistry* **2015**, *106*, 73-76.

(431) Tahar, A. B.; Szymczyk, A.; Tingry, S.; Vadgama, P.; Zelsmann, M.; Tsujumura, S.; Cinquin, P.; Martin, D.; Zebda, A. One-Year stability of Glucose Dehydrogenase Confined in a 3D Carbon Nanotube Electrode with Coated Poly-Methylene Green: Application as Bioanode for a Glucose Biofuel Cell. *J. Electroanal. Chem.* **2019**, DOI:<https://doi.org/10.1016/j.jelechem.2019.04.029>  
<https://doi.org/10.1016/j.jelechem.2019.04.029>.

(432) Lian, X.; Fang, Y.; Joseph, E.; Wang, Q.; Li, J.; Banerjee, S.; Lollar, C.; Wang, X.; Zhou, H. C. Enzyme-MOF (Metal-Organic Framework) Composites. *Chem. Soc. Rev.* **2017**, *46*, 3386-3401.

(433) Patra, S.; Sene, S.; Mousty, C.; Serre, C.; Chausse, A.; Legrand, L.; Steunou, N. Design of Laccase-Metal Organic Framework-Based Bioelectrodes for Biocatalytic Oxygen Reduction Reaction. *ACS Appl. Mater. Interfaces* **2016**, *8*, 20012-20022.

(434) Gkaniatsou, E.; Sicard, C.; Ricoux, R.; Mahy, J.-P.; Steunou, N.; Serre, C. Metal–Organic Frameworks: A Novel Host Platform for Enzymatic Catalysis and Detection. *Mater. Horiz.* **2017**, *4*, 55-63.

- (435) Majewski, M. B.; Howarth, A. J.; Li, P.; Wasielewski, M. R.; Hupp, J. T.; Farha, O. K. Enzyme Encapsulation in Metal–Organic Frameworks for Applications in Catalysis. *CrystEngComm* **2017**, *19*, 4082-4091.
- (436) Liu, X.; Qi, W.; Wang, Y.; Su, R.; He, Z. A Facile Strategy for Enzyme Immobilization with Highly Stable Hierarchically Porous Metal–Organic Frameworks. *Nanoscale* **2017**, *9*, 17561-17570.
- (437) Cabana, H.; Jones, J. P.; Agathos, S. N. Preparation and Characterization of Cross-Linked Laccase Aggregates and Their Application to the Elimination of Endocrine Disrupting Chemicals. *J. Biotechnol.* **2007**, *132*, 23-31.
- (438) Barbosa, O.; Ortiz, C.; Berenguer-Murcia, Á.; Torres, R.; Rodrigues, R. C.; Fernandez-Lafuente, R. Glutaraldehyde in Bio-Catalysts Design: a Useful Crosslinker and a Versatile Tool in Enzyme Immobilization. *RSC Adv.* **2014**, *4*, 1583-1600.
- (439) Xia, H. Q.; Kitazumi, Y.; Shirai, O.; Kano, K. Direct Electron Transfer-Type Bioelectrocatalysis of Peroxidase at Mesoporous Carbon Electrodes and Its Application for Glucose Determination Based on Bienzyme System. *Anal. Sci.* **2017**, *33*, 839-844.
- (440) Bahar, T. Preparation of a Ferrocene Mediated Bioanode for Biofuel Cells by MWCNTs, Polyethylenimine and Glutaraldehyde: Glucose Oxidase Immobilization and Characterization. *Asia-Pac. J. Chem. Eng.* **2016**, *11*, 981-988.
- (441) Beneyton, T.; El Harrak, A.; Griffiths, A. D.; Hellwig, P.; Taly, V. Immobilization of CotA, an Extremophilic Laccase from *Bacillus subtilis*, on Glassy Carbon Electrodes for Biofuel Cell Applications. *Electrochem. Commun.* **2011**, *13*, 24-27.
- (442) Rengaraj, S.; Kavanagh, P.; Leech, D. A Comparison of Redox Polymer and Enzyme Co-Immobilization on Carbon Electrodes to Provide Membrane-Less Glucose/O<sub>2</sub> Enzymatic Fuel Cells with Improved Power Output and Stability. *Biosens. Bioelectron.* **2011**, *30*, 294-299.
- (443) Lopez, F.; Zerria, S.; Ruff, A.; Schuhmann, W. An O<sub>2</sub> Tolerant Polymer/Glucose Oxidase Based Bioanode as Basis for a Self-Powered Glucose Sensor. *Electroanalysis* **2018**, *30*, 1311-1318.
- (444) Ruff, A.; Szczesny, J.; Zacarias, S.; Pereira, I. A. C.; Plumeré, N.; Schuhmann, W. Protection and Reactivation of the [NiFeSe] Hydrogenase from *Desulfovibrio vulgaris* Hildenborough under Oxidative Conditions. *ACS Energy Lett.* **2017**, *2*, 964-968.
- (445) Pöller, S.; Koster, D.; Schuhmann, W. Stabilizing Redox Polymer Films by Electrochemically Induced Crosslinking. *Electrochem. Commun.* **2013**, *34*, 327-330.
- (446) Marquitan, M.; Bobrowski, T.; Ernst, A.; Wilde, P.; Clausmeyer, J.; Ruff, A.; Schuhmann, W. Miniaturized Amperometric Glucose Sensors Based on Polymer/ Enzyme Modified Carbon Electrodes in the Sub-Micrometer Scale. *J. Electrochem. Soc.* **2018**, *165*, G3008-G3014.
- (447) Matijošytė, I.; Arends, I. W. C. E.; de Vries, S.; Sheldon, R. A. Preparation and Use of Cross-Linked Enzyme Aggregates (CLEAs) of Laccases. *J. Mol. Catal. B: Enzym.* **2010**, *62*, 142-148.
- (448) Dumorne, K.; Cordova, D. C.; Astorga-Elo, M.; Renganathan, P. Extremozymes: A Potential Source for Industrial Applications. *J. Microbiol. Biotech.* **2017**, *27*, 649-659.
- (449) Zhang, Y. H. P. Production of Biocommodities and Bioelectricity by Cell-Free Synthetic Enzymatic Pathway Biotransformations: Challenges and Opportunities. *Biotechnol. Bioeng.* **2010**, *105*, 663-677.
- (450) Wang, X. Y.; Li, D.; Watanabe, T.; Shigemori, Y.; Mikawa, T.; Okajima, T.; Mao, L. Q.;

Ohsaka, T. A Glucose/O<sub>2</sub> Biofuel Cell Using Recombinant Thermophilic Enzymes. *Int. J. Electrochem. Sc.* **2012**, *7*, 1071-1078.

(451) Kwan, P.; McIntosh, C. L.; Jennings, D. P.; Hopkins, R. C.; Chandrayan, S. K.; Wu, C.-H.; Adams, M. W. W.; Jones, A. K. The [NiFe]-Hydrogenase of *Pyrococcus furiosus* Exhibits a New Type of Oxygen Tolerance. *J. Am. Chem. Soc.* **2015**, *137*, 13556-13565.

(452) Zhu, Z.; Zhang, Y. H. P. *In Vitro* Metabolic Engineering of Bioelectricity Generation by the Complete Oxidation of Glucose. *Metab. Eng.* **2017**, *39*, 110-116.

(453) Campbell, A. S.; Murata, H.; Carmali, S.; Matyjaszewski, K.; Islam, M. F.; Russell, A. J. Polymer-Based Protein Engineering Grown Ferrocene-Containing Redox Polymers Improve Current Generation in an Enzymatic Biofuel Cell. *Biosens. Bioelectron.* **2016**, *86*, 446-453.

(454) Rodrigues, R. C.; Ortiz, C.; Berenguer-Murcia, A.; Torres, R.; Fernandez-Lafuente, R. Modifying Enzyme Activity and Selectivity by Immobilization. *Chem. Soc. Rev.* **2013**, *42*, 6290-6307.

(455) Wong, T. S.; Schwaneberg, U. Protein Engineering in Bioelectrocatalysis. *Curr. Opin. Biotechnol.* **2003** *14*, 590-596.

(456) Eijsink, V. G. H.; Gaseidnes, S.; Borchert, T. V.; van den Burg, B. Directed Evolution of Enzyme Stability. *Biomol. Eng.* **2005**, *22*, 21-30.

(457) Yuhashi, N.; Tomiyama, M.; Okuda, J.; Igarashi, S.; Ikebukuro, K.; Sode, K. Development of a Novel Glucose Enzyme Fuel Cell System Employing Protein Engineered PQQ Glucose Dehydrogenase. *Biosens. Bioelectron.* **2005**, *20*, 2145-2150.

(458) Tanaka, S.; Igarashi, S.; Ferri, S.; Sode, K. Increasing Stability of Water-Soluble PQQ Glucose Dehydrogenase by Increasing Hydrophobic Interaction at Dimeric Interface. *BMC Biochem.* **2005**, *6*, 1.

(459) Mate, Diana M.; Gonzalez-Perez, D.; Falk, M.; Kittl, R.; Pita, M.; De Lacey, Antonio L.; Ludwig, R.; Shleev, S.; Alcalde, M. Blood Tolerant Laccase by Directed Evolution. *Chem. Biol.* **2013**, *20*, 223-231.

(460) Pereira, A. R.; Luz, R. A. S.; Lima, F. C. D. A.; Crespilho, F. N. Protein Oligomerization Based on Brønsted Acid Reaction. *ACS Catal.* **2017**, *7*, 3082-3088.

(461) Campbell, E.; Meredith, M.; Minteer, S. D.; Banta, S. Enzymatic Biofuel Cells Utilizing a Biomimetic Cofactor. *Chem. Commun.* **2012**, *48*, 1898-1900.

(462) Chen, H.; Zhu, Z. G.; Huang, R.; Zhang, Y. H. P. Coenzyme Engineering of a Hyperthermophilic 6-Phosphogluconate Dehydrogenase from NADP<sup>+</sup> to NAD<sup>+</sup> with Its Application to Biobatteries. *Sci. Rep.* **2016**, *6*, 36311.

(463) Lee, S. Y.; Choi, J. H.; Xu, Z. Microbial Cell-Surface Display. *Trends Biotechnol.* **2003**, *21*, 45-52.

(464) Van Bloois, E.; Winter, R. T.; Kolmar, H.; Fraaije, M. W. Decorating Microbes: Surface Display of Proteins on *Escherichia coli*. *Trends Biotechnol.* **2011**, *29*, 79-86.

(465) Shimazu, M.; Mulchandani, A.; Chen, W. Cell Surface Display of Organophosphorus Hydrolase Using Ice Nucleation Protein. *Biotechnol. Prog.* **2001**, *17*, 76-80.

(466) Yang, C.; Zhu, Y.; Yang, J.; Liu, Z.; Qiao, C.; Mulchandani, A.; Chen, W. Development of an Autofluorescent Whole-Cell Biocatalyst by Displaying Dual Functional Moieties on *Escherichia coli* Cell Surfaces and Construction of a Coculture with Organophosphate-Mineralizing Activity. *Appl. Microbiol. Biotechnol.* **2008**, *74*, 7733-7739.

- (467) Yang, T. H.; Kwon, M. A.; Song, J. K.; Pan, J. G.; Rhee, J. S. Functional Display of *Pseudomonas* and *Burkholderia* Lipases Using a Translocator Domain of EstA Autotransporter on the Cell Surface of *Escherichia coli*. *J. Biotechnol.* **2010**, *146*, 126-129.
- (468) Samuelson, P.; Gunneriusson, E.; Nygren, P. A.; Stahl, S. Display of Proteins on Bacteria. *J. Biotechnol.* **2002**, *96*, 129-154.
- (469) Daugherty, P. S. Protein Engineering with Bacterial Display. *Curr. Opin. Struct. Biol.* **2007**, *17*, 474-480.
- (470) Jahns, A. C.; Rehm, B. H. A. Relevant uses of surface proteins – display on self-organized biological structures. *Microb. Biotechnol.* **2012**, *5*, 188-202.
- (471) Tang, X.; Liang, B.; Yi, T.; Manco, G.; IlariaPalchetti; Liu, A. Cell Surface Display of Organophosphorus Hydrolase for Sensitive Spectrophotometric Detection of *P*-Nitrophenol Substituted Organophosphates. *Enzyme Microb. Technol.* **2014**, *55*, 107-112.
- (472) Lee, J.-S.; Shin, K.-S.; Pan, J.-G.; Kim, C.-J. Surface-Displayed Viral Antigens on *Salmonella* carrier Vaccine. *Nat. Biotech.* **2000**, *18*, 645-648.
- (473) Binder, U.; Matschiner, G.; Theobald, I.; Skerra, A. High-Throughput Sorting of an Anticalin Library via EspP-Mediated Functional Display on the *Escherichia coli* Cell Surface. *J. Mol. Biol.* **2010**, *400*, 783-802.
- (474) Saleem, M.; Brim, H.; Hussain, S.; Arshad, M.; Leigh, M. B.; Zia ul, h. Perspectives on Microbial Cell Surface Display in Bioremediation. *Biotechnol. Adv.* **2008**, *26*, 151-161.
- (475) Jin, Z.; Han, S.-Y.; Zhang, L.; Zheng, S.-P.; Wang, Y.; Lin, Y. Combined Utilization of Lipase-Displaying *Pichia pastoris* Whole-Cell Biocatalysts to Improve Biodiesel Production in Co-Solvent Media. *Bioresour. Technol.* **2013**, *130*, 102-109.
- (476) Liang, B.; Wang, G.; Yan, L.; Ren, H.; Feng, R.; Xiong, Z.; Liu, A. Functional Cell Surface Displaying of Acetylcholinesterase for Spectrophotometric Sensing Organophosphate Pesticide. *Sens. Actuat. B: Chem.* **2019**, *279*, 483-489.
- (477) Amir, L.; Carnally, S. A.; Rayo, J.; Rosenne, S.; Melamed Yerushalmi, S.; Schlesinger, O.; Meijler, M. M.; Alfonta, L. Surface Display of a Redox Enzyme and Its Site-Specific Wiring to Gold Electrodes. *J. Am. Chem. Soc.* **2013**, *135*, 70-73.
- (478) Simon Fishilevich; Liron Amir; Yearit Fridman; Amir Aharoni; Alfonta, L. Surface Display of Redox Enzymes in Microbial Fuel Cells. *J. Am. Chem. Soc.* **2009**, *131*, 12052–12053.
- (479) Alfonta, L. Genetically Engineered Microbial Fuel Cells. *Electroanalysis* **2010**, *22*, 822-831.
- (480) Osman, M. H.; Shah, A. A.; Walsh, F. C. Recent Progress and Continuing Challenges in Bio-Fuel Cells. Part I: Enzymatic Cells. *Biosens. Bioelectron.* **2011**, *26*, 3087-3102.
- (481) Xie, X.; Ye, M.; Hsu, P.-C.; Liu, N.; Criddle, C. S.; Cui, Y. Microbial Battery for Efficient Energy Recovery. *Proc. Natl. Acad. Sci.* **2013**, *110*, 15925-15930.
- (482) Herrero-Hernandez, E.; Smith, T. J.; Akid, R. Electricity Generation from Wastewaters with Starch as Carbon Source Using a Mediatorless Microbial Fuel Cell. *Biosens. Bioelectron.* **2013**, *39*, 194-198.
- (483) Liang, B.; Li, L.; Mascin, M.; Liu, A. Construction of Xylose Dehydrogenase Displayed on the Surface of Bacteria Using Ice Nucleation Protein for Sensitive D-Xylose Detection. *Anal. Chem.* **2012**, *84*, 275-282.
- (484) Liang, B.; Li, L.; Tang, X.; Lang, Q.; Wang, H.; Li, F.; Shi, J.; Shen, W.; Palchetti, I.

Mascini, M.*et al.* Microbial Surface Display of Glucose Dehydrogenase for Amperometric Glucose Biosensor. *Biosens. Bioelectron.* **2013**, *45*, 19-24.

(485) Liang, B.; Lang, Q.; Tang, X.; Liu, A. Simultaneously Improving Stability and Specificity of Cell Surface Displayed Glucose Dehydrogenase Mutants to Construct Whole-Cell Biocatalyst for Glucose Biosensor Application. *Bioresour. Technol.* **2013**, *147*, 492-498.

(486) Liang, B.; Zhang, S.; Lang, Q.; Song, J.; Han, L.; Liu, A. Amperometric L-Glutamate Biosensor Based on Bacterial Cell-Surface Displayed Glutamate Dehydrogenase. *Anal. Chim. Acta* **2015**, *884*, 83-89.

(487) Liu, A.; Liang, B.; Feng, R. Microbial Surface Displaying Formate Dehydrogenase and Its Application in Optical Detection of Formate. *Enzyme Microb. Technol.* **2016**, *91*, 59-65.

(488) Wang, H.; Lang, Q.; Li, L.; Liang, B.; Tang, X.; Kong, L.; Mascini, M.; Liu, A. Yeast Surface Displaying Glucose Oxidase as Whole-Cell Biocatalyst: Construction, Characterization, and Its Electrochemical Glucose Sensing Application. *Anal. Chem.* **2013**, *85*, 6107-6112.

(489) Lang, Q.; Wang, F.; Yin, L.; Liu, M.; Petrenko, V. A.; Liu, A. Specific Probe Selection from Landscape Phage Display Library and Its Application in Enzyme-Linked Immunosorbent Assay of Free Prostate-Specific Antigen. *Anal. Chem.* **2014**, *86*, 2767-2774.

(490) Han, L.; Liu, A. Novel Cell-Inorganic Hybrid Catalytic Interfaces with Enhanced Enzymatic Activity and Stability for Sensitive Biosensing of Paraoxon. *ACS Appl. Mater. Interfaces* **2017**, *9*, 6894-6901.

(491) Han, L.; Xia, H.; Yin, L.; Petrenko, V. A.; Liu, A. Selected Landscape Phage Probe as Selective Recognition Interface for Sensitive Total Prostate-Specific Antigen Immunosensor. *Biosens. Bioelectron.* **2018**, *106*, 1-6.

(492) Xia, L.; Liang, B.; Li, L.; Tang, X.; Palchetti, I.; Mascini, M.; Liu, A. Direct Energy Conversion from Xylose Using Xylose Dehydrogenase Surface Displayed Bacteria Based Enzymatic Biofuel Cell. *Biosens. Bioelectron.* **2013**, *44*, 160-163.

(493) Feng, R.; Liang, B.; Hou, C.; Han, D.; Han, L.; Lang, Q.; Liu, A.; Han, L. Rational Design of Xylose Dehydrogenase for Improved Thermostability and Its Application in Development of Efficient Enzymatic Biofuel Cell. *Enzyme Microb. Technol.* **2016**, *84*, 78-85.

(494) Lang, Q.; Yin, L.; Shi, J.; Li, L.; Xia, L.; Liu, A. Co-Immobilization of Glucoamylase and Glucose Oxidase for Electrochemical Sequential Enzyme Electrode for Starch Biosensor and Biofuel Cell. *Biosens. Bioelectron.* **2014**, *51*, 158-163.

(495) Yamamoto, K.; Matsumoto, T.; Shimada, S.; Tanaka, T.; Kondo, A. Starchy Biomass-Powered Enzymatic Biofuel Cell Based on Amylases and Glucose Oxidase Multi-Immobilized Bioanode. *New Biotech.* **2013**, *30*, 531-535.

(496) Bahartan, K.; Amir, L.; Israel, A.; Lichtenstein, R. G.; Alfonta, L. *In situ* Fuel Processing in a Microbial Fuel Cell. *ChemSusChem* **2012**, *5*, 1820-1825.

(497) Dijkman, W. P.; de Gonzalo, G.; Mattevi, A.; Fraaije, M. W. Flavoprotein Oxidases: Classification and Applications. *Appl. Microbiol. Biotechnol.* **2013**, *97*, 5177-5188.

(498) Gadda, G. Oxygen Activation in Flavoprotein Oxidases: The Importance of Being Positive. *Biochemistry* **2012**, *51*, 2662-2669.

(499) PrévotEAU, A.; Mano, N. How the Reduction of O<sub>2</sub> on Enzymes and/or Redox Mediators Affects the Calibration Curve of “Wired” Glucose Oxidase and Glucose Dehydrogenase Biosensors.

*Electrochim. Acta* **2013**, *112*, 318-326.

- (500) Wilson, R.; Turner, A. P. F. Glucose Oxidase: An Ideal Enzyme. *Biosens. Bioelectron.* **1992**, *7*, 165-185.
- (501) Brusova, Z.; Gorton, L.; Magner, E. Comment on "Direct Electrochemistry and Electrocatalysis of Heme Proteins Entrapped in Agarose Hydrogel Films in Room-Temperature Ionic Liquids". *Langmuir* **2006**, *22*, 11453-11455.
- (502) Scodeller, P.; Carballo, R.; Szamocki, R.; Levin, L.; Forchiassin, F.; Calvo, E. J. Layer-by-Layer Self-Assembled Osmium Polymer-Mediated Laccase Oxygen Cathodes for Biofuel Cells: The Role of Hydrogen Peroxide. *J. Am. Chem. Soc.* **2010**, *132*, 11132-11140.
- (503) Milton, R. D.; Giroud, F.; Thumser, A. E.; Minter, S. D.; Slade, R. C. T. Bilirubin Oxidase Bioelectrocatalytic Cathodes: The Impact of Hydrogen Peroxide. *Chem. Commun.* **2014**, *50*, 94-96.
- (504) Willner, I.; Arad, G.; Katz, E. A Biofuel Cell Based on Pyrroloquinoline Quinone and Microperoxidase-11 Monolayer-Functionalized Electrodes. *Bioelectrochem. Bioenerg.* **1998**, *44*, 209-214.
- (505) Katz, E.; Lioubashevski, O.; Willner, I. Magnetic Field Effects on Bioelectrocatalytic Reactions of Surface-Confined Enzyme Systems: Enhanced Performance of Biofuel Cells. *J. Am. Chem. Soc.* **2005**, *127*, 3979-3988.
- (506) Koushanpour, A.; Gamella, M.; Katz, E. A Biofuel Cell Based on Biocatalytic Reactions of Lactate on Both Anode and Cathode Electrodes – Extracting Electrical Power from Human Sweat. *Electroanalysis* **2017**, *29*, 1602-1611.
- (507) Ruff, A.; Pinyou, P.; Nolten, M.; Conzuelo, F.; Schuhmann, W. A Self-Powered Ethanol Biosensor. *ChemElectroChem* **2017**, *4*, 890-897.
- (508) Cheng, F.; Zhu, L.; Schwaneberg, U. Directed Evolution 2.0: Improving and Deciphering Enzyme Properties. *Chem. Commun.* **2015**, *51*, 9760-9772.
- (509) Klinman, J. P. How Do Enzymes Activate Oxygen without Inactivating Themselves? *Acc. Chem. Res.* **2007**, *40*, 325-333.
- (510) Petrović, D.; Frank, D.; Kamerlin, S. C. L.; Hoffmann, K.; Strodel, B. Shuffling Active Site Substrate Populations Affects Catalytic Activity: The Case of Glucose Oxidase. *ACS Catal.* **2017**, *7*, 6188-6197.
- (511) Roth, J. P.; Klinman, J. P. Catalysis of Electron Transfer During Activation of O<sub>2</sub> by the Flavoprotein Glucose Oxidase. *Proc. Natl. Acad. Sci.* **2003**, *100*, 62-67.
- (512) Arango Gutierrez, E.; Mundhada, H.; Meier, T.; Duefel, H.; Bocola, M.; Schwaneberg, U. Reengineered Glucose Oxidase for Amperometric Glucose Determination in Diabetes Analytics. *Biosens. Bioelectron.* **2013**, *50*, 84-90.
- (513) Horaguchi, Y.; Saito, S.; Kojima, K.; Tsugawa, W.; Ferri, S.; Sode, K. Construction of Mutant Glucose Oxidases with Increased Dye-Mediated Dehydrogenase Activity. *Int. J. Mol. Sci.* **2012**, *13*.
- (514) Horaguchi, Y.; Saito, S.; Kojima, K.; Tsugawa, W.; Ferri, S.; Sode, K. Engineering Glucose Oxidase to Minimize the Influence of Oxygen on Sensor Response. *Electrochim. Acta* **2014**, *126*, 158-161.
- (515) Suraniti, E.; Courjean, O.; Gounel, S.; Tremey, E.; Mano, N. Uncovering and Redesigning a Key Amino Acid of Glucose Oxidase for Improved Biotechnological Applications. *Electroanalysis*



2013, 25, 606-611.

- (516) Tremey, E.; Stines-Chaumeil, C.; Gounel, S.; Mano, N. Designing an O<sub>2</sub>-Insensitive Glucose Oxidase for Improved Electrochemical Applications. *ChemElectroChem* **2017**, *4*, 2520-2526.
- (517) Hiraka, K.; Kojima, K.; Lin, C.-E.; Tsugawa, W.; Asano, R.; La Belle, J. T.; Sode, K. Minimizing the Effects of Oxygen Interference on L-Lactate Sensors by a Single Amino Acid Mutation in *Aerococcus Viridans* L-Lactate Oxidase. *Biosens. Bioelectron.* **2018**, *103*, 163-170.
- (518) Gorton, L.; Domínguez, E. Electrocatalytic Oxidation of NAD(P)H at Mediator Modified Electrodes. *Rev. Mol. Biotechnol.* **2002**, *82*, 371-392.
- (519) Durand, F.; Stines-Chaumeil, C.; Flexer, V.; André, I.; Mano, N. Designing a Highly Active Soluble PQQ-Glucose Dehydrogenase for Efficient Glucose Biosensors and Biofuel Cells. *Biochem. Biophys. Res. Commun.* **2010**, *402*, 750-754.
- (520) Schubart, I. W.; Göbel, G.; Lisdat, F. A Pyrroloquinolinequinone-Dependent Glucose Dehydrogenase (PQQ-GDH)-Electrode with Direct Electron Transfer Based on Polyaniline Modified Carbon Nanotubes for Biofuel Cell Application. *Electrochim. Acta* **2012**, *82*, 224-232.
- (521) Giroud, F.; Milton, R. D.; Tan, B.-X.; Minteer, S. D. Simplifying Enzymatic Biofuel Cells: Immobilized Naphthoquinone as a Biocathodic Orientational Moiety and Bioanodic Electron Mediator. *ACS Catal.* **2015**, *5*, 1240-1244.
- (522) Tanne, C.; Göbel, G.; Lisdat, F. Development of a (PQQ)-GDH-Anode Based on MWCNT-Modified Gold and its Application in a Glucose/O<sub>2</sub>-Biofuel Cell. *Biosens. Bioelectron.* **2010**, *26*, 530-535.
- (523) Flexer, V.; Durand, F.; Tsujimura, S.; Mano, N. Efficient Direct Electron Transfer of PQQ-Glucose Dehydrogenase on Carbon Cryogel Electrodes at Neutral pH. *Anal. Chem.* **2011**, *83*, 5721-5727.
- (524) Xiao, X.; Conghaile, P. Ó.; Leech, D.; Ludwig, R.; Magner, E. An Oxygen-Independent and Membrane-Less Glucose Biobattery/Supercapacitor Hybrid Device. *Biosens. Bioelectron.* **2017**, *98*, 421-427.
- (525) Milton, R. D.; Giroud, F.; Thumser, A. E.; Minteer, S. D.; Slade, R. C. T. Glucose Oxidase Progressively Lowers Bilirubin Oxidase Bioelectrocatalytic Cathode Performance in Single-Compartment Glucose/Oxygen Biological Fuel Cells. *Electrochim. Acta* **2014**, *140*, 59-64.
- (526) Yehezkeli, O.; Tel-Vered, R.; Raichlin, S.; Willner, I. Nano-engineered Flavin-Dependent Glucose Dehydrogenase/Gold Nanoparticle-Modified Electrodes for Glucose Sensing and Biofuel Cell Applications. *ACS Nano* **2011**, *5*, 2385-2391.
- (527) Tsujimura, S.; Kojima, S.; Kano, K.; Ikeda, T.; Sato, M.; Sanada, H.; Omura, H. Novel FAD-Dependent Glucose Dehydrogenase for a Dioxygen-Insensitive Glucose Biosensor. *Biosci. Biotechnol. Biochem.* **2006**, *70*, 654-659.
- (528) Okuda-Shimazaki, J.; Kakehi, N.; Yamazaki, T.; Tomiyama, M.; Sode, K. Biofuel Cell System Employing Thermostable Glucose Dehydrogenase. *Biotechnol. Lett.* **2008**, *30*, 1753-1758.
- (529) Zafar, M. N.; Beden, N.; Leech, D.; Sygmund, C.; Ludwig, R.; Gorton, L. Characterization of Different FAD-Dependent Glucose Dehydrogenases for Possible Use in Glucose-Based Biosensors and Biofuel Cells. *Anal. Bioanal. Chem.* **2012**, *402*, 2069-2077.
- (530) Milton, R. D.; Giroud, F.; Thumser, A. E.; Minteer, S. D.; Slade, R. C. T. Hydrogen Peroxide

Produced by Glucose Oxidase Affects the Performance of Laccase Cathodes in Glucose/Oxygen Fuel Cells: FAD-Dependent Glucose Dehydrogenase as a Replacement. *Phys. Chem. Chem. Phys.* **2013**, *15*, 19371-19379.

(531) Milton, R. D.; Lim, K.; Hickey, D. P.; Minter, S. D. Employing FAD-Dependent Glucose Dehydrogenase Within a Glucose/Oxygen Enzymatic Fuel Cell Operating in Human Serum. *Bioelectrochemistry* **2015**, *106*, Part A, 56-63.

(532) Osadebe, I.; Leech, D. Effect of Multi-Walled Carbon Nanotubes on Glucose Oxidation by Glucose Oxidase or a Flavin-Dependent Glucose Dehydrogenase in Redox-Polymer-Mediated Enzymatic Fuel Cell Anodes. *ChemElectroChem* **2014**, *1*, 1988-1993.

(533) Iwasa, H.; Hiratsuka, A.; Yokoyama, K.; Uzawa, H.; Orihara, K.; Muguruma, H. Thermophilic *Talaromyces emersonii* Flavin Adenine Dinucleotide-Dependent Glucose Dehydrogenase Bioanode for Biosensor and Biofuel Cell Applications. *ACS Omega* **2017**, *2*, 1660-1665.

(534) Tan, T. C.; Spadiut, O.; Wongnate, T.; Sucharitakul, J.; Krondorfer, I.; Sygmond, C.; Haltrich, D.; Chaiyen, P.; Peterbauer, C. K.; Divne, C. The 1.6 Å Crystal Structure of Pyranose Dehydrogenase from *Agaricus meleagris* Rationalizes Substrate Specificity and Reveals a Flavin Intermediate. *PLOS ONE* **2013**, *8*, e53567.

(535) Zafar, M. N.; Tasca, F.; Boland, S.; Kujawa, M.; Patel, I.; Peterbauer, C. K.; Leech, D.; Gorton, L. Wiring of Pyranose Dehydrogenase with Osmium Polymers of Different Redox Potentials. *Bioelectrochemistry* **2010**, *80*, 38-42.

(536) Yakovleva, M. E.; Killyéni, A.; Seubert, O.; Ó Conghaile, P.; MacAodha, D.; Leech, D.; Gonaus, C.; Popescu, I. C.; Peterbauer, C. K.; Kjellström, S. *et al.* Further Insights into the Catalytical Properties of Deglycosylated Pyranose Dehydrogenase from *Agaricus meleagris* Recombinantly Expressed in *Pichia pastoris*. *Anal. Chem.* **2013**, *85*, 9852-9858.

(537) Yakovleva, M. E.; Gonaus, C.; Schropp, K.; Oconghaile, P.; Leech, D.; Peterbauer, C. K.; Gorton, L. Engineering of Pyranose Dehydrogenase for Application to Enzymatic Anodes in Biofuel Cells. *Phys. Chem. Chem. Phys.* **2015**, *17*, 9074-9081.

(538) Sygmond, C.; Kittl, R.; Volc, J.; Halada, P.; Kubátová, E.; Haltrich, D.; Peterbauer, C. K. Characterization of Pyranose Dehydrogenase from *Agaricus meleagris* and Its Application in the C-2 Specific Conversion of *D*-Galactose. *J. Biotechnol.* **2008**, *133*, 334-342.

(539) Wait, A. F.; Parkin, A.; Morley, G. M.; dos Santos, L.; Armstrong, F. A. Characteristics of Enzyme-Based Hydrogen Fuel Cells Using an Oxygen-Tolerant Hydrogenase as the Anodic Catalyst. *J. Phys. Chem. C* **2010**, *114*, 12003-12009.

(540) Plumeré, N.; Rüdiger, O.; Oughli, A. A.; Williams, R.; Vivekananthan, J.; Pöller, S.; Schuhmann, W.; Lubitz, W. A Redox Hydrogel Protects Hydrogenase from High-Potential Deactivation and Oxygen Damage. *Nat. Chem.* **2014**, *6*, 822.

(541) Fourmond, V.; Stapf, S.; Li, H.; Buesen, D.; Birrell, J.; Rüdiger, O.; Lubitz, W.; Schuhmann, W.; Plumeré, N.; Léger, C. Mechanism of Protection of Catalysts Supported in Redox Hydrogel Films. *J. Am. Chem. Soc.* **2015**, *137*, 5494-5505.

(542) Oughli, A. A.; Conzuelo, F.; Winkler, M.; Happe, T.; Lubitz, W.; Schuhmann, W.; Rüdiger, O.; Plumeré, N. A Redox Hydrogel Protects the O<sub>2</sub>-Sensitive [FeFe]-Hydrogenase from

- Chlamydomonas reinhardtii from Oxidative Damage. *Angew. Chem. Int. Ed.* **2015**, *54*, 12329-12333.
- (543) Ruff, A.; Szczesny, J.; Marković, N.; Conzuelo, F.; Zacarias, S.; Pereira, I. A. C.; Lubitz, W.; Schuhmann, W. A Fully Protected Hydrogenase/Polymer-Based Bioanode for High-Performance Hydrogen/Glucose Biofuel Cells. *Nat. Commun.* **2018**, *9*, 3675.
- (544) Lopez, F.; Ma, S.; Ludwig, R.; Schuhmann, W.; Ruff, A. A Polymer Multilayer Based Amperometric Biosensor for the Detection of Lactose in the Presence of High Concentrations of Glucose. *Electroanalysis* **2017**, *29*, 154-161.
- (545) Barfidokht, A.; Gooding, J. J. Approaches Toward Allowing Electroanalytical Devices to be Used in Biological Fluids. *Electroanalysis* **2014**, *26*, 1182-1196.
- (546) Wisniewski, N.; Reichert, M. Methods for Reducing Biosensor Membrane Biofouling. *Coll. Surf. B: Biointerfaces* **2000**, *18*, 197-219.
- (547) Trouillon, R.; Combs, Z.; Patel, B. A.; O'Hare, D. Comparative Study of the Effect of Various Electrode Membranes on Biofouling and Electrochemical Measurements. *Electrochem. Commun.* **2009**, *11*, 1409-1413.
- (548) Wu, H.; Lee, C.-J.; Wang, H.; Hu, Y.; Young, M.; Han, Y.; Xu, F.-J.; Cong, H.; Cheng, G. Highly Sensitive and Stable Zwitterionic Poly(Sulfobetaine-3,4-Ethylenedioxythiophene) (PSBEDOT) Glucose Biosensor. *Chem. Sci.* **2018**, *9*, 2540-2546.
- (549) Daggumati, P.; Matharu, Z.; Wang, L.; Seker, E. Biofouling-Resilient Nanoporous Gold Electrodes for DNA Sensing. *Anal. Chem.* **2015**, *87*, 8618-8622.
- (550) El Ichi-Ribault, S.; Alcaraz, J.-P.; Boucher, F.; Boutaud, B.; Dalmolin, R.; Boutonnat, J.; Cinquin, P.; Zebda, A.; Martin, D. K. Remote Wireless Control of an Enzymatic Biofuel Cell Implanted in a Rabbit for 2 Months. *Electrochim. Acta* **2018**, *269*, 360-366.
- (551) Falk, M.; Andoralov, V.; Blum, Z.; Sotres, J.; Suyatin, D. B.; Ruzgas, T.; Arnebrant, T.; Shleev, S. Biofuel Cell as a Power Source for Electronic Contact Lenses. *Biosens. Bioelectron.* **2012**, *37*, 38-45.
- (552) Falk, M.; Pankratov, D.; Lindh, L.; Arnebrant, T.; Shleev, S. Miniature Direct Electron Transfer Based Enzymatic Fuel Cell Operating in Human Sweat and Saliva. *Fuel Cells* **2014**, *14*, 1050-1056.
- (553) Göbel, G.; Beltran, M. L.; Mundhenk, J.; Heinlein, T.; Schneider, J.; Lisdat, F. Operation of a Carbon Nanotube-Based Glucose/Oxygen Biofuel Cell in Human Body Liquids-Performance Factors and Characteristics. *Electrochim. Acta* **2016**, *218*, 278-284.
- (554) Bollella, P.; Fusco, G.; Stevar, D.; Gorton, L.; Ludwig, R.; Ma, S.; Boer, H.; Koivula, A.; Tortolini, C.; Favero, G. *et al.* A Glucose/Oxygen Enzymatic Fuel Cell Based on Gold Nanoparticles modified Graphene Screen-Printed Electrode. Proof-of-Concept in Human Saliva. *Sens. Actuat. B: Chem.* **2018**, *256*, 921-930.
- (555) Falk, M.; Andoralov, V.; Silow, M.; Toscano, M. D.; Shleev, S. Miniature Biofuel Cell as a Potential Power Source for Glucose-Sensing Contact Lenses. *Anal. Chem.* **2013**, *85*, 6342-6348.
- (556) Xiao, X.; Siepenkoetter, T.; Conghaile, P. Ó.; Leech, D.; Magner, E. Nanoporous Gold-Based Biofuel Cells on Contact Lenses. *ACS Appl. Mater. Interfaces* **2018**, *10*, 7107-7116.
- (557) Kai, H.; Yamauchi, T.; Ogawa, Y.; Tsubota, A.; Magome, T.; Miyake, T.; Yamasaki, K.; Nishizawa, M. Accelerated Wound Healing on Skin by Electrical Stimulation with a Bioelectric Plaster. *Adv. Healthc. Mater.* **2017**, *6*, 1700465.

- (558) Ogawa, Y.; Kato, K.; Miyake, T.; Nagamine, K.; Ofuji, T.; Yoshino, S.; Nishizawa, M. Organic Transdermal Iontophoresis Patch with Built-in Biofuel Cell. *Adv. Healthc. Mater.* **2015**, *4*, 506-510.
- (559) Kizling, M.; Biedul, P.; Zabost, D.; Stolarczyk, K.; Bilewicz, R. Application of Hydroxyethyl Methacrylate and Ethylene Glycol Methacrylate Phosphate Copolymer as Hydrogel Electrolyte in Enzymatic Fuel Cell. *Electroanalysis* **2016**, *28*, 2444-2451.
- (560) Xiao, X.; Magner, E. A Quasi-Solid-State and Self-Powered Biosupercapacitor Based on Flexible Nanoporous Gold Electrodes. *Chem. Commun.* **2018**, *54*, 5823-5826.
- (561) Gamella, M.; Koushanpour, A.; Katz, E. Biofuel Cells – Activation of Micro- and Macro-Electronic Devices. *Bioelectrochemistry* **2018**, *119*, 33-42.
- (562) Shleev, S.; Bergel, A.; Gorton, L. Biological Fuel Cells: Divergence of Opinion. *Bioelectrochemistry* **2015**, *106*, 1-2.
- (563) Mark, A. G.; Suraniti, E.; Roche, J.; Richter, H.; Kuhn, A.; Mano, N.; Fischer, P. On-Chip Enzymatic Microbiofuel Cell-Powered Integrated Circuits. *Lab Chip* **2017**, *17*, 1761-1768.
- (564) Hu, H.; Islam, T.; Kostyukova, A.; Ha, S.; Gupta, S. From Battery Enabled to Natural Harvesting: Enzymatic BioFuel Cell Assisted Integrated Analog Front-End in 130 nm CMOS for Long-Term Monitoring. *IEEE Trans. Circuits Syst. I, Reg. Papers* **2018**, *66*, 534-545.
- (565) Winkler, W.; Nehter, P. In *Modeling Solid Oxide Fuel Cells: Methods, Procedures and Techniques*; Springer Netherlands: Dordrecht, 2008.
- (566) Alberty, R. A. Calculating Apparent Equilibrium Constants of Enzyme-Catalyzed Reactions at pH 7. *Biochem. Mol. Biol. Educ.* **2000**, *28*, 12-17.
- (567) Bard, A. J.; Faulkner, L. R. *Electrochemical Methods—Fundamental and Applications*. John Wiley & Sons Inc., New York (2001) **2001**.
- (568) Umasankar, Y.; Brooks, D. B.; Brown, B.; Zhou, Z.; Ramasamy, R. P. Three Dimensional Carbon Nanosheets as a Novel Catalyst Support for Enzymatic Bioelectrodes. *Adv. Energy Mater.* **2014**, *4*, 1301306.
- (569) Xiao, X.; Magner, E. A Biofuel Cell in Non-Aqueous Solution. *Chem. Commun.* **2015**, *51*, 13478-13480.
- (570) Richardson, D. J. Bacterial Respiration: A Flexible Process for a Changing Environment. *Microbiology* **2000**, *146*, 551-571.
- (571) Rabaey, K.; Verstraete, W. Microbial Fuel Cells: Novel Biotechnology for Energy Generation. *Trends Biotechnol.* **2005**, *23*, 291-298.
- (572) Katz, E.; Schlereth, D. D.; Schmidt, H.-L. Electrochemical Study of Pyrroloquinoline Quinone Covalently Immobilized as a Monolayer onto a Cystamine-Modified Gold Electrode. *J. Electroanal. Chem.* **1994**, *367*, 59-70.
- (573) Coman, V.; Vaz-Dominguez, C.; Ludwig, R.; Harreither, W.; Haltrich, D.; De Lacey, A. L.; Ruzgas, T.; Gorton, L.; Shleev, S. A Membrane-, Mediator-, Cofactor-Less Glucose/Oxygen Biofuel Cell. *Phys. Chem. Chem. Phys.* **2008**, *10*, 6093-6096.
- (574) Gallaway, J. W.; Calabrese Barton, S. A. Kinetics of Redox Polymer-Mediated Enzyme Electrodes. *J. Am. Chem. Soc.* **2008**, *130*, 8527-8536.
- (575) Kavanagh, P.; Leech, D. Mediated Electron Transfer in Glucose Oxidising Enzyme

Electrodes for Application to Biofuel Cells: Recent Progress and Perspectives. *Phys. Chem. Chem. Phys.* **2013**, *15*, 4859-4869.

(576) Heller, A. Electrical Connection of Enzyme Redox Centers to Electrodes. *J. Phys. Chem.* **1992**, *96*, 3579-3587.

(577) Heller, A.; Feldman, B. Electrochemical Glucose Sensors and Their Applications in Diabetes Management. *Chem. Rev.* **2008**, *108*, 2482-2505.

(578) Soukharev, V.; Mano, N.; Heller, A. A Four-Electron O<sub>2</sub>-Electroreduction Biocatalyst Superior to Platinum and a Biofuel Cell Operating at 0.88 V. *J. Am. Chem. Soc.* **2004**, *126*, 8368-8369.

(579) Hickey, D. P.; Halmes, A. J.; Schmidtke, D. W.; Glatzhofer, D. T. Electrochemical Characterization of Glucose Bioanodes Based on Tetramethylferrocene-Modified Linear Poly(ethylenimine). *Electrochim. Acta* **2014**, *149*, 252-257.

(580) Liu, A.; Anzai, J.-i. Ferrocene-Containing Polyelectrolyte Multilayer Films: Effects of Electrochemically Inactive Surface Layers on the Redox Properties. *Langmuir* **2003**, *19*, 4043-4046.

(581) Tapia, C.; Milton, R. D.; Pankratova, G.; Minter, S. D.; Åkerlund, H.-E.; Leech, D.; De Lacey, A. L.; Pita, M.; Gorton, L. Wiring of Photosystem I and Hydrogenase on an Electrode for Photoelectrochemical H<sub>2</sub> Production by using Redox Polymers for Relatively Positive Onset Potential. *ChemElectroChem* **2017**, *4*, 90-95.

(582) Pinyou, P.; Ruff, A.; Pöller, S.; Alsaoub, S.; Leimkühler, S.; Wollenberger, U.; Schuhmann, W. Wiring of the Aldehyde Oxidoreductase PaoABC to Electrode Surfaces via Entrapment in Low Potential Phenothiazine-Modified Redox Polymers. *Bioelectrochemistry* **2016**, *109*, 24-30.

(583) Abdellaoui, S.; Milton, R. D.; Quah, T.; Minter, S. D. NAD-Dependent Dehydrogenase Bioelectrocatalysis: The Ability of a Naphthoquinone Redox Polymer to Regenerate NAD. *Chem. Commun.* **2016**, *52*, 1147-1150.

(584) Hou, C.; Lang, Q.; Liu, A. Tailoring 1,4-Naphthoquinone with Electron-Withdrawing Group: Toward Developing Redox Polymer and FAD-GDH Based Hydrogel Bioanode for Efficient Electrocatalytic Glucose Oxidation. *Electrochim. Acta* **2016**, *211*, 663-670.

(585) Liu, A.; Anzai, J.-i.; Wang, J. Multilayer Assembly of Calf Thymus DNA and Poly(4-Vinylpyridine) (PVP) Derivative Bearing [Os(bpy)<sub>2</sub>Cl]<sup>2+</sup>: Redox Behavior within DNA Film. *Bioelectrochem.* **2005**, *67*, 1-6.

(586) Liu, A.; Anzai, J.-i. Use of Polymeric Indicator for Electrochemical DNA Sensors: Poly(4-Vinylpyridine) Derivative Bearing [Os(5,6-Dimethyl-1,10-Phenanthroline)<sub>2</sub>Cl]<sup>2+</sup>. *Anal. Chem.* **2004**, *76*, 2975-2980.

(587) Pinyou, P.; Ruff, A.; Pöller, S.; Ma, S.; Ludwig, R.; Schuhmann, W. Design of an Os Complex-Modified Hydrogel with Optimized Redox Potential for Biosensors and Biofuel Cells. *Chem. Eur. J.* **2016**, *22*, 5319-5326.

(588) Guschin, D. A.; Castillo, J.; Dimcheva, N.; Schuhmann, W. Redox Electrodeposition Polymers: Adaptation of the Redox Potential of Polymer-Bound Os Complexes for Bioanalytical Applications. *Anal. Bioanal. Chem.* **2010**, *398*, 1661-1673.

(589) Bartlett, P. N.; Pratt, K. F. E. Theoretical Treatment of Diffusion and Kinetics in Amperometric Immobilized Enzyme Electrodes Part I: Redox Mediator Entrapped Within the Film. *J. Electroanal. Chem.* **1995**, *397*, 61-78.

(590) Zafar, M. N.; Wang, X.; Sygmund, C.; Ludwig, R.; Leech, D.; Gorton, L. Electron-Transfer

Studies with a New Flavin Adenine Dinucleotide Dependent Glucose Dehydrogenase and Osmium Polymers of Different Redox Potentials. *Anal. Chem.* **2012**, *84*, 334-341.

(591) Liu, A.; Anzai, J.-i. A Poly(4-Vinylpyridine) Derivative Bearing Os(5,6-Dmphen)<sub>2</sub>Cl (5,6-Dmphen=5,6-Dimethyl-1,10-Phenanthroline): a Novel Electrochemical Indicator for Detecting DNA Hybridization. *Mater. Sci. Eng. C* **2004**, *24*, 503-505.

(592) Pinyou, P.; Pöller, S.; Chen, X.; Schuhmann, W. Optimization of Os-Complex Modified Redox Polymers for Improving Biocatalysis of PQQ-sGDH Based Electrodes. *Electroanalysis* **2015**, *27*, 200-208.

(593) Oughli, A. A.; Vélez, M.; Birrell, J. A.; Schuhmann, W.; Lubitz, W.; Plumeré, N.; Rüdiger, O. Viologen-Modified Electrodes for Protection of Hydrogenases from High Potential Inactivation While Performing H<sub>2</sub> Oxidation at Low Overpotential. *Dalton Trans.* **2018**, *47*, 10685-10691.

(594) Mao, F.; Mano, N.; Heller, A. Long Tethers Binding Redox Centers to Polymer Backbones Enhance Electron Transport in Enzyme "Wiring" Hydrogels. *J. Am. Chem. Soc.* **2003**, *125*, 4951-4957.

(595) PrévotEAU, A.; Mano, N. Oxygen Reduction on Redox Mediators May Affect Glucose Biosensors Based on "Wired" Enzymes. *Electrochim. Acta* **2012**, *68*, 128-133.

(596) Oh, S. E.; Logan, B. E. Voltage Reversal During Microbial Fuel Cell Stack Operation. *J. Power Sources* **2007**, *167*, 11-17.

(597) Yoshino, S.; Oike, M.; Yatagawa, Y.; Haneda, K.; Miyake, T.; Nishizawa, M. In *6th World Congress of Biomechanics (WCB 2010). August 1-6, 2010 Singapore: In Conjunction with 14th International Conference on Biomedical Engineering (ICBME) and 5th Asia Pacific Conference on Biomechanics (APBiomech)*; Lim, C. T.; Goh, J. C. H., Eds. Berlin, Heidelberg, 2010.

(598) Galindo-de-la-Rosa, J.; Arjona, N.; Moreno-Zuria, A.; Ortiz-Ortega, E.; Guerra-Balcázar, M.; Ledesma-García, J.; Arriaga, L. G. Evaluation of Single and Stack Membraneless Enzymatic Fuel Cells Based on Ethanol in Simulated Body Fluids. *Biosens. Bioelectron.* **2017**, *92*, 117-124.

(599) Shitanda, I.; Nohara, S.; Hoshi, Y.; Itagaki, M.; Tsujimura, S. A Screen-Printed Circular-Type Paper-Based Glucose/O<sub>2</sub> Biofuel Cell. *J. Power Sources* **2017**, *360*, 516-519.

(600) Pan, F.; Samaddar, T. *Charge Pump Circuit Design*; McGraw Hill Professional: New York, 2006.

(601) Southcott, M.; MacVittie, K.; Halamek, J.; Halamkova, L.; Jemison, W. D.; Lobel, R.; Katz, E. A Pacemaker Powered by an Implantable Biofuel Cell Operating under Conditions Mimicking the Human Blood Circulatory System - Battery Not Included. *Phys. Chem. Chem. Phys.* **2013**, *15*, 6278-6283.

(602) Katz, E.; Bückmann, A. F.; Willner, I. Self-Powered Enzyme-Based Biosensors. *J. Am. Chem. Soc.* **2001**, *123*, 10752-10753.

(603) Sekretaryova, A. N.; Beni, V.; Eriksson, M.; Karyakin, A. A.; Turner, A. P. F.; Vagin, M. Y. Cholesterol Self-Powered Biosensor. *Anal. Chem.* **2014**, *86*, 9540-9547.

(604) Jeerapan, I.; Sempionatto, J. R.; Pavinatto, A.; You, J.-M.; Wang, J. Stretchable Biofuel Cells as Wearable Textile-Based Self-Powered Sensors. *J. Mater. Chem. A* **2016**, *4*, 18342-18353.

(605) Wen, D.; Deng, L.; Guo, S.; Dong, S. Self-Powered Sensor for Trace Hg<sup>2+</sup> Detection. *Anal. Chem.* **2011**, *83*, 3968-3972.

(606) Deng, L.; Chen, C.; Zhou, M.; Guo, S.; Wang, E.; Dong, S. Integrated Self-Powered Microchip Biosensor for Endogenous Biological Cyanide. *Anal. Chem.* **2010**, *82*, 4283-4287.

- (607) Wang, T.; Milton, R. D.; Abdellaoui, S.; Hickey, D. P.; Minteer, S. D. Laccase Inhibition by Arsenite/Arsenate: Determination of Inhibition Mechanism and Preliminary Application to a Self-Powered Biosensor. *Anal. Chem.* **2016**, *88*, 3243-3248.
- (608) Hou, C.; Fan, S.; Lang, Q.; Liu, A. Biofuel Cell Based Self-Powered Sensing Platform for L-Cysteine Detection. *Anal. Chem.* **2015**, *87*, 3382-3387.
- (609) Conzuelo, F.; Vivekananthan, J.; Pöller, S.; Pingarrón José, M.; Schuhmann, W. Immunologically Controlled Biofuel Cell as a Self-Powered Biosensor for Antibiotic Residue Determination. *ChemElectroChem* **2014**, *1*, 1854-1858.
- (610) Gai, P.; Song, R.; Zhu, C.; Ji, Y.; Wang, W.; Zhang, J.-R.; Zhu, J.-J. Ultrasensitive Self-Powered Cytosensors Based on Exogenous Redox-Free Enzyme Biofuel Cells as Point-of-Care Tools for Early Cancer Diagnosis. *Chem. Commun.* **2015**, *51*, 16763-16766.
- (611) Wang, L.-L.; Shao, H.-H.; Wang, W.-J.; Zhang, J.-R.; Zhu, J.-J. Nitrogen-Doped Hollow Carbon Nanospheres for High-Energy-Density Biofuel Cells and Self-Powered Sensing of MicroRNA-21 and MicroRNA-141. *Nano Energy* **2018**, *44*, 95-102.
- (612) Zhou, M.; Zhou, N.; Kuralay, F.; Windmiller, J. R.; Parkhomovsky, S.; Valdés-Ramírez, G.; Katz, E.; Wang, J. A Self-Powered “Sense-Act-Treat” System that is Based on a Biofuel Cell and Controlled by Boolean Logic. *Angew. Chem. Int. Ed.* **2012**, *51*, 2686-2689.
- (613) Gamella, M.; Guz, N.; Pingarrón, J. M.; Aslebagh, R.; Darie, C. C.; Katz, E. A Bioelectronic System for Insulin Release Triggered by Ketone Body Mimicking Diabetic Ketoacidosis *in vitro*. *Chem. Commun.* **2015**, *51*, 7618-7621.
- (614) Mailloux, S.; Halánek, J.; Katz, E. A Model System for Targeted Drug Release Triggered by Biomolecular Signals Logically Processed through Enzyme Logic Networks. *Analyst* **2014**, *139*, 982-986.
- (615) Mailloux, S.; Halánek, J.; Halámková, L.; Tokarev, A.; Minko, S.; Katz, E. Biomolecular Release Triggered by Glucose Input-Bioelectronic Coupling of Sensing and Actuating Systems. *Chem. Commun.* **2013**, *49*, 4755-4757.
- (616) Kohlmann, C.; Märkle, W.; Lütz, S. Electroenzymatic Synthesis. *J. Mol. Catal. B: Enzym.* **2008**, *51*, 57-72.
- (617) Mazurenko, I.; Etienne, M.; Kohring, G.-W.; Lapique, F.; Walcarius, A. Enzymatic Bioreactor for Simultaneous Electrosynthesis and Energy Production. *Electrochim. Acta* **2016**, *199*, 342-348.
- (618) Wu, R.; Zhu, Z. Self-Powered Enzymatic Electrosynthesis of l-3,4-Dihydroxyphenylalanine in a Hybrid Bioelectrochemical System. *ACS Sustainable Chem. Eng.* **2018**, *6*, 12593-12597.

## Bios

Xinxin Xiao is currently a postdoctoral researcher at the Technical University of Denmark working with Prof. Jingdong Zhang. He received his Ph.D. in January 2019 at the University of Limerick under the supervision of Prof. Edmond Magner. He was a visiting researcher in

Prof. Aihua Liu's group at Qingdao University in October 2017. His research interests are focused on the immobilization of enzymes on solid surfaces for bioelectrochemistry studies and the development of unique hybrid devices such as biosupercapacitors.

Hong-qi Xia received his Ph.D. degree at Kyoto University in 2017 under the supervision of Prof. Kenji Kano. He then worked as a research associate at Key Lab of Electroanalytical Chemistry, Changchun Institute of Applied Chemistry, Chinese Academy of Science. He was a visiting researcher at Qingdao University (with Prof. Aihua Liu) in 2018 before he moved to Sun Yat-sen University and conducted his postdoctoral research. His research interests focus on bioelectrocatalysis and its application in biofuel cells, biosensors and bioreactors.

Ranran Wu received her Ph.D. degree at the Institute of Urban Environment, Chinese Academy of Sciences in 2015. She then undertook postdoctoral research at the Technical University of Denmark until 2016. She is currently an assistant professor at Tianjin Institute of Industrial Biotechnology, Chinese Academy of Sciences. Her research interests focus on the bioelectrochemical systems, electroenzymatic synthesis and bio-nanomaterials.

Lu Bai received her B.S. degree in Chemistry from Nankai University in 2008. She obtained her Ph.D. degree in Analytical Chemistry from the Changchun Institute of Applied Chemistry, Chinese Academy of Sciences under the supervision of Prof. Shaojun Dong in 2013. She is presently an associate professor in the Institute for Biosensing at Qingdao University. Her major research interests focus on biofuel cells, biosensors and self-powered devices.

Lu Yan is currently pursuing his Master's degree under the supervision of Prof. Aihua Liu at the Institute of Life Sciences & Institute for Biosensing at Qingdao University. He received his bachelor's degree in biology from Yantai University in 2017. His research focuses on microbial surface display based nanomedicine.

Professor Edmond Magner studied at University College Cork (B.Sc. in chemistry) and then obtained his Ph.D. at the University of Rochester under the supervision of Prof. G McLendon. He was a postdoctoral fellow at Imperial College (with Prof. W.J. Albery) and at the Massachusetts Institute of Technology (with Prof. A.M. Klibanov). Subsequently he was a senior research scientist at MediSense, Inc. and at Abbott Laboratories where he worked on the development of biosensors for the detection of glucose and ketones, devices that are still commercially available. In 1997, he joined the academic staff at the University of Limerick and is now Professor Electrochemistry and Dean of the Faculty of Science and Engineering.



His current research interests are in bioelectrochemistry and biocatalysis with a particular focus on the immobilisation of enzymes on surfaces. To date he has supervised the theses of 22 Ph.D. and 10 M.Sc. researchers and published over 100 papers. He is a member of the Council of the Bioelectrochemical Society,

Dr. Serge Cosnier is currently Research Director at CNRS and director of the Department of Molecular Chemistry at the Grenoble Alpes University (France) where he began his research career in 1983. He received his doctoral degree in Chemistry from the Toulouse University (1982) and was an Alexander von Humboldt postdoctoral fellow at the University of Munich, Germany. Cosnier's activity is focused on molecular electrochemistry and bioelectrochemistry for the development of biological sensors, enzymatic fuel cells and bio-nanomaterials based on carbon nanotubes. He has also worked on the development of electrogenerated polymers for applications as organometallic films, biofilms and films with photoactivable, chiral or fluorescent properties applied to bioelectrochemistry. He has authored over 355 publications (h-index 60), 3 books and holds 25 patents.

Elisabeth Lojou is research director at the CNRS, France. She obtained her degree in engineering from the National School of Chemistry, Rennes, France in 1985 and her PhD degree from Paris XII University in 1988. After a post-doctoral position in SAFT-Leclanché Company, Poitiers, France where she developed Li/Liquid cathode batteries, and several positions at CNRS, she integrated the Bioenergetic and Protein Engineering laboratory, Marseille (France) leading a group focusing on the functional immobilization of redox enzymes on nanostructured electrochemical interfaces. Her aim is to understand the molecular basis for the oriented immobilization of enzymes on electrochemical interfaces favoring fast electron transfer process. She developed original electrochemical interfaces for catalytic reduction of metals by cytochromes, as well as for catalytic transformations of H<sub>2</sub> and O<sub>2</sub> by hydrogenases and multi copper oxidases respectively. Recently she designed the first high temperature H<sub>2</sub>/O<sub>2</sub> enzymatic fuel cell. She has authored over 100 publications. She is currently chair-elect of the Bioelectrochemistry division of the International Society of Electrochemistry, and a member of the Council of the Bioelectrochemical Society.

Zhiguang Zhu is currently a Professor at Tianjin Institute of Industrial Biotechnology, Chinese Academy of Sciences. He received his B.Sc. degree in Biotechnology from Huazhong University of Science and Technology in 2007, and Ph.D. degree in Biological Systems Engineering from Virginia Tech in 2013. His research interests focus on the construction and engineering of bioelectrocatalytic systems using the interdisciplinary approaches of biochemical engineering, bioelectrochemistry, and synthetic biology.

Dr. Aihua Liu is a Professor and Director of the Institute for Biosensing, Qingdao University (2016-present). Previously he was a Professor at the Key Laboratory of Biofuels, Qingdao Institute of Bioenergy & Bioprocess Technology, Chinese Academy of Sciences, where he led the Biosensing Group (2010-2016). He received his Ph.D. in Pharmaceutical Physico-chemistry from Tohoku University, Japan in 2004. Then he worked in the National Institute of Advanced Industrial Science & Technology (AIST) at Tsukuba, Japan under the Japanese Society for the Promotion of Sciences (JSPS) fellowship (2004-2006). He subsequently moved to the US to conduct postdoctoral research at Michigan State University, the University of Oklahoma, and the University of Texas at Arlington (2006-2010). His research interests cover microbial surface display, bioelectrochemistry, biosensors, bioenergy and nanomedicine. He has authored over 80 papers and 3 book chapters.

## Graphic TOC

